Title
Maximum Entropy for Resource Allocation: a quantitative theory of species coexistence and population demographics

Author
Zhang, Yu

Publication Date
2016

Peer reviewed|Thesis/dissertation

Maximum Entropy for Resource Allocation: a quantitative theory of species coexistence and population demographics

by

Yu Zhang

A dissertation submitted in partial satisfaction of the
requirements for the degree of
Doctor of Philosophy

in

Environmental Science, Policy and Management

in the

Graduate Division

of the

University of California, Berkeley

Committee in charge:

Professor John Harte, Chair
Professor David Ackerly
Associate Professor Perry de Valpine

Fall 2016

Maximum Entropy for Resource Allocation: a quantitative theory of species coexistence and population demographics

Abstract

Maximum Entropy for Resource Allocation: a quantitative theory of species coexistence and population demographics

by

Yu Zhang

Doctor of Philosophy in Environmental Science, Policy and Management

University of California, Berkeley

Professor John Harte, Chair

In the past few decades, ecology has gone through exciting breakthroughs in developing and applying quantitative methods to more accurately describe and predict patterns and dynamics. However, a theoretical framework under which models could be built and results interpreted in one language is still missing, impeding the communication and collaboration among subfields of ecology. To serve the ultimate goal of developing such a framework, in this dissertation, a theory is developed to make unified predictions of several facets of ecology that have so far been addressed mostly in independent ways: starting from a simple scenario of resource allocation, the theory simultaneously predicts species coexistence, community-level energy distribution, population demographic growth function, evolutionary tradeoffs and life history strategies. The approach of maximizing information entropy (MaxEnt) is used to make sure that the theory makes the most objective predictions from the fewest *ad hoc* assumptions. Previous applications of MaxEnt in ecology are reviewed in Chapter 1. In Chapter 2, the fundamental framework and a first model of the theory is introduced. Based on the same framework, several different approaches to expand model predictions are explored in Chapters 3 and 4. As is discussed in Chapters 2-4, the assumptions and parameters of the theory can be related to many important concepts in ecology (e.g. fitness equality, stabilizing effect, niche and neutrality), and the predictions reveal many previously unidentified links between patterns and processes at the population and community level to metabolism and functional traits. Combining all above, the work in this dissertation is potentially a first step towards a unified theoretical framework of ecology.

Contents

List of Figures

List of Tables

Acknowledgments

I would like to thank Prof. John Harte for his passion, intelligence and support as an excellent academic advisor and a most respectable scientist. You are the best role model for a young researcher. I also want to thank the rest of my dissertation committee members, Prof. David Ackerly and Prof. Perry de Valpine, for providing genuinely insightful comments and constructive advice for publication. I am grateful to everyone else who has provided comments on all or part of this dissertation and below is an incomplete list: Dr. Peter Chesson, Dr. Bill Shipley, Dr. Annette Ousting, Dr. Neo Martinez, Dr. Jennifer Dunne, Dr. Stephen Hubbell, Dr. Mark Ritchie, Dr. Thilo Gross, Dr. Brian Enquist. I owe a lot of what I have accomplished to my brilliant labmates, Danielle Christianson, Justin Kitzes, Andy Rominger, Lydia Smith, Manisha Anantharaman, Meredith Jabis and Katerina Georgiou, who have given me endless inspirations in research and made my everyday as a Ph.D student more enjoyable than I ever imagined. I want to acknowledge the department graduate student officer Roxanne Heglar, who has made all department-required procedures and paperwork much less painful. Finally, a big thanks to my family and friends whose love and encouragement supported me through the most difficult times in graduate school: my parents, Hui Zhang, Kelly Iknayan, Dharshi Devendran, Franco Pallete and Hang Deng.

Chapter 1

Applications of the principle of maximum entropy in ecological models: challenges and opportunities

Abstract

In this chapter I review models using the Maximum Entropy principle (MaxEnt) to predict patterns in ecology. Models will be categorized based on their purpose, i.e. the metric to be predicted, with challenges identified for each category. Based on the review, connections among information entropy, stochasticity and neutrality will be discussed and new directions for model developing and theoretical integration identified.

1.1 Introduction

The principle of Maximum Entropy, also known as MaxEnt, is a method that makes the most objective inference for a probability distribution given the information available (Jaynes 1957). More specifically, MaxEnt predicts the flattest and thus least informative shape of a probability distribution given constraints from prior knowledge. The fundamental idea of this method has been introduced for more than half a century, but only in the recent decade did it start to play an active role in theories and models of ecology (Phillips *et al.* 2006a; Shipley *et al.* 2006a; Pueyo *et al.* 2007; Banavar *et al.* 2010; Harte *et al.* 2008).

The absence of an explicit mechanistic basis for models based on MaxEnt has been noted and questioned (McGill 2006; Haegeman & Loreau 2008; McGill & Nekola 2010). A recent paper (Harte & Newman 2014a) has addressed this issue within the context of a particular theory, METE (the maximum entropy theory of ecology) (Harte 2011a). Meanwhile, MaxEnt has been compared to another mechanistically simplified theory of ecology, the neutral theory of biodiversity and biogeography or NTB (Hubbell 2001). However, the links between them are hard to identify. For example, it is unclear whether there is an effective assumption of

species or individual neutrality in MaxEnt-based models. It is also unclear as to whether the distribution of species abundances that emerges from METE describes demographic stochasticity, which is the basis of NTB.

To clarify these points and identify potential future directions, it is necessary to review the existing applications of MaxEnt in ecology. Previously there have been a number of reviews for this purpose (Baldwin 2009; Banavar *et al.* 2010; Petchey 2010; Harte & Newman 2014a) but each focuses on one specific type of application, e.g. spatial distribution modeling. In the following I will try to summarize on a broader scale all ecological applications of MaxEnt. After that I discuss the linkages between MaxEnt and concepts like stochasticity and neutrality and how to incorporate these linkages in future studies.

1.2 The general procedure of MaxEnt

Information entropy is defined over a probability distribution. Given a probability mass function (for a discrete random variable) or a probability density function (for a continuous random variable) $p(X)$ (X is the random variable) , the equation for Shannon information entropy H over $p(X)$ is shown in Eq. 1.1 (Shannon 1951).

$$\begin{aligned} H &= -\sum_X p(X)\log p(X) && \text{(X is discrete)} \\ &= -\int_X p(X)\log p(X) && \text{(X is continuous)} \end{aligned} \tag{1.1}$$

Note that X can be multiple random variables, in which case $p(X)$ would be a joint distribution over all of them. Shannon information entropy as in Eq. 1.1 is the only formula that satisfies the four information criterion (Shannon 1949; Khinchin 1957; Jaynes 1957). The more generalized forms of information entropy, e.g. Renyi entropy (Renyi 1961), and their applications are beyond the scope of this review.

From Eq. 1.1 one can derive that H is maximized when $p(X)$ is completely flat, i.e. a uniform distribution. In general, the bigger the information entropy, the flatter the probability distribution, and the less information it contains. This is because if a probability distribution is very sharp at some value, we can have a better guess about the random variable compared to when the probability distribution is flat over all values. In other words, maximizing information entropy is equivalent to maximizing our ignorance and therefore minimizing bias in making inferences. Using the predicted least informative distribution as a prior, information we get from extra measurements can be maximized.

With no further information, maximizing H leads to a uniform distribution for X. However, we sometimes have prior knowledge about the probability distribution that can be incorporated into the inference. For example, if the mean of a random variable $f(X)$ that is a function of X is known, it can be used as a constraint on $p(X)$ (Eq. 1.2).

$$\begin{aligned} \sum_X f(X)p(X) &= \bar{f}(X) && \text{(X is discrete)} \\ \text{or } \int_X f(X)p(X) &= \bar{f}(X) && \text{(X is continuous)} \end{aligned} \tag{1.2}$$

Maximizing H subject to constraints like Eq. 1.2 yields a non-uniform distribution for $p(X)$ (Eq. 1.3).

$$p(X) = \frac{e^{-\sum_i \lambda_i f_i(X)}}{Z} \tag{1.3}$$

In Eq. 1.3, $f_i(X)$ is the i_{th} function of X whose mean $\bar{f}_i(X)$ is known. λ_i is a constant that is determined by $\bar{f}_i(X)$. Z is the normalization constant which ensures that the sum (or integral) of $p(X)$ over all values of X equals to 1. The derivation of Eq. 1.3 can be found in the original work of Jaynes (Jaynes 1957) and will not be elaborated on here. It is worth noticing, however, that $p(X)$ in Eq. 1.3 is a very general distribution from which many of the well-known distributions emerge, e.g. normal distribution (for continuous X) and geometric distribution (for discrete X), depending on what prior knowledge is assumed.

Introduced above is how to incorporate prior knowledge through constraints on the probability distribution. Sometimes we have prior knowledge in the form of a distribution. In that case, the procedure of maximizing relative information entropy can be useful (Kullback 1959):

$$\begin{aligned} H &= -\sum_X p(X)\ln\frac{p(X)}{p_0(X)} && \text{(X is discrete)} \\ &= -\int_X p(X)\ln\frac{p(X)}{p_0(X)} && \text{(X is continuous)} \end{aligned} \tag{1.4}$$

In Eq. 1.4, $p_0(X)$ is the prior distribution of X, or the probability distribution when no other constraints exist. Comparing Eqs. 1.1 & 1.4 we can see that, maximizing information entropy without a prior distribution is equivalent to assuming that the prior distribution is uniform ($p_0(X)$ is a constant for all X).

All applications of MaxEnt in ecological modeling stem from the simple framework described above. In the following, I will categorize these applications by their purposes, i.e. the metric to predict, with their connections and distinctions clarified.

1.3 An overall review of ecological modeling with MaxEnt

Spatial distribution modeling (SDM)

One question in biodiversity research is that given limited samples in space, how can we predict the spatial distribution of a particular species. Since the first model was proposed (Phillips *et al.* 2006a), MaxEnt has been shown to be a powerful method for this purpose. In this scenario, $p(x)$ is the probability that a random individual of the species is present at a location x given the values of the environmental variables $(f_1(x), f_2(x), ...)$. The information entropy H over $p(x)$ will be maximized subject to constraints on the environmental variables, usually their mean values across the landscape $(\bar{f}_1(x), \bar{f}_2(x), ...)$. This procedure yields a probability distribution of the same form as Eq. 1.3:

$$p(x) = \frac{e^{-\sum_i \lambda_i f_i(x)}}{Z} \tag{1.5}$$

In Eq. 1.5, x is a grid cell in space, $f_i(x)$ is the value of the i_{th} environmental variable at cell x.

Though powerful, this model also has its issues. For example, it is sometimes difficult to determine the landscape boundary. Also there is a tendency to overfit (Hernandez *et al.* 2006; Phillips & Dudík 2008; Baldwin 2009). In spite of these issues, it is still an active area of study that produces an abundance of literature both on improving the model itself and applying it to new systems (Kramer-Schadt *et al.* 2013; Merow *et al.* 2013; Mainali *et al.* 2015). It is worth noticing that this procedure is mathematically equivalent to logistic regression between species presence and the environmental variables based on a Poisson point process model (He 2010; Renner & Warton 2013).

Relative abundance from traits (trait-based community assembly)

Another application of MaxEnt in ecology is to predict relative abundance of species in a community from functional traits (Shipley *et al.* 2006a; Shipley 2010a). The mathematical setting is very similar to that of SDM, just with a different interpretation for $p(x)$: in this context, it is the probability that a random individual in the community belongs to species x given the values of traits $(f_1(x), f_2(x), ...)$. Correspondingly, the constraints are the mean values of the traits over all species $(\bar{f}_1(x), \bar{f}_2(x), ...)$.

$$p(x) = \frac{e^{-\sum_i \lambda_i f_i(x)}}{Z} \tag{1.6}$$

In Eq. 1.6, x is a species in the community, $f_i(x)$ is the value of the i_{th} trait for species x.

While similar, technically, to the MaxEnt SDM, this application has been much more criticized. One argument against it is on the circularity of the logic: while the model aims to predict the abundances, one has to know the abundances of all species to calculate the constraints, i.e. the community level mean values of the trait variables (Marks & Muller-Landau 2007; Roxburgh & Mokany 2007). Another more important issue about it is that it is seriously over constrained. It has been shown that with the number of constraints used in the original study (Shipley *et al.* 2006a), any information criteria (not limited to MaxEnt) can give an equally good estimate for the relative abundances (Haegeman & Loreau 2008, 2009). One reason for this is that unlike in SDM, no cross-validation is done in this application to make sure that the parameters for the traits (the λ_is) are not overfitted: the whole dataset is used to train the model as well as to test the model. This may be due to the fact that the number of species (around 30 in Shipley *et al.* 2006a) is too small to be further split for training, cross-validation and testing, which is also the reason the model is doomed to overfit.

Although controversial, this study has certainly posed important questions for ecologists looking to apply MaxEnt in their models. For example, what makes an application of MaxEnt more productive than alternative approaches? Summarizing different critiques so far, first, we need to have knowledge of the system that is relevant to the pattern or the process of interest, i.e. the constraints; second, that knowledge has to be "lean" so that it is highly distilled on a coarser grain and not overly constraining.

Species-level spatial abundance distribution (SSAD)

Aside from environmental effects as accounted for in SDMs, the spatial distribution of a species is also shaped by demographic processes (e.g. birth, death, immigration) and intraspecific interactions (Durrett & Levin 1998; Nathan & Muller-Landau 2000). Empirical evidence has shown that individuals of the same species tend to aggregate at the local scale, even when the environment is comparatively homogeneous (Plotkin *et al.* 2000; Green *et al.* 2003). To explain this pattern, ecologists sometimes look at the species-level spatial abundance distribution (SSAD), which is the probability that a certain number of individuals n is observed in area A given the total number of individuals n_0 of the species and the total area of the landscape A_0 (Harte *et al.* 2005; Green & Plotkin 2007). It is sometimes denoted by $P(n|A, A_0, n_0)$.

There have been several attempts to derive the form of the SSAD from a MaxEnt-based approach. The simplest approach is introduced as part of the Maximum Entropy Theory of Ecology or METE (Harte *et al.* 2008; Harte 2011a). It applies the general MaxEnt procedure introduced in section 2 to the $P(n|A, A_0, n_0)$ distribution using the mean number of individuals in a cell across the landscape as the constraint. The solution is shown in Eq. 1.7.

$$P(n|A, A_0, n_0) = \frac{e^{-\lambda n}}{Z} \tag{1.7}$$

In Eq. 1.7, n is the abundance class, or the possible numbers of individuals in one cell (n = 0, 1, 2, ...). Notice that here the only constraint variable is n itself ($f(n) = n$). The λ parameter is determined by the mean number of individuals in a cell ($n_0\frac{A}{A_0}$); Z is still the normalization constant. Since n can only take integer values (0, 1, 2, ...), Eq. 1.7 is a geometric distribution with a mean that equals to $n_0\frac{A}{A_0}$.

However, empirical studies show that the shape of the SSAD depends on scale (Conlisk *et al.* 2007). Notice that the above is not the only way to derive SSAD from MaxEnt, nor is geometric distribution the only prediction. In a review on this topic (Haegeman & Etienne 2010), it has been shown that a number of different predictions for SSAD can emerge from a MaxEnt framework, depending on the choice of the probability distribution to conduct the MaxEnt procedure over. In particular, if we maximize information entropy over a probability distribution of individual-cell configurations, such as $P(c_1, c_2, ...|A, A_0, n_0)$, where c_i is the identity of the cell that the i_{th} individual is in, and then derive $P(n|A, A_0, n_0)$ from that distribution, we actually get a different answer from directly maximizing information entropy over $P(n|A, A_0, n_0)$. The difference is whether individual identity matters: when conducting MaxEnt over $P(c_1, c_2, ...|A, A_0, n_0)$, we are assuming a uniform prior distribution among all configurations of individuals among cells (identity acknowledged representation in Fig. 1.1), in which case individual identity matters. When directly applying MaxEnt to $P(n|A, A_0, n_0)$, we are assuming a uniform prior distribution among all configurations of cells among abundance classes ($n = 0, 1, 2, ...$) (identity ignored representation in Fig .1.1). In this case, individual identity does not matter. Fig. 1.1 shows the difference between these two definitions of configurations.

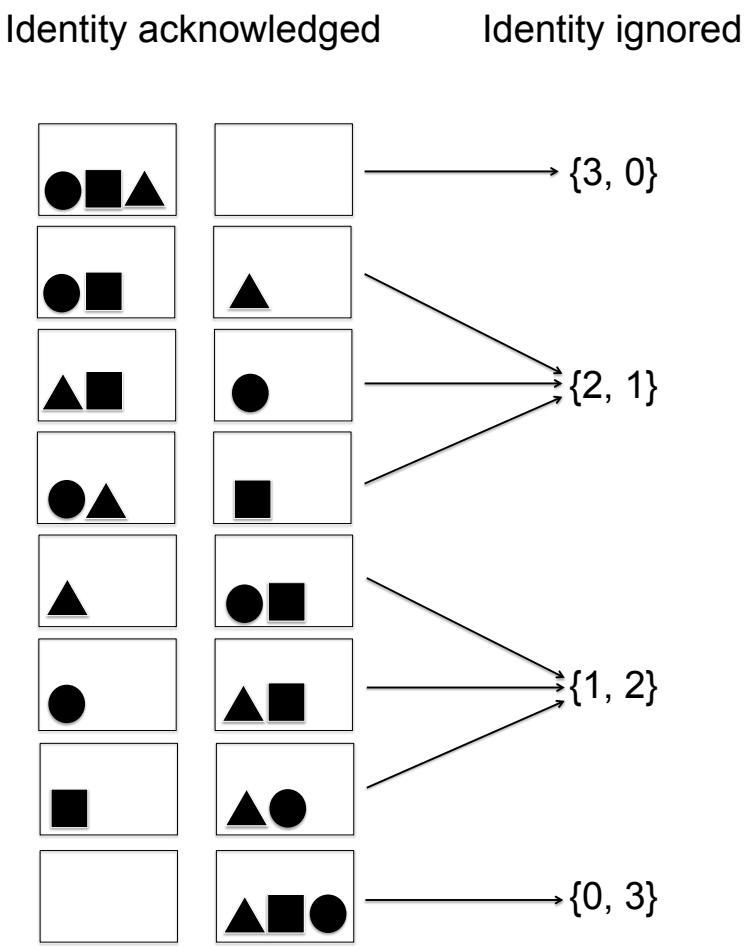

Figure 1.1: Two ways to represent different configurations of allocating three individuals to two cells.
The configurations on the left consider individual identity while the configurations on the right do not, where the numbers in the brackets indicate the numbers of individuals in each cell. When assuming a uniform probability distribution among configurations on the left, {2,1} is three times the probability of {3,0}. When assuming a uniform probability distribution among configurations on the right, {2,1} has the same probability as {3,0}.

The same paper also showed that the choice of constraints can be exchangeable with the choice of prior distribution and the probability distribution to which MaxEnt is applied. Scale inconsistency is another potential problem that emerges from these methods: if one applies MaxEnt to the SSAD at one scale (a certain value of A) and scale transform to a higher scale (merge cells of area A into bigger cells), one usually gets a different SSAD from directly applying MaxEnt to the SSAD at the higher scale. This could be reconciled by allowing for certain spatial autocorrelation among individuals, for example, the probability of presence in one cell is contingent on presence in adjacent cells. The accurate form of spatial autocorrelation that makes MaxEnt consistent across scales has not been solved yet.

There have been other studies exploring the use of MaxEnt in predicting SSAD (Young & Willson 1987a) or biodiversity distribution among sites (Kelly *et al.* 2011, where species is used in place of individuals and sites in place of cells), but all fall within the general framework introduced here.

Species abundance distribution (SAD)

The species abundance distribution $P(n)$ is the probability that a species has n individuals (usually conditional on the total number of individuals N_0 and total number of species S_0 in the community and therefore denoted by $P(n|N_0, S_0)$). Empirical studies show that the species abundance distribution tends to follow a Fisher log-series in stable communities (Fisher *et al.* 1943; Pueyo 2006; White *et al.* 2012). There have been multiple attempts to derive this distribution from fundamental principles (Kendall 1948; MacArthur 1957; Tokeshi 1993; Hubbell 2001). Here I will only focus on the approaches based on MaxEnt.

The first approach (Pueyo *et al.* 2007) used an informative prior distribution (as opposed to the uninformative uniform distribution used in all applications above):

$$P_0(n|N_0, S_0) = Cn^{-1} \tag{1.8}$$

In Eq. 1.8, C is a constant determined by N_0 and S_0. This is derived from a negative binomial SSAD combined with the hypothesis of scale invariance (Dewdney 1998; Pueyo *et al.* 2007): the abundance of a random species in a plot is independent of the size of the plot. The rationale is that it is hard to distinguish between the sample of a rarer species at a larger scale from that of a more common species at a smaller scale, since they should result in very similar sample abundances. Using Eq. 1.8 as the prior distribution, maximizing relative information entropy (Eq. 1.4) subject to a constraint on the mean species abundance yields a log-series distribution for SAD:

$$P(n|N_0, S_0) = Cn^{-1}e^{-\lambda n} \tag{1.9}$$

In Eq. 1.9, n is the abundance class, or the possible numbers of individuals in one species ($n = 0, 1, 2, ...$). λ is a constant determined by the constraint.

One could also obtain the same prior distribution in Eq. 1.8 by assuming that without any constraints, the system goes through a Markov birth-death process (Kendall 1948; Hubbell

2001; Banavar *et al.* 2010) and that birth and death rates are equal and completely density independent.

Another approach that successfully derived a log-series SAD used an uninformative prior distribution but made different choices for the constraints and the probability distribution to conduct MaxEnt over (Harte *et al.* 2008; Harte 2011a). A joint distribution between abundance and metabolic energy is defined, and constraints on both mean abundance and mean metabolic energy are used. More details on this approach will be discussed in Section 1.3.5: metabolic energy distribution.

In general, predicting SAD is technically very similar to predicting SSAD with MaxEnt: instead of allocating individuals of one species among cells in space, we allocate individuals of the whole community among species. The same issues for SSAD also hold: the choice of probability distribution is crucial. Conducting MaxEnt over $P(s_1, s_2, ...)$ where individuals are all labeled with their species identities gives a different SAD from conducting MaxEnt over $P(n|N_0, S_0)$ as defined above (Banavar *et al.* 2010). Constraints and prior distributions also immensely affect the result. Similar to the scale inconsistency issue with SSAD, applying MaxEnt to different taxonomic scales might lead to different solutions to certain metrics. Choice of taxonomic levels to include in the model needs to be made with caution.

Metabolic energy distribution

Aside from the SSAD and the SAD, METE also predicts the metabolic energy distribution within and across species. In the first model of METE (Harte *et al.* 2008), the probability distribution over which the information entropy is maximized is defined as a joint distribution $R(n, \epsilon)$ between n, the abundance of a random species in the community, and ϵ, the metabolic energy of a random individual of that species. Using total number of species S_0, total number of individuals N_0 and total metabolic energy E_0 as state variables from which the constraints can be calculated (mean species abundance N_0/S_0, mean species metabolic energy E_0/S_0), this model predicts the shape of $R(n, \epsilon)$ (Eq. 1.10).

$$R(n, \epsilon) = \frac{e^{-\lambda_1 n - \lambda_2 n\epsilon}}{Z} \tag{1.10}$$

In Eq. 1.10, λ_1 and λ_2 are constants determined by the constraints; Z is the normalization constant. From $R(n, \epsilon)$ one can derive the metabolic energy distribution across all individuals in the community (denoted by $\Psi(\epsilon)$ in METE) as well as the metabolic energy distribution within a species given its abundance (denoted by $\theta(\epsilon|n)$ in METE). Here I will not go over the derivations and interested readers should refer to the original publications of METE (Harte *et al.* 2008; Harte 2011a).

In this very first model, the energetic equivalence rule (EER, Damuth 1981) is predicted: all species have the same total metabolic energy. However, data shows that there is often a lot of scatter around the prediction of EER (Marquet *et al.* 1995a; George-Nascimento *et al.* 2004; White *et al.* 2007b). In a later extension of METE (Harte *et al.* 2015), a new model

incorporating constraints on higher taxonomic levels (mean number of species in a family) is developed. It predicts a different total species metabolic energy in each family which better fits empirical patterns than EER.

Population dynamics and species coexistence

As mentioned above, the choice of probability distribution to conduct MaxEnt over is of crucial importance. The pressing question is which distribution we should assume to be uniform without further constraints. For example in SSAD, should it be the distribution over all individual-cell configurations or the distribution over all cell-abundance class configurations? Although this remains an open question, there have been attempts using a generalized MaxEnt framework based on the fundamental concepts of microstate and macrostate that provide insights into this decision.

It has been known in physics that the thermodynamic entropy of a macrostate is a function of the number of microstates associated with it:

$$S = k_B \log W \tag{1.11}$$

Eq. 1.11 is the Boltzmann's entropy formula (Boltzmann & Gibbs 1870), which states that the thermodynamic entropy S of any macrostate for ideal gas is the natural log of the number of microstates W associated with that macrostate times a constant ($k_B \approx 1.38065 \times 10^{-23} J/K$, the Boltzmann constant). In this context, macrostates are particular values for temperature, volume and pressure, while microstates are particular allocation patterns of particles among energy levels (Dewar 2009; Banavar *et al.* 2010). In general, a macrostate can be understood as a coarse-grain observation at the macroscopic level, e.g. three balls in a box, while a microstate is a fine-grain observation at the microscopic level, e.g. two red balls and one white ball in the box. A microstate contains more information than a macrostate: a macrostate can correspond to multiple microstates but one microstate can only be associated with one macrostate. Furthermore, assuming all microstates are equally probable, the number of microstates W of a macrostate is proportional to the probability of the macrostate.

Given this framework, one can find the most probable macrostate by maximizing S, the Boltzmann entropy. This is equivalent to maximizing W since according to Eq. 1.11 S is a positive function of W and W only. This makes it possible to make inferences about any macroscopic variables, without having to define a probability distribution or choosing constraints. One study explored the prediction for population dynamics in a simple chemostat scenario for microbes (Neill *et al.* 2009b): defining the number of resource units each species gets as the macrostate variable while specific resource allocation between species as microstates (middle column of Fig. 1.2), the model is able to derive the most probable resource allocation pattern between the two species at each time step and thereby a population dynamic path. However, the equally probable microstates in this model are defined at the

species level, and therefore individual identity within each species does not matter when counting the number of microstates. When individual identity within each species matters, each microstate diversifies into multiple scenarios (right column of Fig. 1.2).

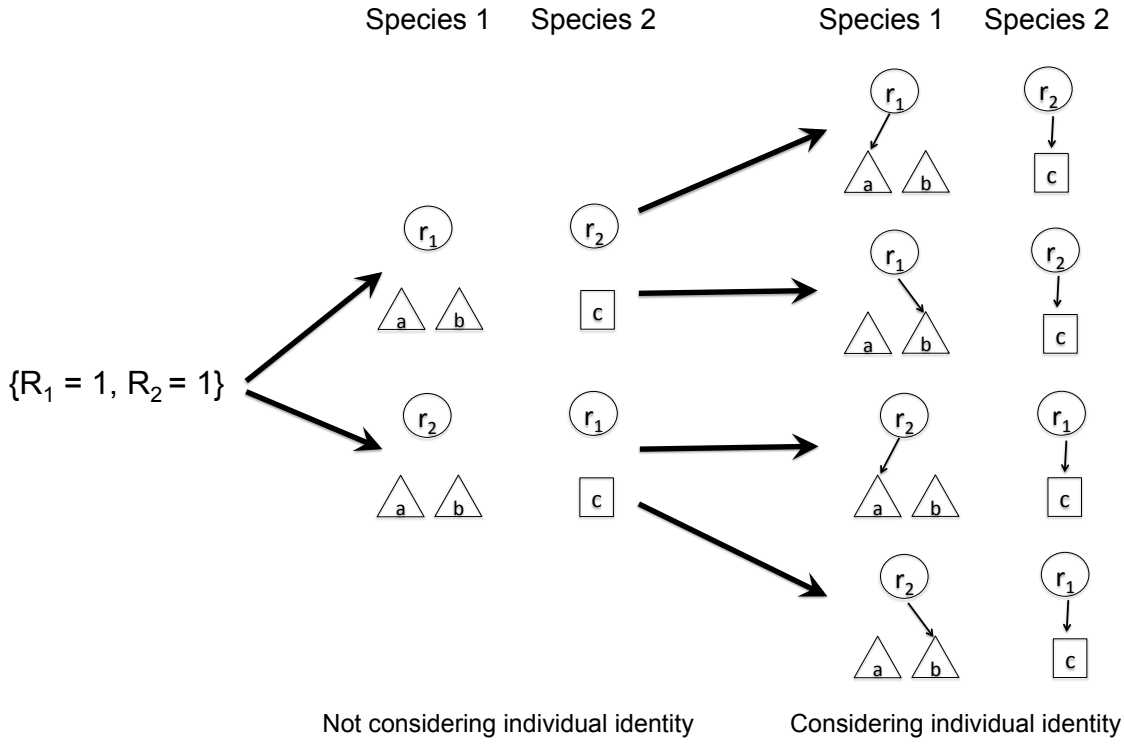

Figure 1.2: Macrostate and microstates for resource allocation between two species. The macrostate is each species gets one resource unit ($R_1 = R_2 = 1$). Not considering individual identity (a, b, c), microstates are the two ways to shuffle resource units between the species. When individual identity is considered, microstates also include the different ways to shuffle resource units between individuals within the species.

In a paper published by this author (Zhang & Harte 2015), a model is developed in which it is possible to switch between the two options: acknowledging or ignoring individual identities. This is realized through the definition of relative distinguishability D_r, a continuous variable between 0 and 1 and potentially different for each species. When $D_r = 0$, individual identity within the species can be ignored; when $D_r = 1$, individual identity should be fully considered when counting the number of microstates. Connections have been made between D_r and functional dispersion as well as genetic variation within- compared to across-species. This model predicts the condition for species to coexist through time, a distinct steady state abundance-metabolic rate relationship that generalizes the prediction of the energetic equivalence rule (EER), and a relationship between population stability and metabolic rate.

1.4 Discussion

Mechanisms and tests

The assumptions of most models introduced above are not based on specific processes. Therefore, tests of these models are targeted towards the potential mechanisms shaping the patterns of interest (spatial distribution, abundance distribution, etc.). Instead of precisely "what is going on and how", these models focus on the broader question of "what matters", more specifically "what it is that mechanisms should incorporate to be able to predict certain patterns". For example, in an SDM, including temperature as a variable assumes that temperature matters to the presence of a species without specifying how exactly it takes effect. If including temperature does not significantly improve the prediction on species presence, then this assumption is falsified. For another example, in METE, including three state variables (total number of species, total abundance and total energy) yields pretty good predictions for species abundance distributions (SAD) in stable ecosystems. This means that in these ecosystems, mechanisms determining the three state variables are the key mechanisms determining the shape of SAD. The fact that the METE model does not work as well in disturbed ecosystems suggests that there are additional important mechanisms involved in those systems, which can be manifested once a new state variable (e.g. total water use) that significantly improves predictions is found.

Links to other concepts in ecology

From the introductions in previous sections we can see that, the choice of model setting (constraint, prior distribution, definition of probability distribution) can hugely affect the predictions in MaxEnt models. However, it is very difficult to justify the choice of one model setting over another, if not by examining *ad hoc* which yields predictions that better describe empirical patterns. Researchers are gradually realizing that this can be enlightened by linking MaxEnt assumptions to processes and mechanisms that ecologists are familiar with (Banavar *et al.* 2010; Haegeman & Etienne 2010; Harte & Newman 2014a). However,

up to this point, models and theories based on MaxEnt have been comparatively independent of other ecological theories. Many questions need to be answered linking specific aspects of MaxEnt to different theories. With these questions not properly addressed, there have been prevalent confusions about MaxEnt and its applications in ecology. Below I will discuss two examples of linkage between MaxEnt and existing concepts in ecological theories. In each example I will try and highlight the ambiguous points, identify the gaps and make suggestions for future model development.

Entropy and stochasticity

It has been a common misunderstanding that MaxEnt models predicting ecological metrics assume stochastic demographic processes, e.g. stochastic birth, death and immigration. In fact, most MaxEnt models are agnostic about processes; they focus on the patterns instead. The stochasticity of MaxEnt lies in the assumption that there is a space consisting of all possible outcomes, i.e. the microstates, corresponding to the pattern of interest, i.e. the macrostate, and the system takes a random walk in the microstate space. The random walk is assumed to be ergodic so through time the macrostate with the most number of microstates is mostly likely to be observed.

This is very different from stochastic birth-death models like the one in NTB (Hubbell 2001), where the transition between any two states correspond to specific demographic processes, i.e. birth, death, immigration, speciation. Instead in MaxEnt, the random walk in the microstate space is merely a theoretical representation and does not correspond to any real processes in nature: we do not know how nature jumps from one microstate to another and whether that has anything to do with ecological processes or mechanisms. In short, MaxEnt is stochastic, but is not mechanistic, in other words does not specify where the stochasticity comes from.

Although MaxEnt has mainly been applied to patterns, it does not mean that MaxEnt is unable to predict processes. Macrostate can be defined based on not only static patterns, but also dynamic terms. As is introduced in Section 1.3.6: population dynamics and species coexistence, the theory developed in this dissertation predicts the most likely birth and death rates (the macrostate) under a simple resource allocation scenario where microstates are defined. The remaining question is how to combine a traditional stochastic model, e.g. the one presented by NTB, with a MaxEnt model on processes. Here we propose two potential solutions. First, apply MaxEnt to derive probability distributions for demographic rates that can be used as parameters in stochastic models. Second, use stochastic models to predict the dynamics of the constraints or the prior distribution for a MaxEnt model. In such applications, one needs to be aware of the combined assumptions of stochasticity at different scales: MaxEnt assumes stochasticity at the microscopic scale but not at the macroscopic scale (there is only one macrostate corresponding to the maximized entropy). Most stochastic models in ecology assume stochasticity at the macroscopic scale. Most importantly, we have to be clear about the choice of microstate as well as constraints and prior distribution; they are the essence of MaxEnt-based models and determine what predictions emerge from them.

Niche and neutrality

For a similar reason as the confusion with stochastic models, the dependence of MaxEnt-based models on the assumption of neutrality has been frequently suspected (Pueyo *et al.* 2007; McGill 2010). A similar argument also applies: MaxEnt *per se* is agnostic about species or individual neutrality; no assumption related to neutrality is needed to apply MaxEnt. In fact, from this review we can see that many ecological models applying MaxEnt have significant non-neutral or niche-based assumptions: SDM predicts that a set of environment variables determine the spatial distribution of a given species in a way specific to that species; trait-based community assembly assumes that the relative abundance of a species is determined by its traits. Even in the original model realization of METE (the ASNE model) where only three state variables (total number of species, total number of individuals, total metabolic rate) are used as input, a non-uniform distribution of metabolic rate among species is predicted.

Such confusion exists partly due to the fact that the definition of neutrality is not clear. The assumption of neutral species has been mostly related to fitness equality and niche irrelevance, where most criticism are also aimed at (Chave 2004; Clark 2009). One common cause of confusion is that the concept of neutrality is relative and always needs a reference. For example, immigration of mammals is probably not neutral about body size (since bigger individuals may be more mobile), but is very likely to be neutral about fur color. The scale at which neutrality is defined also matters: individuals within the same species may be neutral about demographic processes, but different species are not. In future studies involving assumptions related to neutrality, it would be helpful to clarify the subject and scale of concern instead of using the general term which can easily cause confusion.

As is discussed in Section 1.3.6, the relative distinguishability parameter D_r makes it possible to switch between ignoring and acknowledging conspecific individual identity. This parameter could potentially serve as an indicator for the level of neutrality assumed in MaxEnt-based models. Though reasonable hypotheses have been made, It remains to be seen from data whether D_r is related to functional dispersion or genetic variation or something else. Once this is clarified, more connections between MaxEnt model settings and ecological mechanisms as well as neutrality can readily be made.

To summarize, connections among stochasticity, neutrality and MaxEnt do exist but can be versatile depending on the context of a specific application. Interpretation of these concepts should be more open and not limited to views based on established models. Future efforts are needed to expand the horizon of MaxEnt applications in ecology by, for example, modeling not just patterns but also processes, combining with traditional stochastic models, and further clarifying assumptions associated with niche or neutrality at different organization scales.

1.5 Conclusion

Models based on the principle of Maximum Entropy (MaxEnt) have made significant achievements predicting ecological metrics such as SAD (species abundance distribution), IED (individual energy distribution), SSAD (species-level abundance distribution) and SAR (species area relationship). However, there are still challenges regarding choice of constraints, prior distribution and definition of probability distribution. We proposed that one way to tackle these challenges is to link MaxEnt assumptions to existing ecological theories, and based on that we summarized future directions to apply MaxEnt in ecology. With these directions explored in the future, MaxEnt can be a powerful tool to identify crucial ingredients in processes and mechanisms and greatly expand the power of ecological theory.

Chapter 2

Population dynamics and competitive outcome derive from resource allocation statistics: the governing influence of the distinguishability of individuals

Abstract

Model predictions for species competition outcomes highly depend on the assumed form of the population growth function. In this paper we apply an alternative inferential method based on statistical mechanics, maximizing Boltzmann entropy, to predict resource-constrained population dynamics and coexistence. Within this framework, population dynamics and competition outcome can be determined without assuming any particular form of the population growth function. The dynamics of each species is determined by two parameters: the mean resource requirement θ (related to the mean metabolic rate) and individual distinguishability D_r (related to intra- compared to interspecific functional variation). Our theory clarifies the condition for the energetic equivalence rule (EER) to hold, and provide a statistical explanation for the importance of species functional variation in determining population dynamics and coexistence patterns.

2.1 Introduction

Although the competitive exclusion principle has been extensively studied since first proposed, its connection to actual patterns of biodiversity remains elusive (Volterra 1938; Hutchinson 1961; Wilson & Lindow 1994; Anderson *et al.* 2002). Consequently the question of how species diversity is maintained under limited resources continues to intrigue ecologists

(Wright 2002; Kelly & Bowler 2002; Wilson & Abrams 2005; Calcagno *et al.* 2006; Lobry & Harmand 2006; Tokeshi 2009; Siepielski & McPeek 2010).

In a review of this topic, Chesson (2000) identified two properties of mechanisms of population dynamics that shape the species coexistence outcomes: equalizing, which leads to diminishing average fitness difference between species(Tilman 1981; Chave 2004); and stabilizing, which leads to higher intraspecific than interspecific density dependence (Amarasekare 2003; Lobry & Harmand 2006). He then partitioned different models using these two properties and concluded that coexistence is only possible when fitness differences (the opposite of equalizing mechanisms) are compensated by stabilizing mechanisms. The equalizing and stabilizing behaviors of a model, however, are largely determined by the form of the population growth function the model assumes, which is usually chosen phenomenologically, applying functions most familiar to ecologists, e.g. linear, exponential and logistic (Volterra 1938; Hassell 1975).

Although these simple function forms are convenient and neat, nature is undoubtedly more complex (Abrams & Ginzburg 2000; Chase *et al.* 2002; Melbourne & Chesson 2005). And while some competition models have assumed more complex equations, either fitted from data (Leirs *et al.* 1997) or derived from more nonlinear mechanisms (Toro *et al.* 1971; Dennis & Desharnais 1995), the more complex the model, the more vulnerable it usually is to over parameterization, adding to the difficulty of falsification. More importantly, since most studies only look at a handful of species, the form of the population growth function varies from study to study. How this variation is generated would be better understood if a theory involving only general principles, potentially applicable to all species, existed.

Our goal is such a theory, one that predicts the most phenomena with the fewest unverifiable assumptions. Statistical mechanics provides a widely applicable method, maximum entropy (MaxEnt), for inferring the most likely form of the pattern of interest given limited information available. MaxEnt based on Shannon entropy (Jaynes 1982) has been used in ecology to predict species spatial distributions from environmental variables (Phillips *et al.* 2006b) or from the species abundance distribution (Shipley *et al.* 2006b) and has nurtured a comprehensive theory that predicts numerous macroecological metrics including the species abundance distribution, the species level spatial abundance distribution and the species area relationship (Harte 2011b; Harte & Newman 2014b; see also Dewar & Porté 2008).

So far there has been little effort to apply MaxEnt to the study of population dynamics and species interaction. It is not obvious how to do so basing such an application on Shannon entropy. But it is much more straightforward starting with the definition of Boltzmann entropy (Boltzmann 1896), which is applicable to any discrete process, such as resource allocation that can be easily associated with demographic processes. The Boltzmann entropy of a macrostate is defined to be the natural log of the number of microstates compatible with the macrostate:

$$S = \mathrm{k_b} \log(W) \tag{2.1}$$

Where S is the thermodynamic entropy of a macrostate, $\mathrm{k_b}$ is the Boltzmann constant

($\approx 1.38 \times 10^{-23} \mathrm{m^2 kg\ s^{-2} K^{-1}}$), and W is the number of microstates associated with the macrostate. The second law of thermodynamics states that the entropy of an isolated system cannot decrease and the most likely state of a system is the one associated with the highest entropy. Consistent with Eq. 2.1, according to which maximizing the Boltzmann entropy gives the macrostate that is associated with the largest number of microstates, the state with the highest entropy has the highest probability to be observed.

To apply this idea to a resource allocation scenario, a way of counting microstates is needed. A natural approach is to equate the number of microstates with the number of ways the available resources can be allocated to the individuals in the system. In a first attempt in this direction (Neill *et al.* 2009a), the number of resource allocations for two species is maximized in each constant growth period subject to an energy constraint, from which the form of population growth function is derived. This innovative model, however, leads to the conclusion that coexistence is the ultimate competition outcome under all circumstances, contradicting both theory and observation (Phillips *et al.* 2004; Fargione & Tilman 2005). Their model fails for several reasons. First, the MaxEnt part of the model predicted birth rate only, while death was introduced by imposing a constant per capita death rate, making the theoretical basis for birth and death inconsistent. Second, this model only includes between-species allocation but not within-species allocation, which as we will show later, can flip the coexistence outcome under certain conditions; third, the model allocates two resources (a constrained "energy" and an unconstrained "resource") at the same time, adding to the number of parameters and *ad hoc* assumptions, while the more fundamental scenario of allocating one resource was unexamined. Another study uses a similar method to derive abundance distributions by maximizing the number of ways to allocate total biomass to each species subject to constraints on traits (Shipley 2010b). Unlike Neill *et al.* (2009a), this model does not separately specify the birth and death processes and also does not account for within-species allocation.

Here we propose and explore a theory that simultaneously predicts the birth and death rates of two species competing for one constrained resource. It is based on maximizing the Boltzmann entropy of resource allocation, or as will be elaborated on later, the number of ways in which resources can be allocated to individuals and species. Within-species allocation is included using an adjustable exponent corresponding to the within-species individual distinguishability relative to the between-species individual distinguishability. Under this framework, the population growth function, the steady state abundance distribution, the metabolic rate-abundance relationship and the form of the population dynamics can be analytically or numerically determined. Implications of the results and future extensions of this simplest scenario are discussed.

Table 2.1: Symbols used

Symbols ($i = 1, 2$)	Interpretations
R, R_i	The total amount of resources allocated in one allocation period or the amount allocated to species i.
N_i, $N_{i,t}, \hat{N}_i$	The abundance of species i (i=1,2) at any given time, at the t_{th} allocation period, or at steady state.
B_i, D_i	Species level birth and death rates, i.e. the total number of births and deaths for species i in one allocation period.
Ω_{B_i,D_i}	A macrostate of resource allocation, indicating that in the given allocation period, species i has B_i births and D_i deaths
$W_{grouping}$	Number of ways to group individuals into demographic groups, i.e. individuals that reproduce, survive, or die (Fig. 2.1a).
$W_{between}$	Number of ways to allocate resources between the two species (Fig. 2.1b).
$W_{within,i}$	Number of ways to allocate resources within species i (Fig. 2.1c).
W_{total}	Total number of ways to allocate resources, combining demographic grouping, between-species allocation and within-species allocation (see Eq 2.4).
g_i	Per capita net population growth rate at any allocation period.
t_{ij}	The trait value of the j_{th} individual of species i.
$D_{between}, D_{within}$	Mean pairwise difference of a trait relevant to resource acquisition between or within species (see Eq. 2.5 and 2.6).
D_r	Individual level distinguishability within species relative to across species.
θ_i	Relative resource requirement for species i.
S, λ	The objective function for constrained maximization and the Lagrange multiplier (see Eq. 2.14).

2.2 Materials and Methods

A complete list of symbols used in this paper and their implications is shown in Table 2.1.

Scenario setting

Throughout, the term "community" is interpreted as a group of species that significantly depend on and actively compete for the same resource that is essential for their survival and reproduction; the term "resource" is defined generally as something beneficial, exclusive and potentially limiting that is to be allocated among individuals within and between species. This definition covers 1) material resources such as food, water, and nitrogen, 2) energy, including solar radiation and heat, and 3) others, such as space and transportation medium. While this framework can be extended to more complicated scenarios (see Discussion), we focus here on the case of a two-species community competing for one resource. We assume populations grow in a discrete manner and define an allocation period as a time interval in which the resource is allocated among all individuals of the two species; it is also the shortest interval during which population shifts are assumed to occur. A resource unit is defined as the minimum "batch" of resource that can be allocated independently in an allocation period. We also assume during one allocation period an individual can give birth to at most one offspring. We assume the total amount of resource R that is allocated in each allocation period to be the same, corresponding to both the case that the resource is constantly replenished (e.g. solar radiation, food source) and the case that the resource is a constant stock recycled within the community (e.g. space). Finally we are assuming that in each allocation period, the resource is completely exploited with no resource left, or $R_1 + R_2 = R$, where R_1 and R_2 are the amounts of the resource allocated to species 1 and 2 respectively, in a zero-sum process.

$B_{i,t}$ is defined as the discrete species level birth rate at time t, or the number of births at the t_{th} allocation period for species $i (i = 1, 2)$. $D_{i,t}$ is the corresponding rate for death. Capital letters are used here to indicate that these are measures over the whole species instead of per capita. We make no assumptions about the dependence of $B_{i,t}$ and $D_{i,t}$ on abundance; the theory will determine that dependence. By definition:

$$N_{i,t+1} = N_{i,t} + B_{i,t} - D_{i,t} \ (i = 1,2) \tag{2.2}$$

Next we introduce a simple model to predict birth and death rates at the same time: in any allocation period, each individual of species i requires θ_i resource units to survive; to reproduce, a surviving individual has to acquire an extra amount of θ_i, in total $2\theta_i$ resource units. The values of θ_i are determined by the relative magnitude between the amount of resource required for an individual to survive and the size of a resource unit. Since our theory does not incorporate individual growth (individuals become adults instantly after they are born), the extra resource requirement for reproduction is assumed to be the same as that for

Table 2.2: Resource allocation consequence for an individual of species i

Units of resource allocated to the individual	Consequence
0	Death
θ_i	Survive (but not reproduce)
$2\theta_i$	Survive and reproduce

survival so that the actual resource used is always proportional to the updated abundance of the species (see Eq. 2.3). The ratio θ_1/θ_2 quantifies how resource demanding species 1 is compared to species 2. The consequence for an individual after one allocation is shown in Table 2.2.

Based on the above, we can easily calculate $R_{i,t}$ which is the number of resource units used by species i at allocation period t.

$$\begin{aligned} R_{i,t} = \theta_i \times \text{number of individuals that survive but do not reproduce} \\ +2\theta_i \times \text{number of individuals that reproduce} \\ = \theta_i(N_{i,t} - B_{i,t} - D_{i,t}) + 2\theta_i B_{i,t} \\ = \theta_i(N_{i,t} + B_{i,t} - D_{i,t}) \\ = \theta_i N_{i,t+1} \end{aligned} \tag{2.3}$$

Later we suppress t in the annotation and use R_i, N_i, B_i and D_i to represent the resource consumption, abundance, birth and death rates at any given allocation period for species i.

Allocation macrostate and microstate

A macrostate in a given allocation period (with N_1 and N_2 given as initial abundances) is defined as any particular combination of the species level birth and death rates for each species, represented by Ω_{B_1,D_1,B_2,D_2}. In contrast, a microstate is a unique way to allocate each distinct resource unit to individuals of the two species. Multiple microstates could be associated with the same macrostate.

To better illustrate these concepts, we use a simple example where there are $R = 4$ resource units and two species each with 3 individuals at the start of an allocation period ($N_1 = N_2 = 3$) as is shown in Fig. 2.1. We assume $\theta_1 = \theta_2 = 1$ so that individuals of both species could at most get 2 resource units in one allocation period. One specific example for a macrostate under this scenario is $\Omega_{B_1=1,D_1=1,B_2=0,D_2=2}$, indicating there is one birth and one death for species 1 while no birth and two deaths for species 2. From Eq. 2.3 we can get $R_1 = 3$ and $R_2 = 1$. To see what a microstate of this macrostate looks like, in the following the resource allocation process is broken down to separate steps. We assume that the different patterns within each allocation step should be equally weighted, corresponding to a maximally uninformative prior distribution (Shipley 2010c).

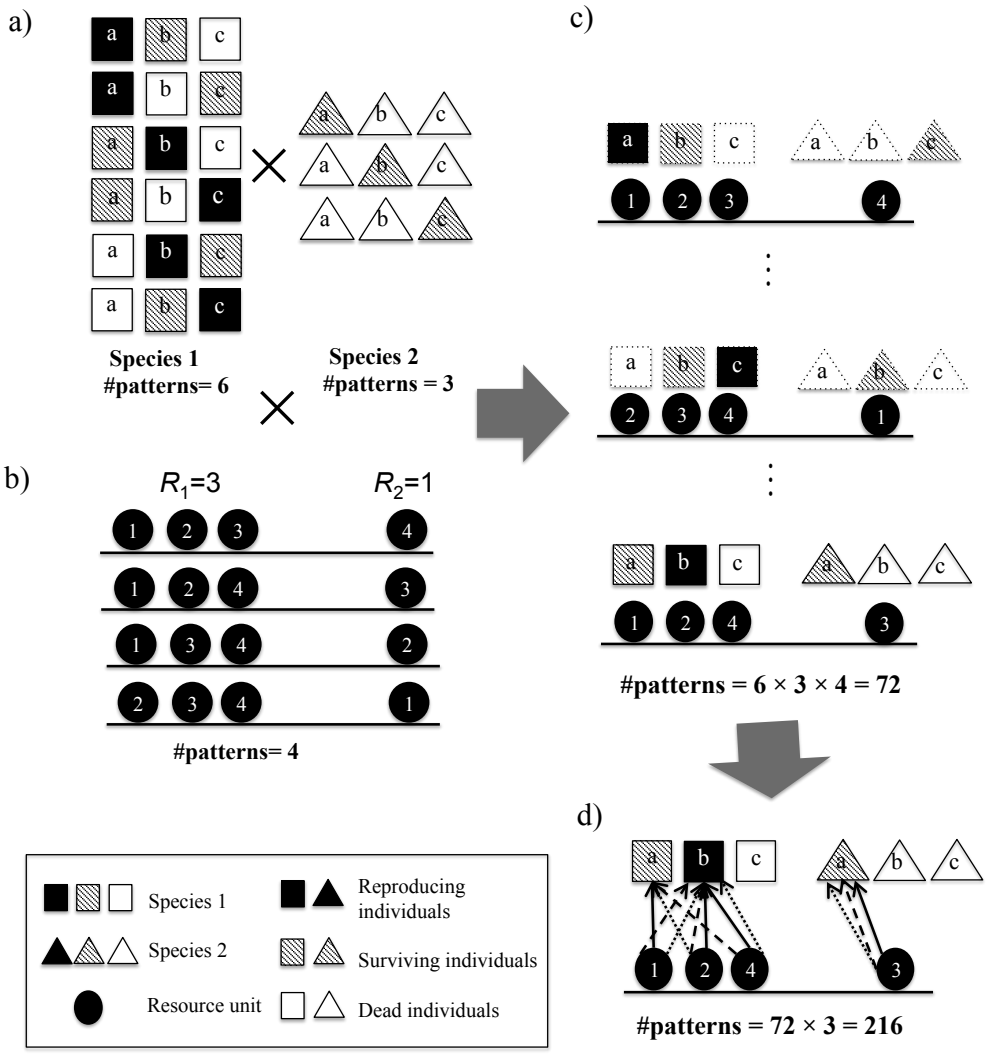

Figure 2.1: Resource allocation process.
With total resource $R = 4$, equal abundances $N_1 = N_2 = 3$ and equal resource requirements $\theta_1 = \theta_2 = 1$, the many ways (microstates) to realize the macrostate $\Omega(B_1 = 1, D_1 = 1, B_2 = 0, D_2 = 2)$ (resulting in $R_1 = 3, R_2 = 1$) is shown in the figure. Resource units and individuals are numerically and alphabetically labeled, respectively, to be differentiated from each other. The three steps of resource allocation are separately shown in a) demographic grouping, divide each species into groups of reproducing, surviving and dead individuals; b) between-species allocation (divide resources into two batches, each for one of the species); c) shows that combining a) and b) gives specific allocation patterns to the demographic group level; d) within-species allocation at the individual level. In this case there are 3 unique ways - each represented by a specific arrow type (solid, dashed or dotted) - to allocate the resource units to the surviving or reproducing individuals chosen in the first two steps within each species.

1. Demographic grouping: Individuals of the same species are divided into three different demographic groups: individuals that reproduce, survive or die. In this example (Fig. 2.1a) there are $\frac{3!}{1!1!1!} = 6$ different ways of grouping for species 1 and $\frac{3!}{0!1!2!} = 3$ different ways of grouping for species 2, combining into $6 \times 3 = 18$ ways of demographic grouping for the two species.
2. Between-species allocation: Resource is divided into two batches, each for one of the species. From Fig. 2.1b we can see that for the macrostate $\Omega_{B_1=1,D_1=1,B_2=0,D_2=2}$ there are $\frac{4!}{3!1!} = 4$ ways to allocate between the two species.

After these two steps, we have a range of combinations between demographic grouping and between-species allocation. If we ignore the difference between the various ways to allocate resource units within each species (among the individuals that reproduce or survive), as is implicitly assumed in Neill *et al.* (2009a), each of the $18 \times 4 = 72$ combinations is a microstate, which can be defined as a unique way to allocate resources between species to individual-specified demographic groups (Fig. 2.1c).

On the other hand, we might not want to ignore the possible difference among various allocation patterns at the individuals-within-species level, which can be specified in a third step where resource is further allocated within each species:
3. Within-species allocation: Resource is allocated within each species among individuals that reproduce or survive (Fig. 2.1d). For species 1 in the above example, for each combination between step 1 and 2, there are $\frac{3!}{2!1!} = 3$ to allocate the $R_1 = 3$ resource units between $B_1 = 1$ individual that reproduces (and thus gets 2 resource units) and $N_1 - B_1 - D_1 = 1$ individual that survives (and thus gets 1 resource unit). Similarly for species 2, there are $\frac{1!}{1!} = 1$ ways of within-species allocation. If we take each of these outcomes where the within-species allocation pattern is specified as a microstate, a microstate can be defined as a specific way to allocate resource units to the individual level.

Relative individual distinguishability

In the section above we introduced two alternative ways to define the microstate (depending on whether within-species allocation is ignored). Here we introduce a critical parameter that makes it possible for our model to switch between the two definitions, and more importantly, to explore the space in between the two underlying assumptions. This parameter is named relative individual distinguishability, represented by D_r, which is defined to be an attribute that quantifies the mean relative distinguishability between two individuals of the same species (conspecific) compared to two individuals of different species (heterospecific). The rationale behind this definition is that, if conspecific individuals are as different from each other as heterospecific individuals, in which case $D_r = 1$, the difference between two microstates generated by relocating resource units between two conspecific individuals should be equally weighted as that generated by relocating resource units between two heterospecific individuals. Therefore in calculating the number of microstates, the number of within-species allocations should be equally weighted as the number of between-species allocations . In contrast, if conspecific individuals are totally indistinguishable from each

other, in which case $D_r = 0$, no difference is generated by relocating resource units within the species, therefore within-species allocation should be ignored and only the number of between-species allocation will be counted as microstates. A case in between is represented by $0 < D_r < 1$. The simplest mathematical representation of the above is:

$$W_{total}(\Omega) = W_{grouping}(\Omega) \times W_{between}(\Omega) \prod_{i}^{2} W_{within,i}(\Omega)^{D_r} \tag{2.4}$$

Where the total number of microstates for a given macrostate Ω (annotated with W_{total}) is the number of ways to group conspecific individuals into demographic groups ($W_{grouping}$) times the number of ways to allocate resource between the species ($W_{between}$) times the weighted number of ways to allocate resource units among the individuals of the same species, the exponent being the relative individual distinguishability of that species ($W_{within,i}^{D_r}$).

Although D_r defined in the above is primarily a statistical attribute, to attach some empirical sense to it, we further interpret D_r as the ecological distinguishability (the converse of substitutability) of conspecific compared to heterospecific individuals. To elaborate on that, the lower the D_r, the more indistinguishable and thus substitutable conspecific individuals are, therefore the smaller the difference among situations where resource units are relocated within the species. While there are many potential measures for ecological substitutability, here we propose one possible approach assuming that the ecological substitutability of individuals is represented by their relative similarity in one or more functional traits. Empirically, which trait(s) to use for D_r measurement depends on the resource as well as the species. To give a specific example, when the resource to be allocated is space and species are plants, the relevant trait might be body size, since it certainly makes a difference for a bigger plant to occupy the space unit compared to when it is occupied by a smaller plant (through influence on the microclimate and biotic interactions). Calculation of D_r for a simple two-species case using trait data is illustrated in Fig. 2.2, where we have used:

$$D_{within} = \frac{2\sum_{i=1}^{2}\sum_{j=1}^{N_i}\sum_{k=i+1}^{N_i}|t_{ij} - t_{ik}|}{N_1(N_1-1) + N_2(N_2-1)} \tag{2.5}$$

$$D_{across} = \frac{\sum_{j=1}^{N_1}\sum_{k=1}^{N_2}|t_{1j} - t_{2k}|}{N_1 N_2} \tag{2.6}$$

$$D_r = D_{within}/D_{across} \tag{2.7}$$

In Eqs. 2.5-2.7, t_{ij} is the trait value of the j_{th} individual in species i. D_{within} is the mean pairwise trait difference between conspecific individuals while D_{across} is that between heterospecific individuals. Substituting the trait values in Fig. 2.2 into Eqs. 2.5-2.7, we get $D_r = 0.9$, indicating that conspecific individuals are 90% as distinguishable as heterospecific individuals. While D_{within}/D_{across} could potentially be bigger than 1 (when the trait distribution is over-dispersed) and so is D_r, in this paper we only discuss the situations where D_r falls within the range [0,1], or within-species variation cannot be bigger than between-species

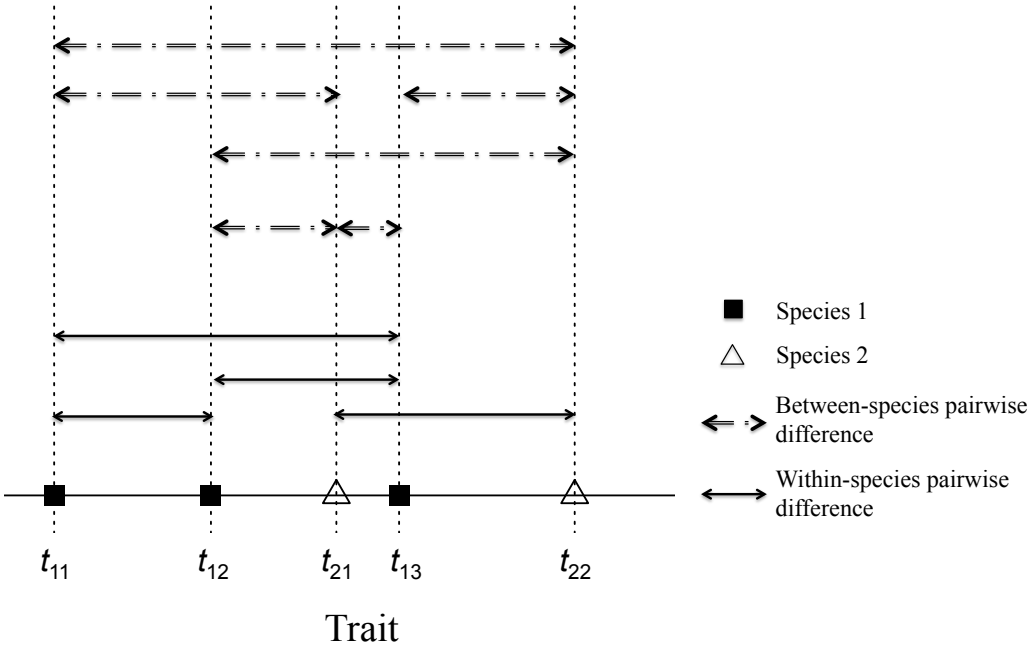

Figure 2.2: Calculation of D_r using a trait relevant to resource acquisition. This is illustrated with a simple two-species case where there are three individuals for the first species and two for the second. Trait values for all individuals are plotted on the trait axis with a distinct point type for each species. t_{ij} represents the trait value of the j_{th} individual in species i. Within- and across- species pairwise distances are represented by line segments of different types. D_r is the relative individual distinguishability calculated from pairwise trait distances using Eqs. 2.5-2.7. In this graph, $t_{11} = 5$, $t_{12} = 30$, $t_{13} = 60$, $t_{21} = 50$, $t_{22} = 90$, substituting in Eqs. 2.5-2.7, we get $D_{within,1} = 2 * (25 + 30 + 55)/6 = 36.67$,$D_{within,2} = 2 * 40/2 = 40$ $D_{across} = (45 + 85 + 20 + 60 + 10 + 30)/6 = 41.67$, $D_{r,1} = 36.67/41.67 = 0.88$, $D_{r,2} = 40/41.67 = 0.96$.

variation. Based on this method, multiple traits and potentially genetic data can be used to calculate D_r.

For simplicity we have assumed that the two species have equal D_r. This can be easily relaxed, with D_{within} calculated separately for each species, and the exponent of W_{within} in Eq. 2.4 being the species specific D_r. Also notice that the measure proposed in the above is only a preliminary attempt based on the assumption that trait difference can be proxy for ecological substitutability (and further for statistical distinguishability). Also if we had used different units for the traits, or a log scale rather than the scale in Fig. 2.2, Eq. 2.7 would be different. Further implications and alternative assumptions will be addressed later in the discussion section.

Calculation

Next we calculate the maximal total number of allocation microstates $W_{total}(\Omega)$ over all possible Ω, with which the most likely macrostate $\hat{\Omega}$ is associated. To do this we first need to express $W_{total}(\Omega)$ as a function of the macrostate variables (B_1, D_1, B_2, D_2). Then we will separately derive each term on the right side of Eq. 2.4. Throughout, $C(x_1, x_2, ...|X)$ denotes the number of ways to combine X individuals into groups of x_i:

$$C(x_1, x_2, ...|X) = \frac{X!}{x_1!x_2!...} \tag{2.8}$$

$W_{grouping}$ is the number of ways to group conspecific individuals into demographic groups, i.e. reproducing, surviving and dead individuals. Using the notation defined above,

$$\begin{aligned} W_{grouping}(\Omega_{B_1,D_1,B_2,D_2}) &= C(B_1, D_1, N_1 - B_1 - D_1|N_1) \\ &\times C(B_2, D_2, N_2 - B_2 - D_2|N_2) \\ &= \prod_{i=1}^{2} \frac{N_i!}{B_i!D_i!(N_i - B_i - D_i)!} \end{aligned} \tag{2.9}$$

$W_{between}$ is the number of ways to divide resource into two batches (R_1, R_2), each for one of the species. Combining Eq. 2.3 and Eq. 2.8, we have

$$\begin{aligned} W_{between}(\Omega_{B_1,D_1,B_2,D_2}) &= C(R_1, R_2|R) \\ = C(\theta_1(N_1 + B_1 - D_1), \theta_2(N_2 + B_2 - D_2)|R) \\ = \frac{R!}{[\theta_1(N_1 + B_1 - D_1)]![\theta_2(N_2 - B_2 - D_2)]!} \end{aligned} \tag{2.10}$$

$W_{within,i}$ is the number of ways the resources allocated to each species are allocated among the reproducing or surviving individuals. For species i, each reproducing individual gets $2\theta_i$ resource units and each surviving individual gets θ_i:

$$W_{within,i}(\Omega_{B_i,D_i,B_i,D_i}) = C(\underbrace{\theta_i,\theta_i,\theta_i,\ ...}_{N_i-B_i-D_i}\underbrace{2\theta_i,2\theta_i,2\theta_i,...}_{B_i}|R_i)$$
$$= \frac{R_i!}{(\theta_i!)^{N_i-B_i-D_i}[(2\theta_i)!]^{B_i}} = \frac{[\theta_i(N_i+B_i-D_i)]!}{(\theta_i!)^{N_i-B_i-D_i}[(2\theta_i)!]^{B_i}} \tag{2.11}$$

Substituting Eqs. 2.9-2.11 into Eq. 2.4, we can get $W_{total}(\Omega_{B_1,D_1,B_2,D_2})$ as a function of B_1, D_1, B_2 and D_2

$$W_{total}(\Omega_{B_1,D_1,B_2,D_2}) = R\prod_{i=1}^{2}\Bigg\{\frac{N_i!}{B_i!D_i!(N_i-B_i-D_i)![\theta_i(N_i-B_i-D_i)]!} \times\Big\{\frac{[\theta_i(N_i+B_i-D_i)]!}{(\theta_i!)^{N_i-B_i-D_i}[(2\theta_i)!]^{B_i}}\Big\}^{D_r}\Bigg\} \tag{2.12}$$

Since the resource in this scenario is assumed to be constrained (see illustration in Section 2.2.1), maximization is subject to the constraint

$$R = R_1 + R_2 = \sum_{i=1}^{2}\theta_i(N_i+B_i-D_i) \tag{2.13}$$

Applying the method of Lagrange multipliers for constrained maximization(Bellman 1956), we define an objective function S as

$$S(\Omega_{B_1,D_1,B_2,D_2}) = \log(W_{total}(\Omega_{B_1,D_1,B_2,D_2}) - \lambda[R - \sum_{i=1}^{2}\theta_i(N_i+B_i-D_i)] \tag{2.14}$$

where λ is the Lagrange multiplier. The constrained maximal $W_{total}(\Omega)$ can be obtained by substituting Eq. 2.12 into Eq. 2.14 and maximizing by setting to zero the derivatives of $S(\Omega_{B_1,D_1,B_2,D_2})$ over each macrostate variable (B_1, D_1, B_2, D_2):

$$\frac{\partial S(\Omega_{B_1,D_1,B_2,D_2})}{\partial B_i} = \log\frac{B_i[\theta_i(N_i+B_i-D_i)]^{\theta_i(1-D_r)}}{N_i-B_i-D_i} + D_r\log\frac{(2\theta_i)!}{\theta_i!} + \lambda\theta_i = 0 \tag{2.15}$$

$$\frac{\partial S(\Omega_{B_1,D_1,B_2,D_2})}{\partial D_i} = \log\frac{D_i}{[\theta_i(N_i+B_i-D_i)]^{\theta_i(1-D_r)}(N_i-B_i-D_i)} - D_r\log\theta_i! - \lambda\theta_i = 0 \tag{2.16}$$

In deriving Eqs. 2.15 - 2.16, Stirling's approximation to a factorial is applied assuming the highest digits are bigger than 10 ($< 1\%$ correction), as is also assumed in Neill *et al.* (2009). These equations combined with the constraint (Eq. 2.13) compose the determining equations of this macrostate. From them the macrostate variables associated with the most

likely macrostate (B_1, D_1, B_2, D_2) can be solved as functions of the initial conditions (N_1, N_2, R, θ_1, θ_2 and D_r).

Combining Eqs. 2.3 and 2.13, we can derive that $\theta_1 N_{1,t} + \theta_2 N_{2,t} = R$ for all $t > 0$. With $g_{i,t}$ defined as the per capita population growth rate of species i at time t, we can further derive that $\theta_1 g_{1,t} + \theta_2 g_{2,t} = 0$ for all $t > 0$ (because $R = \theta_1 N_{1,t} + \theta_2 N_{2,t} = \theta_1 N_{1,t}(1 + g_{1,t}) + \theta_2 N_{2,t}(1+g_{2,t}) = \theta_1 N_{1,t+1} + \theta_2 N_{2,t+1}$). These two equations will be referred to as the zero-sum condition in later discussions.

2.3 Results

In this section we will show the result of solving the determining equations (Eqs. 2.13, 2.15 and 2.16) under various conditions. Specifically, we will derive the population growth function and steady state abundances analytically, and track the population dynamics numerically.

Special case: When $D_r = 1$

Because solving the equations for the most general case (arbitrary θ_i and D_r) is comparatively difficult, we will start with the simplest case where $D_r = 1$ and thus the term $[\theta_i(N_i + B_i - D_i)]^{\theta_i(1-D_r)} = 1$ and can be dropped from the equations. Under this condition, Eqs. 2.15-2.16 reduce to:

$$\frac{B_i}{N_i - B_i - D_i} = \frac{\theta_i! e^{-\lambda\theta_i}}{(2\theta_i)!} \tag{2.17}$$

$$\frac{D_i}{N_i - B_i - D_i} = \theta_i! e^{\lambda\theta_i} \tag{2.18}$$

From which we can solve B_i and D_i:

$$B_i = \frac{N_i}{\frac{(2\theta_i)!}{C^{2\theta_i}} + \frac{(2\theta_i)!}{\theta_i! C^{\theta_i}} + 1} \tag{2.19}$$

$$D_i = \frac{N_i}{\frac{C^{2\theta_i}}{(2\theta_i)!} + \frac{C^{\theta_i}}{\theta_i!} + 1} \tag{2.20}$$

where $C = e^{-\lambda}$, a constant determined by the resource constraint:

$$R = \sum_{i=1}^{2}(N_i + B_i - D_i) = \sum_{i=1}^{2} N_i\theta_i \frac{2C^{2\theta_i} + \frac{(2\theta_i)!}{\theta_i!}C^{\theta_i}}{C^{2\theta_i} + \frac{(2\theta_i)!}{\theta_i!}C^{\theta_i} + (2\theta_i)!} \tag{2.21}$$

The per capita net population growth rate g_i is given by:

$$g_i = \frac{B_i - D_i}{N_i} = \frac{C^{2\theta_i} - (2\theta_i)!}{C^{2\theta_i} + \frac{(2\theta_i)!}{\theta_i!}C^{\theta_i} + (2\theta_i)!} \tag{2.22}$$

From Eq. 2.22 we can see that when $D_r = 1$, $\theta_1 = \theta_2$ always leads to $g_1 = g_2$. Previously we have shown that g_1 and g_2 have to follow the relationship $\theta_1 g_1 + \theta_2 g_2 = 0$ due to the zero-sum condition imposed by the resource constraint. Therefore $g_1 = g_2$ always means $g_1 = g_2 = 0$ since both θ_1 and θ_2 are positive. This means that when $D_r = 1$ and $\theta_1 = \theta_2$, the system has neutral equilibrium states along the resource constraint line, or the community can end up with any N_1 and N_2 that satisfy $\theta_1 N_1 + \theta_2 N_2 = R$.

Given $D_r = 1$, when $\theta_1 \neq \theta_2$, however, the species with smaller θ will always exclude the other. To see this, first $\theta_1 \neq \theta_2$ suggests that $g_1 \neq g_2$. Because $\theta_1 g_1 + \theta_2 g_2 = 0$, g_1 and g_2 cannot be both positive or negative, and therefore $g_1 \neq g_2$ means that g_1 and g_2 are of opposite signs. Eq. 22 suggests that all else equal, the bigger the θ_i, the smaller the g_i. Therefore the g_i corresponding to the lower θ_i is always positive while the other is always negative. This will eventually lead to the species with lower θ_i excluding the other. These inferences will be confirmed below from numerical solutions tracking the population dynamics of the two species.

Population growth rate variation in relation to abundances of both species

When $D_r \neq 1$, B_i and D_i cannot be solved analytically and therefore we take a different approach to determine the g_i by defining a new variable r_i:

$$r_i = \frac{B_i}{D_i} \tag{2.23}$$

Combining r_i with Eqs. 2.15-2.16 we can solve analytically for the relationship between g_i or N_i and r_i(a detailed derivation is in the Appendix)

$$g_i = \frac{r_i - 1}{2^{D_r\theta_i} r_i^{\frac{1}{2}} + r_i + 1} \tag{2.24}$$

$$N_i = \frac{2}{e}(C'\theta_i r_i^{\frac{1}{2\theta_i}})^{\frac{1}{D_r - 1}} \frac{2^{D_r\theta_i} r_i^{\frac{1}{2}} + r_i + 1}{2^{D_r\theta_i} r_i^{\frac{1}{2}} + 2r_i} \tag{2.25}$$

Here C' is another constant that equals $2e^{\lambda - 1}$; given r_1 and r_2, it is determined from

$$\begin{aligned} R = R_1 + R_2 &= \sum_{i=1}^{2} \theta_i (N_i + B_i - D_i) \\ &= \sum_{i=1}^{2} \theta_i N_i (1 + g_i) = \sum_{i=1}^{2} \theta_i \frac{2}{e}(C'\theta_i r_i^{\frac{1}{2\theta_i}})^{\frac{1}{D_r - 1}} \end{aligned} \tag{2.26}$$

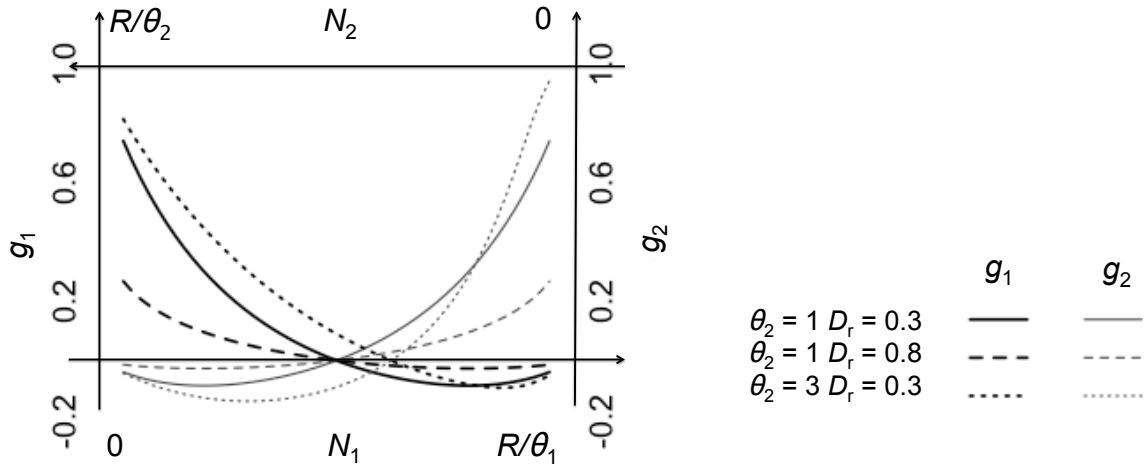

Figure 2.3: Predicted relationship between per capita population growth rate g_i and N_1, N_2. For all calculations, the resource requirement of species 1 and the total resource are fixed ($\theta_1 = 1, R = 200$). Different colors are used for different species (black for species 1, light gray for species 2). Different combinations for resource requirement of species 2 (θ_2) and the relative individual distinguishability (D_r) are represented by curves of different types.

For any given N_1 and N_2 (and R), g_1 and g_2 can be solved by first combining Eqs. 2.25 (for both species) and 2.26 to solve for r_1 and r_2 (and C'), then substituting into Eq. 2.24. Notice that N_1 and N_2 have to satisfy the zero-sum condition ($\theta_1 N_1 + \theta_2 N_2 = R$), therefore an increase in N_1 is always associated with a decrease in N_2 and vice versa. The relationship between g_i and N_i resulting from this procedure is shown in Fig. 2.3.

From Fig. 2.3 we can see that, in all cases, the per capita population growth rate of the species is positive when its abundance is below the steady state level (when $g_1 = g_2 = 0$) and negative when it is above the steady state level, suggesting the steady state in this case ($D_r < 1$) is stable as long as both species start with positive abundances ($0 < N_i < R/\theta_i$). Specifically, the curves for g_1 and g_2 are symmetrical and the steady state abundances for both species are the same when $\theta_1 = \theta_2$, which makes intuitive sense because of the symmetry of the model. However when $\theta_2 > \theta_1$, the curves are asymmetrical and the community converges to a steady state where $N_1 > N_2$, a result that can be analytically proved in the next section. Moreover, the smaller the D_r, the faster the system converges to the steady state, indicated by the bigger absolute values of g_1 and g_2 at any given N_1 and N_2 different from the steady state.

Analytical solution to steady state abundances

When both species are at steady state, $B_1 = D_1$, $B_2 = D_2$ and $r_1 = r_2 = 1$. Substituting this into Eq. 2.24 and again applying Stirling's approximation, we have

$$\hat{N}_i = \frac{2}{e}(C'\theta_i)^{\frac{1}{D_r - 1}} \tag{2.27}$$

$\hat{N}_i$ is the steady state abundance for species i; C' is the same constant as in Eqs. 24-25. Since $D_r < 1$, $\hat{N}_i$ is a negative function of θ_i. Therefore species with higher resource requirement ends up with lower abundance at steady state. Taking the ratio of steady state abundances between the two species we have:

$$\frac{\hat{N}_1}{\hat{N}_2} = (\frac{\theta_1}{\theta_2})^{\frac{1}{D_r - 1}} \tag{2.28}$$

In other words, when $\frac{\theta_1}{\theta_2}$ is constant, the bigger the D_r, the more different the steady state abundances are. When $D_r = 1$ and $\theta_1 \neq \theta_2$, the steady state is complete exclusion of one species ($\hat{N}_1/\hat{N}_2 = 0$ or ∞) as was discussed in Section 2.3.1. On the other hand, holding D_r constant, the abundance distribution at steady state is solely determined by the relative resource requirement θ_1/θ_2. Specifically when $D_r = 0$, Eq. 2.27 indicates that $N_i \propto \theta_i^{-1}$, the implication of which will be discussed later in the next section.

Two-species population dynamics

In this section, the two-species population dynamics under the zero-sum resource constraint is examined by numerically solving the determining equations and updating species abundances through time:

$$N_{i,t+1} = N_{i,t}(1 + g_{i,t}) \tag{2.29}$$

Results are shown in Fig. 2.4. We can see from each graph that given θ_i, the higher the D_r, the more different the steady state abundances between the species, as is suggested by the analytical solution in Section 2.3.3. When $D_r = 1$, our result is consistent with the inference in Section 2.3.1: when resource requirements are equal between the species (Fig. 2.4a), $D_r = 1$ is corresponding to a neutral equilibrium; when resource requirements are not equal (Fig. 2.4b and c), $D_r = 1$ results in the species with higher θ_i to exclude the other. What's more, from the dynamics we can see that the closer the resource requirements between the species (Fig. 2.4c compared to Fig. 2.4b), the longer it takes for exclusion to happen. In spite of that, exclusion is definite eventually as long as $D_r = 1$ and $\theta_1 \neq \theta_2$.

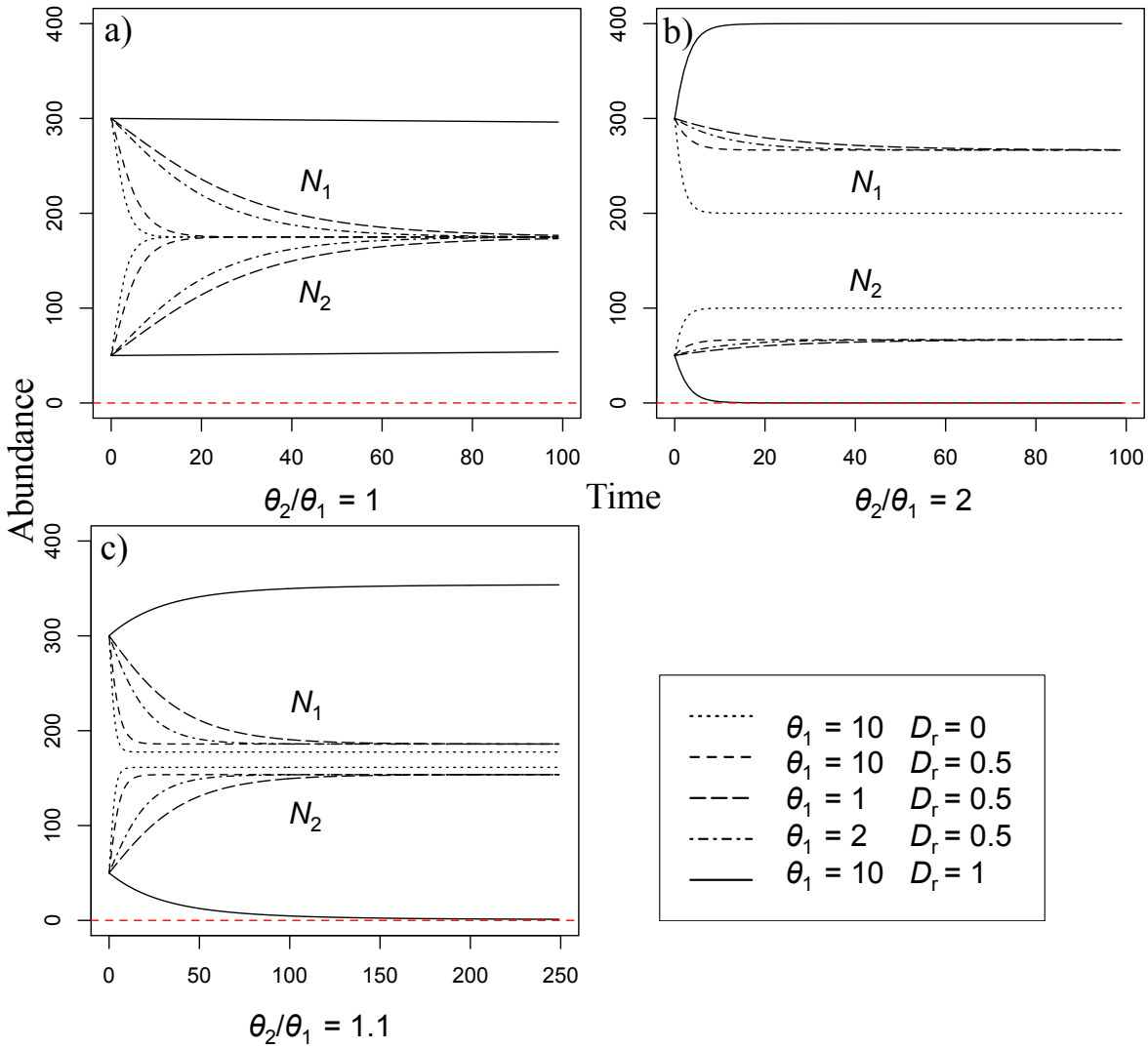

Figure 2.4: Population dynamics through time predicted by maximizing resource allocation entropy between two species.
N_1 and N_2 are the abundances for species 1 and species 2, respectively. At time t=0, $N_1 = 300, N_2 = 50$. D_r is the relative individual distinguishability. Predictions for dynamic variation in abundances for both species are compared for different relative values between θ_1 and θ_2 across the graphs (a, b and c), and within each graph, among different combinations of the absolute values of θ_1 and θ_2 and D_r (represented by different line types).

Compared across graphs, for the same $D_r < 1$, the more different the resource requirements (θ_1 and θ_2), the more different the steady state abundances between the two species, as is also suggested by the analytical solution to the steady state. Specifically when $\theta_1 = \theta_2$, except for the case where $D_r = 1$ which leads to a neutral equilibrium, the two species always end up with the same abundance at steady state. Another implication of the analytical solution is that, when D_r is held constant, the steady state is solely determined by the ratio θ_1/θ_2, which is also demonstrated in Fig. 2.4. In addition, the graph shows that with this ratio held constant, while steady state abundances are the same, it takes longer time for steady state to be reached when θ_1 and θ_2 are both smaller.

2.4 Discussion

In this paper a new theory is established to understand factors affecting the form of the population growth function that leads to various competition outcomes. It reveals the conditions for competitive exclusion or coexistence to happen. Most prominently, we have shown that relative individual distinguishability is a key parameter governing coexistence; a smaller value indicates a higher chance of coexistence. Based on the current results, some important inferences and insights for future studies are discussed in the below.

Species resource requirement and energy equivalence rule (EER)

While the absolute values of the species resource requirements θ_1 and θ_2 do not affect the steady state abundances which only depend on the relative resource requirement θ_1/θ_2, they do affect the time to reach steady state. As discussed when introducing the parameters, the absolute values of θ_1 and θ_2 are determined by the ratio of the amount an individual needs to survive to the size of a resource unit. Our result shows that all else equal, the bigger the resource unit and therefore the smaller the absolute values of θ_1 and θ_2, the longer it takes for steady state to be reached.

In the current framework we have assumed θ_i to be independent of D_r, and that θ_i is the same for all individuals of species i. The alternatives, i.e. D_r is correlated with θ_i and θ_i varies within the species, are worth future examination. Intuitively, the species resource requirement θ can be related to metabolic rate, based on which the implication of our results for the metabolic energy distribution can be examined. Specifically, when $D_r = 0$, $N_i \propto \theta_i^{-1}$, and if we take θ_i as the metabolic rate of species i, Eq. 2.27 is consistent with the energetic equivalence rule (EER, Nee *et al.* 1991), which states that the total metabolic rate is the same across all species in the community. Within the theoretical framework introduced here, the energetic equivalence rule should hold only when conspecific individuals can be treated as identical compared to heterospecific individuals ($D_r = 0$); deviations from $D_r = 0$ could explain the widely observed violations of the energetic equivalence rule (White *et al.* 2007a; Blackburn & Gaston 1994; Marquet *et al.* 1995b).

Notice that we have assumed D_r to be the same for both species but the alternative, i.e. D_r is different between the species, could also be easily explored under this framework, in which case both the relative and the absolute values of θ_1 and θ_2 could potentially affect the steady state. Fig. 2.2 presents one way to measure D_r under both assumptions. Choosing between them, however, requires better understanding of what D_r really means ecologically.

Relative individual distinguishability: Challenges and promises

The distinguishability of conspecific individuals is not a new concept in ecology and has been discussed in the context of species level spatial abundance distributions (Young & Willson 1987b; Harte 2011b), where different levels of distinguishability lead to different distribution patterns. In the context of species coexistence, the effect of social factors, i.e. interactions among conspecific individuals, have been discussed in contrast to niche difference among the species (Chesson 1991; McPeek 2012). So far, however, distinguishability has only been treated as a binary value (distinguishable vs indistinguishable). Neither the continuous definition nor any method to measure this important attribute has been proposed.

In this paper we only gave one example of an interpretation (Fig. 2.2) of this very important attribute D_r, but we do not want to limit its interpretation. Fig. 2.2 assumes that higher relative individual distinguishability (lower ecological substitutability) can be associated with higher intraspecific compared to interspecific variation in functional traits (and vice versa). The latter is also known as functional overdispersion (Swenson & Enquist 2009), the importance of which is an active topic in plant functional ecology (Albert *et al.* 2010; Auger & Shipley 2013). If the relevant functional trait is related to the type of food source, a high D_r could also indicate more generalists in the community. Based on these interpretations, a series of macroecological inferences follow from our result, which can be used to generate hypotheses for empirical studies:

Hypothesis 1 The species abundance distributions are more skewed in communities where functional overdispersion is prevalent (higher D_r).

Hypothesis 2 Steady state can be reached faster, and thus the system is more resilient, when the community has more specialists (lower D_r).

Combined with the assumption that the species resource requirement θ_i is positively correlated to its metabolic rate and therefore to body size, there are two additional inferences:

Hypothesis 3 The body size distribution is more skewed (or difference in body size results in larger difference in abundance) in a community with more generalists/functional overdispersion (higher D_r).

Hypothesis 4 The system is more resilient for a community where individuals of species are generally bigger (bigger absolute values of θ_i)

Notice that in the last hypothesis, it is assumed that the length of allocation period is independent of body size. Violation of this assumption (e.g. a positive relationship between body size and population growth period) might confound the result.

Many other hypotheses can be similarly made from the trait-focused point of view illustrated in the above. Alternatively, the ecological substitutability of conspecific individuals

can be obtained from measures of the population structure, based on the assumption that individuals from the same "subgroup" (e.g. a local population in a metapopulation structure, a certain age group) are more substitutable for each other compared to those outside the subgroup. Under this interpretation, D_r can be measured by the level of intraspecific subgrouping: the more distinct subgroups there are within the species, the less substitutable two random conspecific individuals and thus the higher the D_r. Finally, since within-species variation is also related to evolutionary potential (Lewontin 1974), the interplay between evolutionary mechanisms and species competition could also be studied with this framework.

Comparison with previous theories

Instead of including specific equalizing or stabilizing mechanisms, our theory predicts species interactions from two species attributes, θ and D_r, which are the biological constraints for the stochastic process of the theory and assumed to be fixed for the time being considered. Although this does not affect the formula or predictions, we believe that the mechanism-based explanation of this theory lies in the interpretation of these attributes, which we have made some first attempts in the above two sections. In particular, closer values of θ between species has an effect similar to that obtained from an equalizing mechanism in models describing species interaction (by imposing a similar maximal abundance R/θ_i between the species), while a smaller D_r has an effect similar to that obtained by including a stabilizing mechanism (by causing faster convergence to the steady state). Although the actual values of these attributes are probably the outcome of a series of evolutionary and biophysical mechanisms and have to be empirically determined (guidelines have been given in previous sections), our theory has revealed that species coexistence is the general outcome for most cases ($D_r < 1$), providing a new approach to the long standing conundrum of why species coexistence is possible.

Unlike many models involving spatial or temporal fluctuations (Chesson 2000; Barabás *et al.* 2012), the theory focuses on a zero-sum scenario under fixed resource supply. Under this framework, each species has to have a positive abundance to start with ($N_{i,0} > 0$). However, if we assume a non-zero invasion rate for both species, based on the criterion derived from Kang & Chesson (2010), our model predicts permanent coexistence when $D_r < 1$.

Our theory is more like a null hypothesis (or null theory), with no explicit biological mechanisms incorporated in the resource allocation process. In other words, when our predictions resemble real patterns, it suggests that a stochastic process similar to the one described by this theory is capable of describing the resource allocation process and the associated population dynamics. Similarly, deviations from our predictions suggest the need to incorporate explicit biological mechanisms in describing these dynamics. This, however, does not mean that there is no biology/ecology in this theory. The biology/ecology of this theory lies implicitly in the species attributes: θ (related body size) and D_r (related to functional variation), the determinant parameters for the stochastic process discussed here. The evolutionary and

biophysical mechanisms and constraints influencing these attributes are not the focus of this theory.

Although the key process of the theory is based on a statistical principle (maximum entropy), our result has highlighted the effect of a biological constraint that has previously been neglected: the relative individual distinguishability D_r, which we have suggested could be related to functional variation of the species. In this interpretation, species coexistence might be more governed by internal biological constraints than previously thought. Combining our theory with the theories focusing more on external, abiotic factors (Levin 1970; Armstrong & McGehee 1980; Chesson 2000; Barabás *et al.* 2012), we might ultimately be able to resolve the species coexistence problem combining mechanisms from a spectrum of spatial, ecological and temporal scales.

Future extensions

There are many potential future extensions to this model. To summarize in a most general way, first, more species (> 2) can readily be included, the implication for community structure and species abundance distribution be examined. Second, more than one resource could be incorporated, which might significantly change the model behavior. Third, other types of interaction can be incorporated. For example, instead of allocating resource among two species, individuals of one species could be allocated among another to predict predator-prey interactions. Combining all three directions, the theory can be used to predict the network structure of food web. Finally, by examining the roles of relative individual distinguishability in both processes, insight into the relationship between evolution and competition might be possible with this theory.

The mathematical forms of population growth functions and species interactions vary from species to species in a poorly understood manner, making it hard to make general predictions for species coexistence. In this paper, we started with only a simple rule of maximizing the Boltzmann entropy (number of microstates) for a resource allocation process and predicted a variety of population dynamics and steady state patterns, from which general inferences about conditions leading to species coexistence can be made. Relative individual distinguishability has been highlighted as an important attribute governing species interactions. Our work reveals a promising approach to utilizing fundamental principles of statistics to explain the structure and dynamics of important patterns in ecology.

Appendix: Derivation for the relationship between g_i, N_i and r_i (Eqs. 2.24 -2.25)

Substituting Eq. 2.23 into Eqs. 2.15 - 2.16 then taking Eq. 2.15 - Eq. 2.16, we have

$$2\theta_i(1-D_r)\log[\theta_i(N_i+B_i-D_i)]+\log(r_i)+D_r\log 2\theta_i!+2\lambda\theta_i=0 \tag{2.30}$$

From which we can solve for $N_i + B_i - D_i$, which is also $N_i(1 + g_i)$ based on the definition of g_i (Eq. 2.22):

$$N_i(1 + g_i) = N_i + B_i - D_i = \frac{2}{e}(C'\theta_i r_i^{\frac{1}{2\theta_i}})^{\frac{1}{D_{r,i}-1}} \tag{2.31}$$

Where $C' = 2e^{\lambda-1}$. Combining Eqs. 2.22 and 2.23 we have

$$B_i = \frac{N_i g_i r_i}{r_i - 1} \tag{2.32}$$

$$D_i = \frac{N_i g_i}{r_i - 1} \tag{2.33}$$

Substituting 2.32 and 2.33 back into Eq. 2.15:

$$2\theta_i(1 - D_r)\log[\theta_i N_i(1 + g_i)] + \log\frac{\frac{N_i g_i r_i}{r_i - 1}}{N_i(1 + g_i) - N_i g_i \frac{2r_i}{r_i - 1}} + D_r \log\frac{(2\theta_i)!}{\theta_i!} + \lambda\theta_i = 0 \tag{2.34}$$

Combining A.31 and A.34 we can solve for N_i and g_i separately as functions of r_i, θ_i, D_r and C', as is shown in Eqs. 2.24 - 2.25.

Chapter 3

Modifications for more realistic dynamics: beyond the zero-sum scenario

Abstract

In this chapter, modifications are made to the assumptions of the model in Chapter 2 so that community dynamics can be modeled without the zero-sum constraint for a community with any number of species. Using the same fundamental approach (maximizing resource allocation entropy), this second model gives a number of predictions in addition to those of the first model; it predicts the shape of the within-species resource distribution, thereby revealing the factors influencing population genetic variation. It also predicts a non-trivial population growth pattern for a single species community, which can be compared with the logistic growth equation, and multiple competitor dynamics, which can be compared with the Lotka-Volterra equations. A life span-body size relationship also emerges from this model with one extra assumption about individual selfishness. In addition to supporting most of the conclusions in Chapter 2, the results in this chapter reveal a number of paths linking evolution and ecology.

3.1 Introduction

To begin, we elaborate on a few assumptions of the first model, and then introduce modifications that will lead to a second, more realistic model.

Clarification on assumptions

I. The resource being allocated is constant through time, and is the only essential resource for any individual of the community to survive and to reproduce.

Naturally there can be more than one resource that are essential to survival and reproduction. The resource in our model can be thought of as the most limiting prerequisite for survival and reproduction (e.g. water for a community prone to drought). Of course this does not apply to ecosystems where there are multiple limiting conditions that drive the community dynamics, in which case it may be necessary to include more than one resource types in the model. Such modification is technically simple especially if the multiple resources can be assumed to be independent (in which case the number of microstates can simply be multiplied across resource types to get the total number of microstates). In this chapter we will not explore this direction in depth.

II. Both resource allocation and population growth are discrete in time and happen simultaneously for all species. This means that the time interval for resource allocation is equal to that for population growth. Population growth instantly and fully reflects the result of resource allocation. More specifically, all offspring generated from the last time interval become adults ready for reproduction at the beginning of the next. Therefore in the following we will use "reproductive interval" exchangeably with resource allocation period.

III. The amount of resource required for an adult individual to survive is the same as that for a newborn of the same species to be born and survive through one reproductive interval. This is because the resource requirement parameter θ is defined in such a way that an individual needs θ resource units to survive and another θ to give birth to an offspring (and therefore 2θ to survive and reproduce). In Chapter 2 we have argued that this is an approximation ignoring ontogenetic growth (newborns instantly become adults). Here we want to provide two alternative perspectives that may help justify this assumption. First, since the reproductive interval is defined as the time between birth and adulthood, the additional θ the individual needs to give birth to an offspring that will survive till the end of the current reproductive interval (otherwise there is no reason to count it) actually includes expenses for both the reproductive activities before the offspring is born, and survival of the newborn till it reaches adulthood. By this argument, if we assume ontogenetic growth to be linear with respect to time, the resource a newborn takes to survive should be half of that for its adult parent in one reproductive interval. Adding the cost for reproductive activities to the former, we can assume that the two should be comparable. Second, for each reproductive interval between its birth and death, it has to take exactly the same amount of resource an adult takes to survive. Therefore if we ignore the short-term fluctuations and focus on the general trend through time, survival requirement should be roughly the same as reproduction requirement, and the latter should be defined as "the average amount of resource required in one reproductive interval to produce an individual that will survive more than one reproductive intervals". In reality there are surely newborns that cannot survive till adulthood but still consumes a certain amount of resource. In our models we are assuming that the resource these individuals take is either negligible, or can be instantly recycled for use by other individuals.

IV. Between-species resource allocation matters as much as demographic grouping, while within-species resource allocation matters as much or less than the

former two. In calculating the total number of microstates, the weight for between-species resource allocation (ways to put resource units into different species) and that for demographic grouping (ways to put individuals into death, survival, birth groups) are assumed to be the same. On the other hand, the weight for within-species resource allocation (ways to put resource units into different individuals of the same species) can be smaller than the former two when its exponent $D_r < 1$. This might sound very arbitrary, yet it does reflect prevailing notions in ecology: species identity matters; demographic rates (birth and death) matter; individual identity, however, might not matter as much. In Chapter 4 this particular assumption will be further explored to reveal how important it is to our predictions.

We understand that none of our assumptions are flawless. We are applying them just to initiate this new approach that could potentially provide a valuable insight approach to ecological theory. These assumptions can all be modified and are not essential to the theory. In Chapter 4 we will describe a more thorough roadmap to future modifications and tests of the theory. Here in this chapter, we want to focus on a few modifications that can be done comparatively easily and as will be shown later, add greatly to the number of testable predictions.

Modifications

I. Species specific D_r (for any number of species). In Chapter 2 we have used a common relative individual distinguishability D_r for a two-species community. It was mentioned in the discussion that this can be easily modified so that the model applies to multiple (> 2) species, using a different D_r for each species. That will be done in this chapter. Although potentially variable across species, the interpretation for D_r is the same as before. At one extreme, if species i has $D_{r,i} = 1$, it means each of its individuals is as important as a distinct species in resource allocation. If, at the other extreme, it has $D_{r,i} = 0$, it means that the number and identity of its individuals do not matter and they should always be considered as one whole in resource allocation.

Having species-specific $D_{r,i}$ values does not change the predictions of the first model that we have looked at in Chapter 2: it can be easily shown that wherever D_r shows up in the equations, it can be replaced by the species specific $D_{r,i}$. In some of the following analyses, we will still use a common D_r for all species. However, it is important to notice is that this is not a constraint and D_r by definition can vary from species to species. This is of crucial importance in understanding the interpretation of D_r which will be discussed in more depth later in Chapter 4.

II. Removing the resource constraint. In nature, due to perturbations (e.g. fire, hurricane), a community sometimes is pushed down to a very small size when each species only has a few individuals. In such a case, the total resource use of the community is far less than what the environment provides, and it takes time for the community to grow to the carrying capacity. Because of the constant resource constraint, the first model in Chapter 2 is not able to deal with such a scenario. Besides, it is not realistic to state that the resource can always be exhaustively used: there has to be some portion that is left unused by any

species, either by mere chance or because the community is not always big enough to use all the resource. Therefore, in the modified model that will be introduced in this chapter we eliminate the constant resource constraint but instead let the same procedure of maximum entropy tell us how much resource the community should use given its current size and all the species attributes.

III. Including intrinsic growth rate. The first model assumed the maximum number of offspring in one resource allocation period for each species to be one (so the maximum number resource units an individual gets is $2\theta_i$). In reality, fecundity varies from species to species and in some cases, an adult can give birth to up to thousands of offspring in one reproductive interval. To account for this effect, we are introducing a new species attribute, the intrinsic growth rate r_i, which is the maximum number of offspring an individual can have in one reproductive interval. (We have defined a variable $r_i = \frac{B_i}{D_i}$ in Chapter 2 which will not be used again. Whenever r_i appears later in Chapter 3 and 4, it represents the intrinsic growth rate.) An individual of species i can get any number of resource units between 0 and $(r_i + 1)\theta_i$, the actual distribution of which is determined by the procedure of maximizing resource allocation entropy and depends on the resource availability R_0, the current abundances N_i and all the species attribute parameters (θ_i, D_r, i, r_i) in the community.

The values of r_i determine how fast the community reaches its steady state after perturbation: when the values are bigger, it takes a shorter time since the "steps" each species can take are bigger. Due to other constraints that are not related to resource availability, species cannot grow at an infinite speed even if the resource is infinite, and so r_i cannot be infinite. Previous studies have revealed that r_i is in negative relationship with body size (Fenchel 1974), which will be incorporated in our analyses.

Although another species attribute parameter, r_i, has been introduced, but including r_i actually does not add much complication to the predictions. As will be shown here, it has a minor effect on the steady state predictions. The most important conclusions from our model regarding species coexistence and abundance distribution hold regardless of the values of r_i, whether they are big or small, same or variable across species. This by itself is an interesting revelation: maximal fecundity of species do not significantly affect the community structure at steady state.

IV. Allocation between parent and offspring. In the first model in Chapter 2, we assumed that the individual always acquire resource units with priority (choosing itself over one of its offspring to survive). This is the case where death is minimized and purely determined by resource availability. Here we relax this assumption: while net growth can be determined from the number of resource units allocated to the individual, the actual number of birth or death is not. For example, when an individual gets $2\theta_i$ resource units, it can either die and leave two offspring to survive, or survive and only leave one offspring to survive. The birth and death rates for the former case are both higher. Without further assumptions, our theory is not able to tell these two cases apart. This does not matter if we are only interested in the overall population dynamics and the steady state, for which we only need to know the net growth of all species. It is only when we want to know specifically about birth and death rules that we need to differentiate one case from another. This question will be addressed

Table 3.1: Resource allocation outcome for an individual of species i

# resource units	Outcome
0	net population growth = -1 (0 birth, 1 death)
θ_i	net population growth = 0 (1 birth, 1 death or 0 birth, 0 death)
$2\theta_i$	net population growth = 1 (2 birth, 1 death or 1 birth, 0 death)
$3\theta_i$	net population growth = 2 (3 birth, 1 death or 2 birth, 0 death)
$\vdots$	$\vdots$
$(r_i+1)\theta_i$	net population growth $=r_i$ (r_i+1 birth, 1 death or r_i birth, 0 death)

again later in the analysis. Before that we will just leave it as an open option (Table. 3.1).

Based on the above, we now have a new demographic outcome table, as shown in Table 3.1.

3.2 Method: a modified model for resource allocation

Macrostate: $N_{i,k}$

With the new demographic outcome table (Table. 3.1), the macrostate variable becomes $N_{i,k}$. It denotes the number of individuals in the k_{th} demographic group, i.e. those that get $k\theta_i$ resource units and generate $k-1$ net growth (row $k+1$ in Table. 3.1). The previous macrostate variable B_i and D_i are simply $N_{i,2}$ and $N_{i,0}$ under the special case $r_i = 1$ for all i. For each species i, we have r_i+1 independent macrostate variables $N_{i,k}$ (k from 1 to r_i+1; $N_{i,0}$ can be calculated from $N_i - \sum_{k=1}^{r_i+1} N_{i,k}$).

Expressing and maximizing number of microstates

While the definition of a microstate is the same as in the first model (a particular resource unit - species - individual permutation), the space for possible microstates has been expanded with the relaxation of the resource constraint and the introduction of r_i. In the following we will derive a new equation for the number of microstates W_{total} of a given macrostate $N_{i,k}$ (for all i from 1 to S_0, and for each i, k from 0 to r_i+1). Also in the equations are R_0, the current abundances N_i and the species attributes θ_i, $D_{r,i}$ and r_i.

The general equation for W_{total} is very similar to the previous model (with W_{across} in place of $W_{between}$ since there can be more than two species):

$$W_{total} = W_{across} \times \prod_{i}^{S_0} W_{grouping,i} W_{within,i}^{D_{r,i}} \tag{3.1}$$

Where

$$W_{across} = \frac{R_0!}{\prod_i^{S_0} R_i! R_n!} \tag{3.2}$$

Notice that without the resource constraint, we have an extra box in addition to the species boxes at the cross species allocation step: the null box, the size of which $R_n = R_0 - \sum_i^{S_0} R_i$ determines how many resource units are not allocated to any species. In Chapter 2 we have constrained this box to be empty. Now we can derive the size of it by maximizing the number of microstates in the expanded microstate space. Since there are no individuals in the null box, it does not have a corresponding $W_{within,i}$ like the species boxes.

$$W_{within,i} = \frac{R_i!}{\prod_{k=1}^{r_i+1} (k\theta_i)!^{N_{i,k}}} \tag{3.3}$$

R_i, the total amount of resource allocated to species i, can be calculated by:

$$R_i = \sum_{i}^{S_0} N_{i,k} k\theta_i \tag{3.4}$$

$W_{grouping,i}$ counts the number ways to allocate N_i individuals into different demographic groups.

$$W_{grouping,i} = \frac{N_i!}{\prod_{k=0}^{r_i+1} N_{i,k}!} \tag{3.5}$$

As is mentioned earlier, although k can take $r_i + 2$ different values (0 to $r_i + 1$), for each species i we only have $r_i + 1$ independent $N_{i,k}$ since the last one can be obtained from subtracting the sum of the rest from N_i. Here we are using $N_{i,k}$ where $k = 1, 2, ..., r_i + 1$ as the independent macrostate variables to solve for, and replace $N_{i,0}$ by $N_i - \sum_{k=1}^{r_i+1} N_{i,k}$. log transform W_{total} we get:

$$\begin{aligned} \log W_{total} = \log R_0! - \log (R_0 - \sum_{i}^{S_0} R_i)! + \sum_{i}^{S_0} [(D_{r,i} - 1) \log R_i! \\ - D_{r,i} \sum_{k=1}^{r_i+1} N_{i,k} \log (k\theta_i)! + \log N_i! - \sum_{k=1}^{r_i+1} \log N_{i,k}! - \log (N_i - \sum_{k=1}^{r_i+1} N_{i,k})!] \end{aligned} \tag{3.6}$$

Next we maximize W_{total} by taking the partial derivative of $\log W_{total}$ over $N_{i,k}$ ($k = 1, 2, ..., r_i + 1$) and making it equal to 0:

$$\frac{\partial \log W_{total}}{\partial N_{i,k}} = k\theta_i \log\,(R_0 - \sum_i^{S_0}\sum_{k=1}^{r_i+1} N_{i,k}k\theta_i) + k\theta_i(D_{r,i}-1)\log\,(\sum_{k=1}^{r_i+1} N_{i,k}k\theta_i) \\ -D_{r,i}k\theta_i(\log\,k\theta_i - 1) - \log\,N_{i,k} + \log\,(N_i - \sum_{k=1}^{r_i+1} N_{i,k}) = 0 \tag{3.7}$$

The $\sum_i^{S_0}(r_i+1)$ (r_i+1 for each species) simultaneous equations in the form of Eq. 3.7 are the determining equations from which the macrostate variables $N_{i,k}$ ($k = 1, 2, ..., r_i+1$) can be solved:

$$N_{i,k} = (N_i - \sum_{k=1}^{r_i+1} N_{i,k})[\frac{R_i^{D_{r,i}-1}R_n}{(\frac{k\theta_i}{e})^{D_{r,i}}}]^{k\theta_i} \\ => N_{i,k} = N_i \frac{[\frac{R_i^{D_{r,i}-1}R_n}{(\frac{k\theta_i}{e})^{D_{r,i}}}]^{k\theta_i}}{\sum_{k=1}^{r_i+1}[\frac{R_i^{D_{r,i}-1}R_n}{(\frac{k\theta_i}{e})^{D_{r,i}}}]^{k\theta_i} + 1} \tag{3.8}$$

e is the Euler's number.

Solving for *per capita* net growth rate

Here we use g_i to denote the average *per capita* net growth of species i in one allocation period. By definition

$$g_i(t) = \frac{N_i(t+1) - N_i(t)}{N_i(t)} = \frac{\frac{R_i(t)}{\theta_i} - N_i(t)}{N_i(t)} \tag{3.9}$$

The t in parenthesis indicates that the value is for the t_{th} time interval. g_i is the realized growth of the species and $g_i \leq r_i$. $g_i = r_i$ only happens when resource is in the infinite limit or the current abundances are much lower than the steady state values.

Suppressing t from the subscript and substitute Eq. 3.4 into Eq. 3.9 we get

$$g_i = \frac{\sum_{k=0}^{r_i+1}(k-1)N_{i,k}}{\sum_{k=0}^{r_i+1} N_{i,k}} \tag{3.10}$$

Notice that k starts from 0 in the subscript. Substituting Eq. 3.8 into Eq. 3.10 we get

$$g_i = \frac{\sum_{k=1}^{r_i+1}(k-1)[\frac{R_i^{D_{r,i}-1}R_n}{(\frac{k\theta_i}{e})^{D_{r,i}}}]^{k\theta_i} - 1}{\sum_{k=1}^{r_i+1}[\frac{R_i^{D_{r,i}-1}R_n}{(\frac{k\theta_i}{e})^{D_{r,i}}}]^{k\theta_i} + 1} \tag{3.11}$$

In Eq. 3.11, $R_i = \theta_i N_i(g_i + 1)$ and $R_n = R_0 - \sum_i^{S_0} R_i$ so the only unknown is g_i, which can be solved from S_0 simultaneous equations in the same form.

When $D_{r,i} = 1$

In Chapter 2 we have specifically looked at the case where $D_r = 1$. Here if we substitute $D_{r,i} = 1$ into Eq. 3.11 we get

$$g_i = \frac{\sum_{k=1}^{r_i+1}(k-1)(\frac{eR_n}{k\theta_i})^{k\theta_i} - 1}{\sum_{k=1}^{r_i+1}(\frac{eR_n}{k\theta_i})^{k\theta_i} + 1} \tag{3.12}$$

In Eq. 3.12, R_i does not appear as an independent term (but only in $R_n = R_0 - \sum_i^{S_0} R_i$). First, it means that when θ_i and r_i are both the same for all i, g_i should also be the same regardless of the current R_i for each species. Specifically, the steady state can be any R_i combination that gives an $R_n = R_0 - \sum_i^{S_0} R_i$ that satisfies $g_i = 0$ in Eq. 3.12. This is consistent with our prediction from the first model: when $D_r = 1$ and $\theta_1 = \theta_2$, the community has a neutral steady state.

Second, Eq. 3.12 shows that when $D_r = 1$, net growth rate g_i is independent of N_i and always a negative function of θ_i. This means that when resource limit is reached and therefore species cannot all have positive growth rates, those with bigger θ will have negative growth rates and eventually be excluded. Another way to look at this is that, the dependence of g_i on its own abundance, i.e. conspecific density dependence, is the same as its dependence on abundance of any other species, i.e. heterospecific density dependence. This property tends to enlarge the resource imbalance among species: if the abundance of one species increases, its population growth is not affected more than other species. In other words, there is no feedback to offset the initial increase. In our model, this means the system is prone to competitive exclusion.

Solving for steady state (when $D_{r,i} \neq 1$)

At steady state $\hat{g}_i = 0$ for all i, and $\hat{R}_i = \hat{N}_i\theta_i$. Substituting these into Eq. 3.11 we get

$$\sum_{k=1}^{r_i+1}(k-1)[\frac{(\hat{N}_i\theta_i)^{D_{r,i}-1}(R_0 - \sum_i^{S_0}\hat{N}_i\theta_i)}{(\frac{k\theta_i}{e})^{D_{r,i}}}]^{k\theta_i} = 1 \tag{3.13}$$

The only unknown is $\hat{N}_i$, which can be solved from S_0 simultaneous equations in the form of Eq. 3.13.

When $r_i = 1$ for all i, Eq. 3.13 is simplified into

$$-1 + [\frac{(\hat{N}_i\theta_i)^{D_{r,i}-1}(R_0 - \sum_i^{S_0}\hat{N}_i\theta_i)}{(\frac{2\theta_i}{e})^{D_{r,i}}}]^{2\theta_i} = 0 \tag{3.14}$$

From which $\hat{N}_i$ can be solved:

$$\hat{N}_i = \frac{2}{e}(C\theta_i)^{\frac{1}{D_{r,i}-1}} \tag{3.15}$$

Where $C = \frac{2}{e\hat{R}_n}$. Eq. 3.15 is in exactly the same form with the steady state solution for the first model in Chapter 2. This suggests that the previous model is very close to a special case for this more general model where r_i is constraint to be 1 for all species.

Under the most general condition (different r_i for each species), the steady state cannot be analytically solved. With θ_i, $D_{r,i}$ and r_i known for all species, we can numerically solve Eq. 3.13 to get the steady state. Fig. 3.1 compares between the first model in Chapter 2 and the modified model in this chapter their predictions for steady state abundances.

Previously in the first model, only the ratio between R_0 and θ_i matters. In other words, the unit by which the resource is measured does not matter, as long as it is consistent for all the θ_i and R_0. However, this is not the case for the modified model. In Fig. 3.1, keeping the ratio between θ_i and R_0 constant, the steady state solutions for the modified model can be different if the absolute value of R_0 is different.

We could see that overall, the steady state abundances predicted by the two models are in positive relationship. With the magnitude of R_0 (and θ_i) increasing, the correlation between the two models' steady state predictions becomes better and eventually almost perfect in the last graph. This means that when the absolute amount of resource is not too small, the analytical equation for steady state (Eq. 3.15) still holds for this model, even if there is an extra parameter (intrinsic growth rates r_i) for each species. The property of Eq. 3.15 has been discussed in detail in Chapter 2.

Fig. 3.1 also shows that, when the absolute magnitude of R_0 is small, the modified model predicts more species with low abundances (dots that are below the solid line) at steady state than the first model. This suggests that when resource is limited, there are more rare species and higher risk for extinction even if all species are proportionately smaller.

In the following section we will look at the predictions of the modified model for 1) within-species resource distribution, 2) single species population growth, 3) multiple competitor dynamics and 4) lifespan-body size relationship.

3.3 Result

Within-species resource distribution

Eq. 3.8 gives $N_{i,k}$ as a function of k. Since $k\theta_i$ is the number of resource units an individual gets in the k_{th} demographic group, $\frac{N_{i,k}}{N_i}$ is the relative frequency that an individual of the species gets $k\theta_i$ resource units. In other words, the shape of the $\frac{N_{i,k}}{N_i}$ vs k curve tells us how resource is distributed within the species.

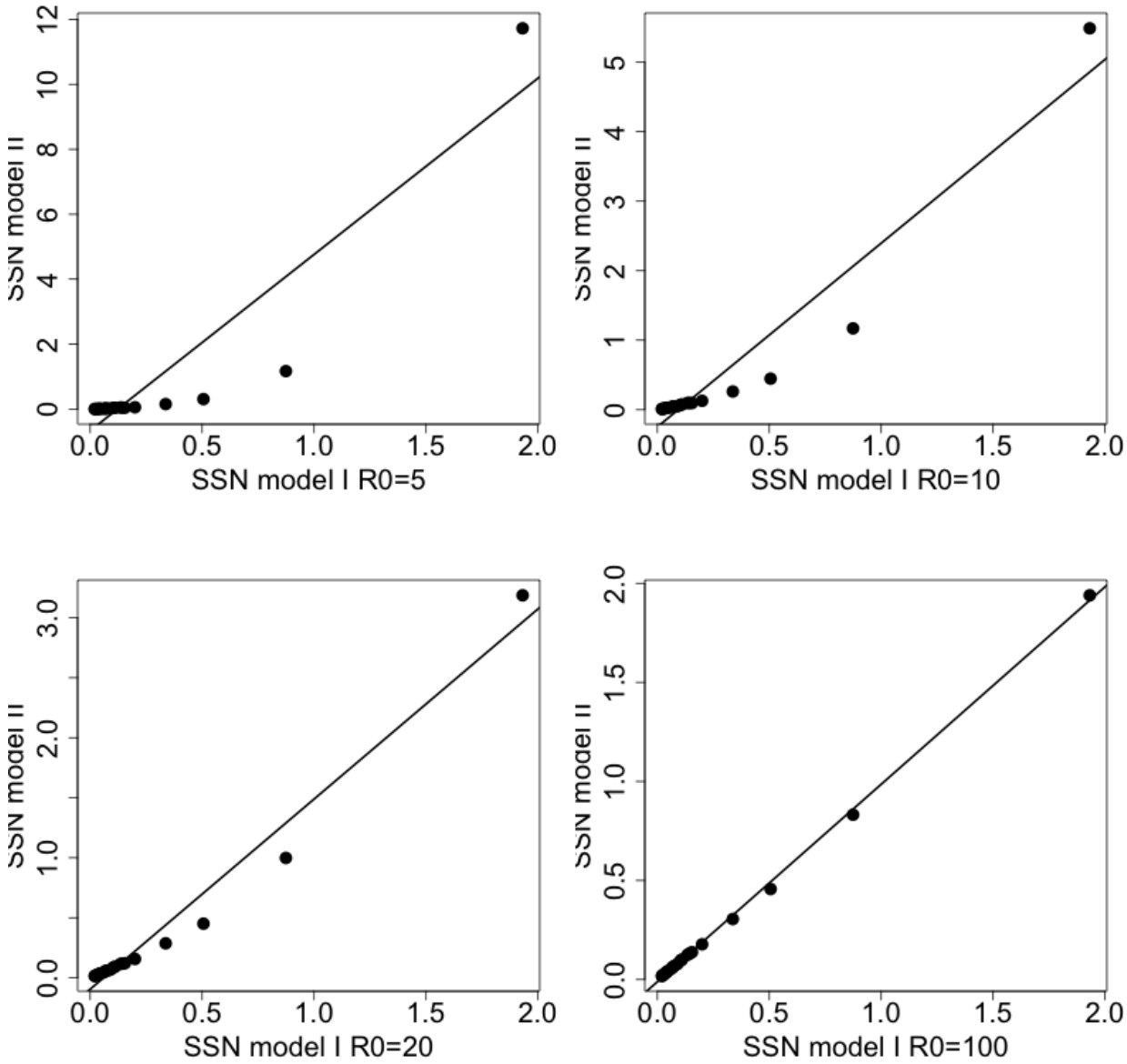

Figure 3.1: Comparing predictions for steady state abundances ($\hat{N}_i$) between the original model in Chapter 2 (X axis) and the modified model (Y axis).
$D_{r,i}$ is uniformly drawn from 0.1 to 0.9, r_i from 1 to 20. For the first graph, θ_i from 1 to 10, $R_0 = 5$. For the other graphs, R_0 and θ_i are both multiplied by a scale factor (2, 4 or 20) so that their relative magnitudes are unchanged. The absolute value of R_0 is shown in the X label. The solid line is a linear fit between X and Y.

In Fig. 3.2 this curve is plotted for the simplest case of single-species community at steady state. When the steady state abundance is controlled, R_0 is determined by θ, r and D_r, which means there are three free parameters. Since there is only one species, i will be suppressed in the notations.

At steady state, the mean of k has to be 1 (g= $\frac{\sum_k (k-1)N_k}{N}$=0 so $\frac{\sum_k kN_k}{N}$=1). However, as Fig. 3.2 shows, the variation of k can be different for different D_r values: when $D_r = 0$, the probability for $k = 0$ (in which case the individual definitely dies) is the highest and decreases as k increases; as D_r increases, the distribution of k becomes more and more peaked around $k = 1$ (in which case either the individual survives with no offspring, or dies with one offspring) and the probability for an individual to get more extreme number of resource units ($k = 0$ or k is big) gets smaller.

We can also see that these variations are more significant at the range where k is much smaller than r. The difference among different D_r diminishes and N_k quickly drops to 0 as k gets bigger. Because of this, the shape of the distribution should not change much if we increase the intrinsic growth rate r ($r + 1$ is the upper limit for k) as is shown in the second row of Fig. 3.2: all else equal, the distribution is the same for $r = 10$ and $r = 20$. From this we can deduce that r is not a very important parameter for the k distribution. Notice that changing $\hat{N}$ does not change the shape of this distribution: all else equal, the same graphs can be obtained from $\hat{N} = 10$ or $\hat{N} = 200$.

Because $k - 1$ is the net growth from any of the N_k individuals that get $k\theta$ resource units, the distribution of k also reflects the distribution of reproductive success: as k gets more and more peaked around $k = 1$, reproductive success gets more and more evenly distributed among individuals while extreme cases (no offspring or a lot of offspring from one individual) become rarer.

The distribution of reproductive success affects the genetic variability of the species: given a background mutation rate, when reproductive success is more evenly distributed or all individuals tend to have the same number of offspring (as when $D_r = 1$ in Fig. 3.2), the genetic variation of the population can steadily increase through time. On the contrary, if reproductive success is unevenly distributed or some individuals tend to have much more offspring than others (as when $D_r = 0$ in Fig. 3.2), the genetic variation of the population increases more slowly or even decreases through time since there are more individuals that are related (offspring of the same individual). Comparing across graphs we can see that this effect is stronger when θ is bigger: when $D_r = 1$, k distribution is more peaked when θ is bigger. These results suggest that, species fitness might be enhanced by large θ and D_r, yielding a more even distribution for reproductive success and higher genetic diversity. More implications will be discussed later in this chapter.

Single species population growth

In the first model in Chapter 2 we compared how *per capita* net growth rate g changes with population size N to reveal the density dependence of population growth in a zero-sum scenario (Fig. 2.3 of Chapter 2). In that scenario, the single species case is trivial because of

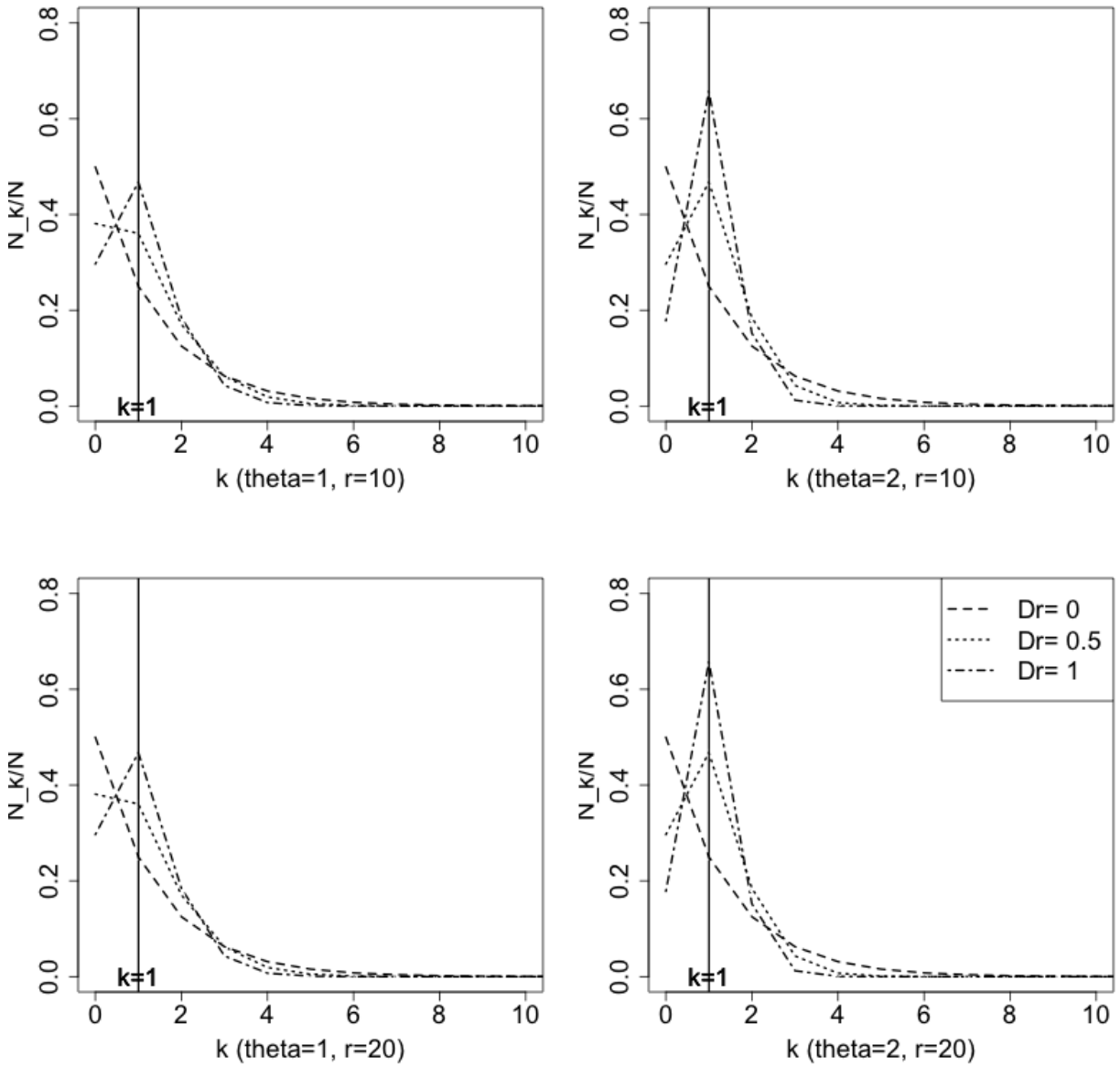

Figure 3.2: Within-species resource distribution for a single species community at steady state ($\hat{N} = 100$).

The Y axis is $\frac{N_k}{\hat{N}}$. The X axis is k. θ is varied between left and right, while r is varied between upper and lower graphs; both are specified in the X label. Within each graph, different line types represent different D_r values (see the legend).

the constant resource constraint: the species has to jump from any initial state to its steady state in one step. Therefore, the first model is not able to predict the gradual increase of population size from a minimal value to the steady state as the logistic growth equation does. This can now be done by the modified model with the zero-sum assumption relaxed and intrinsic growth rate introduced.

Using Eq. 3.11 we can numerically solve for g as a function of all model parameters (R_0, θ, D_r, r) and the current abundance N. To compare our model with the logistic growth equation which has the carrying capacity (equal to the steady state abundance it predicts) as one of its parameters, the steady state abundance $\hat{N}$ will be controlled as a constant. Therefore here we also have three free parameters: θ, D_r and r (R_0 can be obtained by substituting the rest of the parameters into Eq. 3.13).

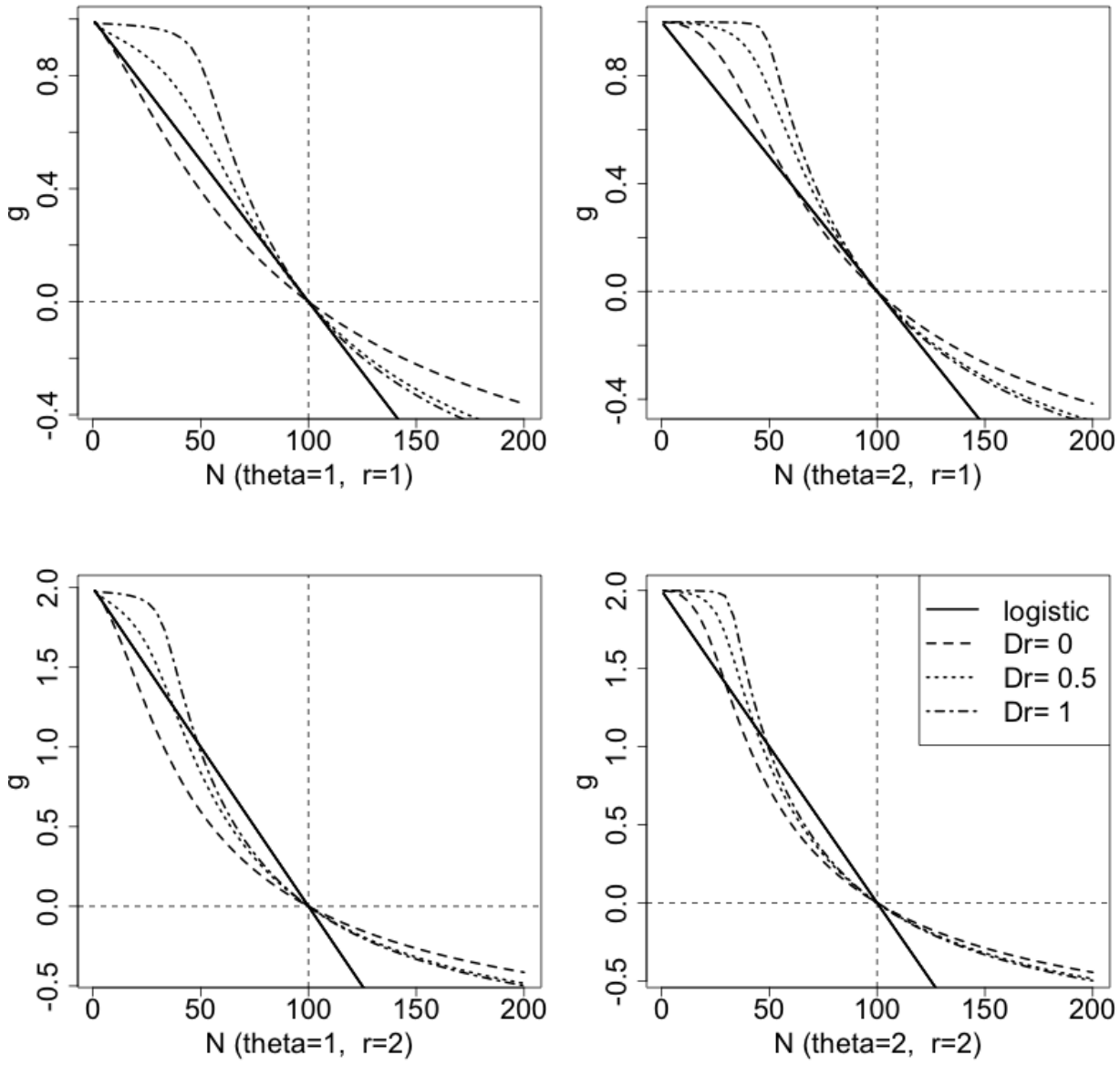

(a) Density dependence of population growth. The horizontal dotted line indicates $g = 0$ the vertical one $N = \hat{N}$.

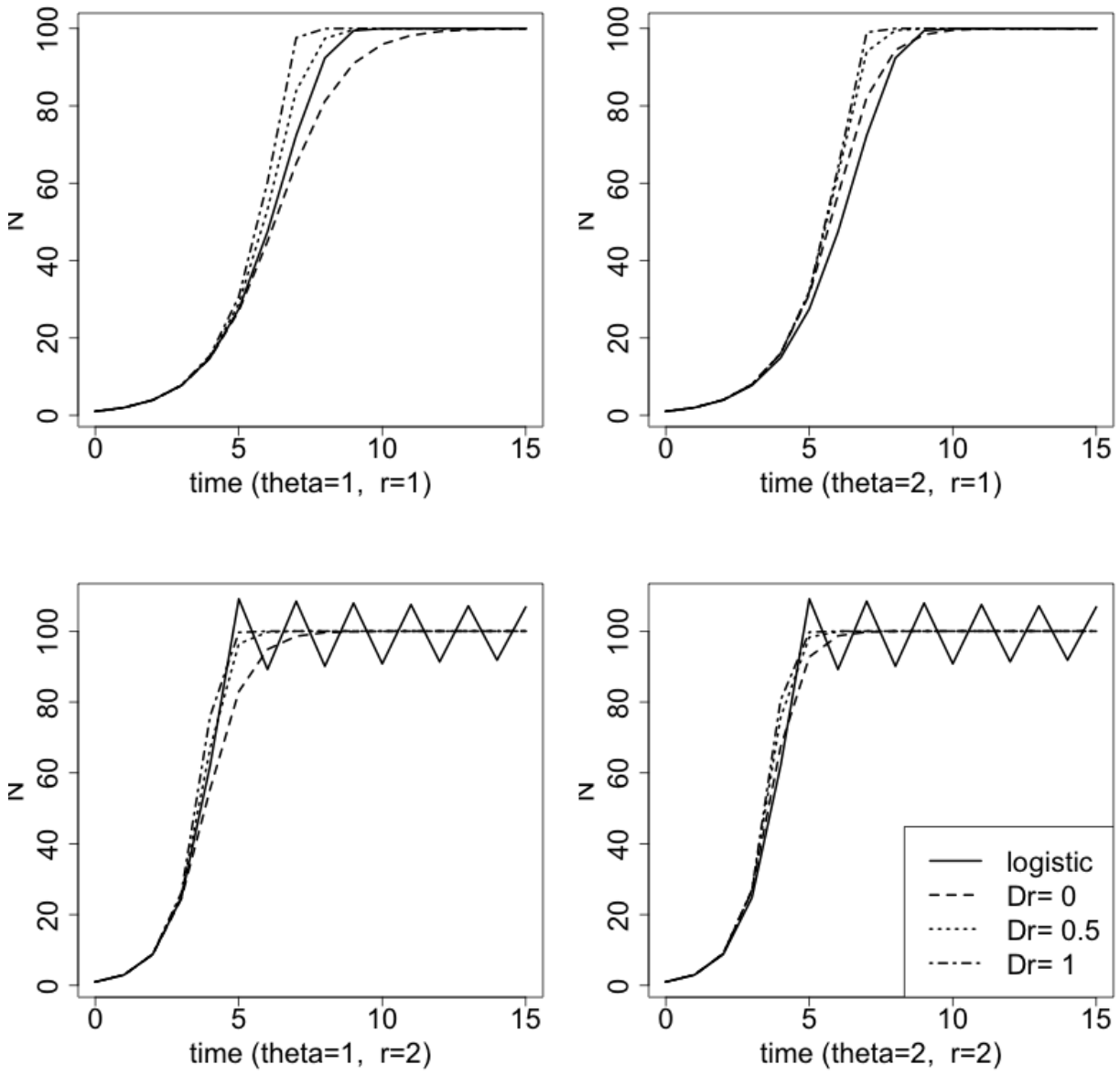

(b) Population dynamic path of the species.

Figure 3.3: Comparing the modified model for a one-species community with the logistic growth equation.

For all graphs $\hat{N} = 100$. θ is varied between left and right while r is varied between upper and lower graphs; both are specified in the X label. Within each graph, different line types represent different D_r values or the logistic growth equation (see the legend).

From Fig. 3.3a we can see that, in the modified model *per capita* net growth rate generally declines with abundance, as is predicted by the logistic growth equation. However, instead of a linear decline like the logistic growth equation predicts, here how fast g decreases with N (i.e. the slope) varies with N: when N is small, g is close to the intrinsic growth rate r and does not decline much with N. As N increases, g starts to decline faster with N, and gets the fastest at a point between 0 and the steady state (the inflection point, where curvature goes from negative to positive). After that point, the decline gets slower with increasing N and keeps that way.

Looking within each graph we can see that, before the steady state is reached, the higher the D_r, the higher the g; after the steady state is reached, however, higher D_r leads to lower g. Therefore all else equal, higher D_r for the species leads to faster convergence to steady state, whether the current abundance is smaller or bigger than the steady state. This means that species with higher D_r have higher resilience: it takes shorter time to resume when the population size is perturbed away from its steady state. This result is the opposite from that of the first model: in the zero-sum scenario, the community is more resilient when D_r is smaller.

Comparing between left and right, when $D_r = 0$, the effect of a bigger θ is similar to that of a bigger D_r given θ. However, the effect is opposite when $D_r = 1$. This suggests that when the species D_r is small, increasing θ increases resilience; when D_r is big, increasing θ decreases resilience. This is also different from the prediction of the first model, where smaller θ always leads to more resilience regardless of the value of D_r.

Comparing between upper and lower graphs, when $r = 2$, the curvature is bigger (i.e. the slope changes faster) with respect to the logistic growth equation: when abundance is small, just like when $r = 1$, g decreases slowly with abundance and is bigger than predicted by the logistic growth equation; as abundance further increases, however, g decreases much faster that it drops below the prediction of the logistic growth equation for all D_r values (this only happens for $D_r = 0$ when $r = 1$). After the intersection with the logistic growth equation, the decrease of g slows down. When abundance approaches the steady state, the decrease of g becomes much slower and again intersects with the logistic growth equation. After that, g stays bigger than the logistic growth equation. This patterns holds for all $r > 1$. In general, when $r > 1$, our model predicts that the population growth to be more "sluggish" than the logistic growth equation around the steady state: slower increase right before the steady state is reached and slower decrease after the steady state is reached. As will be shown in the following, this leads to less fluctuation in population dynamics in our model compared to the logistic growth equation,

In Fig. 3.3a the curves predicted by the modified model are clearly differentiable from the logistic growth equation. In practice, we do not usually compare the pattern of g vs N but instead how abundance changes through time, i.e. N vs t, since that is usually what we directly observe from data and what we want to predict. In Fig. 3.3b, I have plotted the predicted N against time, where time is a discrete variable, i.e. the number of reproductive intervals from the initial point.

From the $r = 1$ case we can also see that, regardless of the obvious differences on the

g vs N plot, all model predictions tend to follow a similar shape to that predicted by the logistic growth equation on the N vs time plot: an S-shaped curve. This suggests that the commonly observed S-shaped population dynamic curve could be the result of many different functions other than the logistic equation (including the ones predicted by our theory), and it is easiest to tell them apart using g vs N plot instead of N vs time plot.

When $r = 2$, one distinct difference is that while there are fluctuations in the prediction by the discrete logistic growth equation, in our model there are not. This is mostly due to our assumptions that 1) the resource constraint has to be satisfied every time resource is allocated and 2) population instantly and fully reflects the resource allocation outcome. This means that the population cannot overshoot since that will violate the resource constraint. Therefore there are no fluctuations in the predicted abundance by our model. Fluctuations will emerge if we relax the above assumptions by either 1) making resource fluctuates or 2) creating a time lag between population growth and resource allocation so the population does not have to meet the resource constraint at all times. Since our model is discrete in time, an interesting revelation here is that there can be more factors complicating the mechanism of population fluctuation in addition to the discreteness or continuity of population growth, which is the most important factor that affects population fluctuation for populations obeying the logistic growth equation (discrete and continuous).

The results of this section inform us that for the one species case, 1) D_r and θ both affect how fast population converges to steady state and therefore the resilience of the population but in different ways from predicted by the first model, 2) actual density dependence of growth can be much more complicated than the logistic growth equation, even if they all generate an S-shaped population dynamic curve, 3) the model does not predict population fluctuations even when $r > 1$, indicating more potential complication than the simple discrete vs continuous-time dichotomy in temporal behavior of populations.

Two competitors population dynamics

To make it easier to compare with the results in Chapter 2, we assume that the two competitors have equal D_r although this model can be applied to multiple (> 3) species each with a different D_r. Also to compare with the competitive Lotka-Volterra equations, we assume that the carrying capacity for each species (the K parameter) is the abundance of the species if all resource at steady state of the community is allocated to it (as in the competitive Lotka-Volterra equations, K is the abundance of the species if no other species exists at steady state).

$$K_i = \frac{\sum_j^{S_0} \theta_j \hat{N}_j}{\theta_i} \tag{3.16}$$

Also since we are only considering exploitative competition (consumption of the resource by one species makes it unavailable to the other), we assume that the α_{ij} parameter of the Lotka-Volterra equations, i.e. the effect of species j on species i, is simply the ratio between

the resource requirements of species j and i, or the number of individuals of species i from which resource will be deprived of if one extra individual of species j survives.

$$\alpha_{ij} = \frac{\theta_j}{\theta_i} \tag{3.17}$$

With K_i and α_{ij} defined within our framework, we can then use the classic form of competitive Lotka-Volterra equations (Gilpin & Ayala 1973):

$$g_i = r_i(1 - \frac{\sum_j^{S_0} \alpha_{ij} N_j}{K_i}) = r_i(1 - \frac{\sum_j^{S_0} \frac{\theta_j}{\theta_i} N_j}{\sum_j^{S_0} \frac{\theta_j}{\theta_i} \hat{N}_j}) \tag{3.18}$$

We can see that g_i is linearly related to N_j (both when $j = i$ and $j \neq i$) and the coefficient is r_i.

With these assumptions clarified, now we can compare our model prediction with that of the Lotka-Volterra equations. First we look at the case where $\theta_1 = \theta_2$.

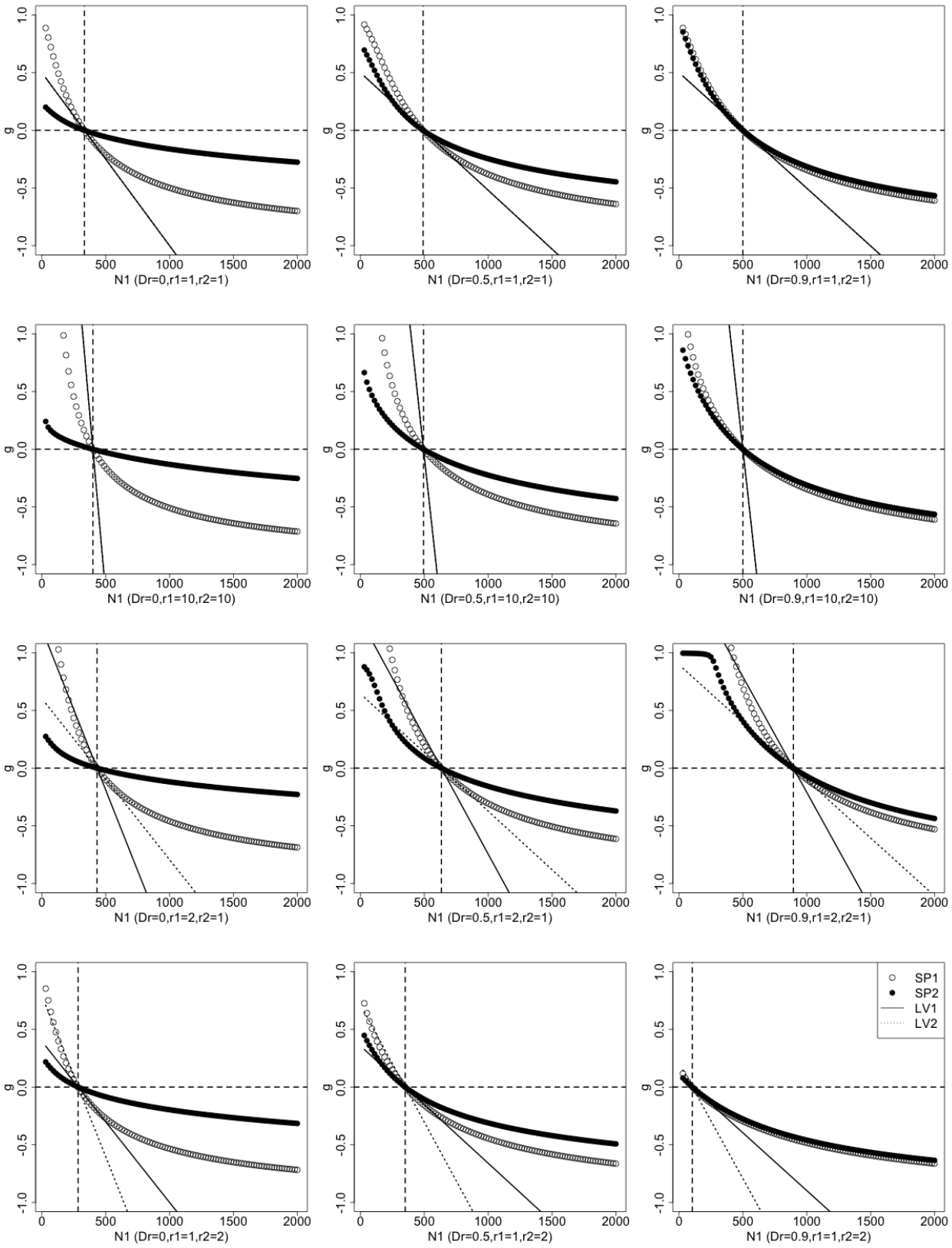

(a) $\theta_1 = \theta_2 = 1$.

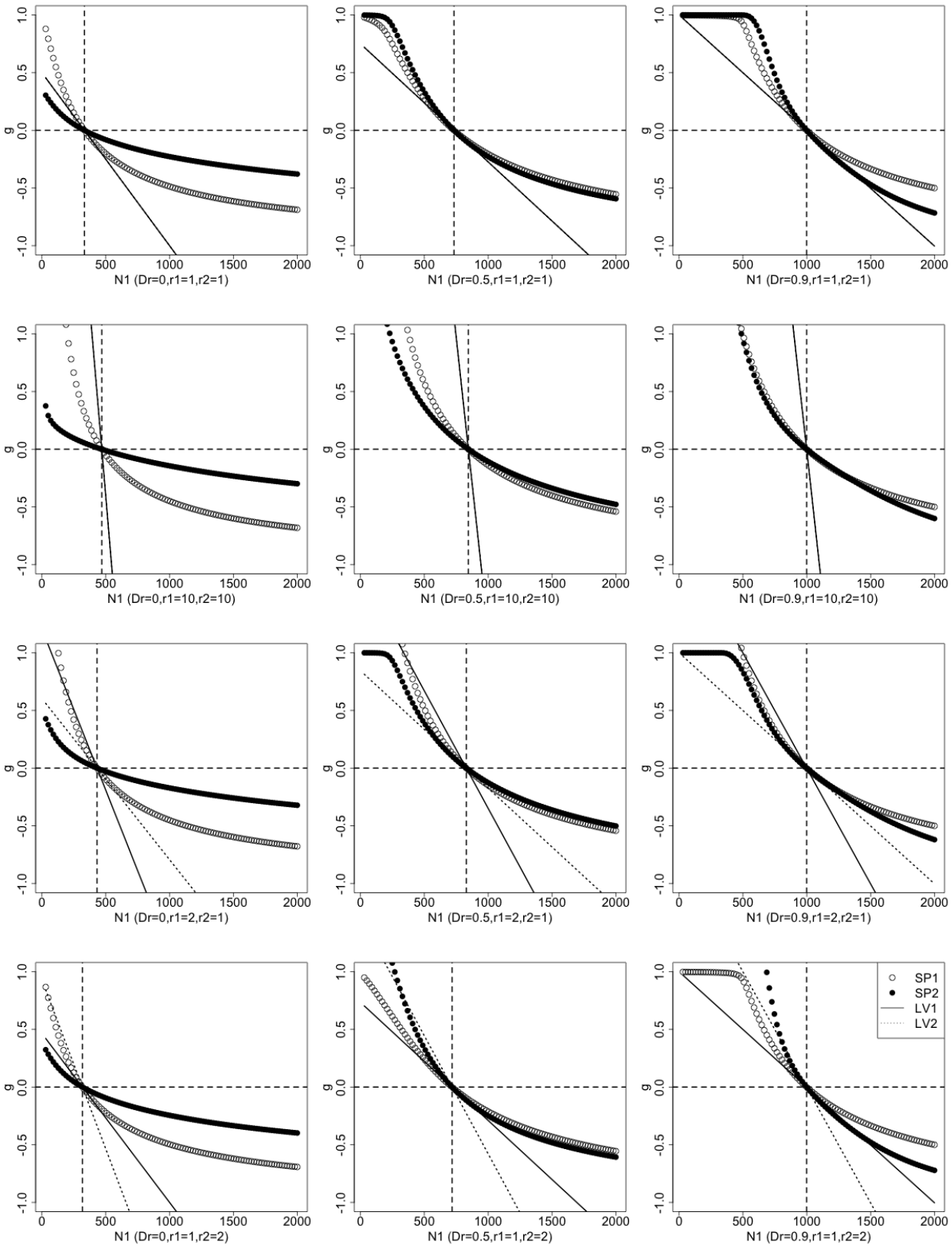

(b) $\theta_1 = 1$, $\theta_2 = 3$.

Figure 3.4: Dependence of *per capita* net growth rate on population size of the species and its competitor in a two-species community.

Species 2 is set at its steady state level ($N_2 = \hat{N}_2$) while the abundance of species 1 is varied (X axis). *per capita* net growth rate (Y axis) is plotted for the two species, each with a different point type. Predictions of the Lotka-Volterra equations are plotted with a different line type for each species (see the legend). D_r is varied among columns (left: 0, middle: 0.5 middle, right: 0.9), and r_1 and r_2 are varied among the rows (row 1: $r_1 = r_2 = 1$, row 2: $r_1 = r_2 = 10$, row 3: $r_1 = 2, r_2 = 1$, row 4: $r_1 = 1, r_2 = 2$). D_r, r_1 and r_2 are specified in the X label. The horizontal dotted line is $g = 0$ and the vertical $N_1 = \hat{N}_1$.

In each graph of Fig. 3.4a, the hollow dots show us how the net growth rate of species 1 changes with its own abundance, i.e. conspecific density dependence of growth, while the solid dots tell us how the net growth rate of species 2 changes with the abundance of species 1, i.e. heterospecific density dependence of growth. For convenience in the following, I will refer to them as simply conspecific and heterospecific density dependence. Meanwhile, the abundance of species 2 is controlled to be at its steady state ($N_2 = \hat{N}_2$). Since $D_r = 1$ will lead to no single steady state solution (exclusion or neutral steady state), in this section the highest D_r value we will look at is 0.9.

For all graphs in Fig. 3.4a, the conspecific density dependence is more negative than heterospecific density dependence. This suggests a stabilizing effect in our model because increasing the abundance of species 1 tends to decrease its own growth more than the growth of species 2, which is a negative feedback that tends to offset the initial increase.

Comparing across the columns we can see that, the difference between conspecific and heterospecific density dependence of growth diminishes as D_r increases. When $D_r = 0.9$, increasing the abundance of one species has basically the same impact on its own population growth as on the other species. This means there is little stabilizing effect to offset the initial increase. As we have discussed earlier in 2.4, when $D_r = 1$, conspecific density dependence equals heterospecific density dependence, which means stabilizing effect is zero. This is consistent with our conclusion from Chapter 2: the bigger the D_r, the smaller the stabilizing effect and the less the chance for coexistence.

Comparing across the rows we can see that, especially when D_r is small, the patterns look very similar regardless of the values of r_1 and r_2. While the predictions from the Lotka-Volterra equations change significantly with r (since r is the slope of the g vs N curve), in our model, having different r mostly just changes the starting point of g when N_1 is small but does not significantly change the relative magnitude of g_1 and g_2 or how they each vary with N_1.

So far θ has been set to be equal for the two species. In Fig. 3.4b, we examine the case where they are different. From Fig. 3.4b we can see that when $\theta_1 \neq \theta_2$, big D_r can lead to a reversal of the relative magnitude of g_1 and g_2: while in all cases where $\theta_1 = \theta_2$, $g_2 < g_1$ when $N_1 < \hat{N}_1$ and $g_2 > g_1$ when $N_1 > \hat{N}_1$, here when $\theta_1 \neq \theta_2$, there are exceptions when $D_r > 0$. This means that when D_r is big enough, increasing the abundance of species 1 could negatively affect the growth of species 2 more than itself (and vice versa), which is a positive feedback and will lead to exclusion of species 2. This result is also consistent with the conclusion in Chapter 2: when θ is different between the species, having high D_r leads to exclusion of the species with bigger θ (species 2 in this case). Again changing r_1 or r_2 does not change the shape of the density dependence curves much especially when N_1 is close to or bigger than its steady state value.

In summary, the result in this section shows that in the modified model, 1) D_r is still the key parameter that determines whether coexistence or exclusion happens: the higher the D_r, for more chance for exclusion; 2) the effect of θ is similar to that in the first model (Chapter 2): difference in θ can lead to exclusion when $D_r > 0$; 3) unlike the Lotka-Volterra equations, in our model intrinsic growth rates affects the growth curve only when abundance

is much smaller than the steady state value. Finally, despite the connection we have made between α and θ (Eq. 3.17), in our model θ does not have the dominating effect α has in the Lotka-Volterra equations (Gause 1934). Instead, conspecific and heterospecific density dependence are determined by θ and D_r together.

Lifespan-body size relationship

So far we have only looked at the overall change in population size, where only net growth (birth minus death) matters. If we are interested in predicting specifically birth and death rates and related to which, species lifespan, we will need to make further assumptions.

By looking at Table. 3.1 again, we can see that the missing information is the death probability when an individual gets a number of resource units that is between 0 (in which case death probability is definitely 1) and $(r+1)\theta$ (in which case death probability is definitely 0). An extra assumption is needed to fill this gap.

To see what exactly this assumption should be, let's look at the specific case where an individual gets 2θ resource units. As is mentioned earlier in section 3.1.2 IV, the individual can either die and give birth to 2 offspring (one death, two births), or survive and give birth to only 1 offspring (zero death, one birth). The difference lies in whether the individual keeps the resource to itself or gives it to an offspring. With no existing metric for this behavior, we will define it as "selfishness", denoted by S_f, which is equal to the probability of survival when the number of resource units an individual gets is bigger than 0 but smaller than $(r+1)\theta$. If $S_f = 0$, the individual is perfectly selfless and always give the resource to its offspring with priority, in which case all individuals die after one reproductive interval. This is true for species with non-overlapping generations. At the opposite extreme, if $S_f = 1$, the individual is perfectly selfish and always prioritize itself in resource allocation, which means death (and birth, since they are equal at steady state) is minimized and individuals all tend to live longer. Other than these two extremes, there can be states in-between. For example, if $S_f = 0.5$, there is a 50% chance the individual can survive when the resource is not zero or absolutely abundant. In the following this will be referred to as the indifferent case, indicating that the individual is indifferent to giving the resource to itself or to its offspring. These three cases and their interpretations are illustrated in Table 3.2.

Table 3.2: Three cases for individual selfishness

Scenario	S_f	death probability*	Number of deaths for the species
Selfless	0	1	N_i
Indifferent	0.5	0.5	$N_{i,0} + 0.5 \sum_k^{r_i} N_{i,k}$
Selfish	1	0	$N_{i,0}$

*Here it refers to the death probability for an individual when the number of resource units the individual gets is between 0 and $(r + 1)\theta$.

Once the value for S_f is specified, our model can predict not just net growth, but also birth and death specifically from the resource allocation outcome.

With birth and death resolved, we can further look at lifespan. By lifespan we mean the average lifetime over all individuals of the species. Lifetime here is a random variable representing the number of reproductive intervals before death happens, which follows a geometric distribution with a success rate that equals to the *per capita* death rate (assuming this rate is constant through time once steady state is reached). Since the expectation of a geometric distribution is one over the success rate, lifespan is always equal to one over the steady state *per capita* death rate (or birth rate, since they are equal).

The perfectly selfless case (S_f=0) is straightforward: all individuals die after one reproductive interval (since they always prioritize their offspring in resource allocation) so death rate is always 1 and the lifespan is one reproductive interval regardless of the species attributes (θ, D_r and r). The selfish case and indifferent case, however, could each predict a non-trivial relationship between birth rate or death rate or lifespan and the species attributes of our model. It has been widely observed that bigger species (with bigger θ) tend to live longer and have fewer offspring in each reproductive interval. In the following, we will use our model to predict the species lifespan in the single species community for different θ values keeping all other parameters constant (Fig. 3.5a).

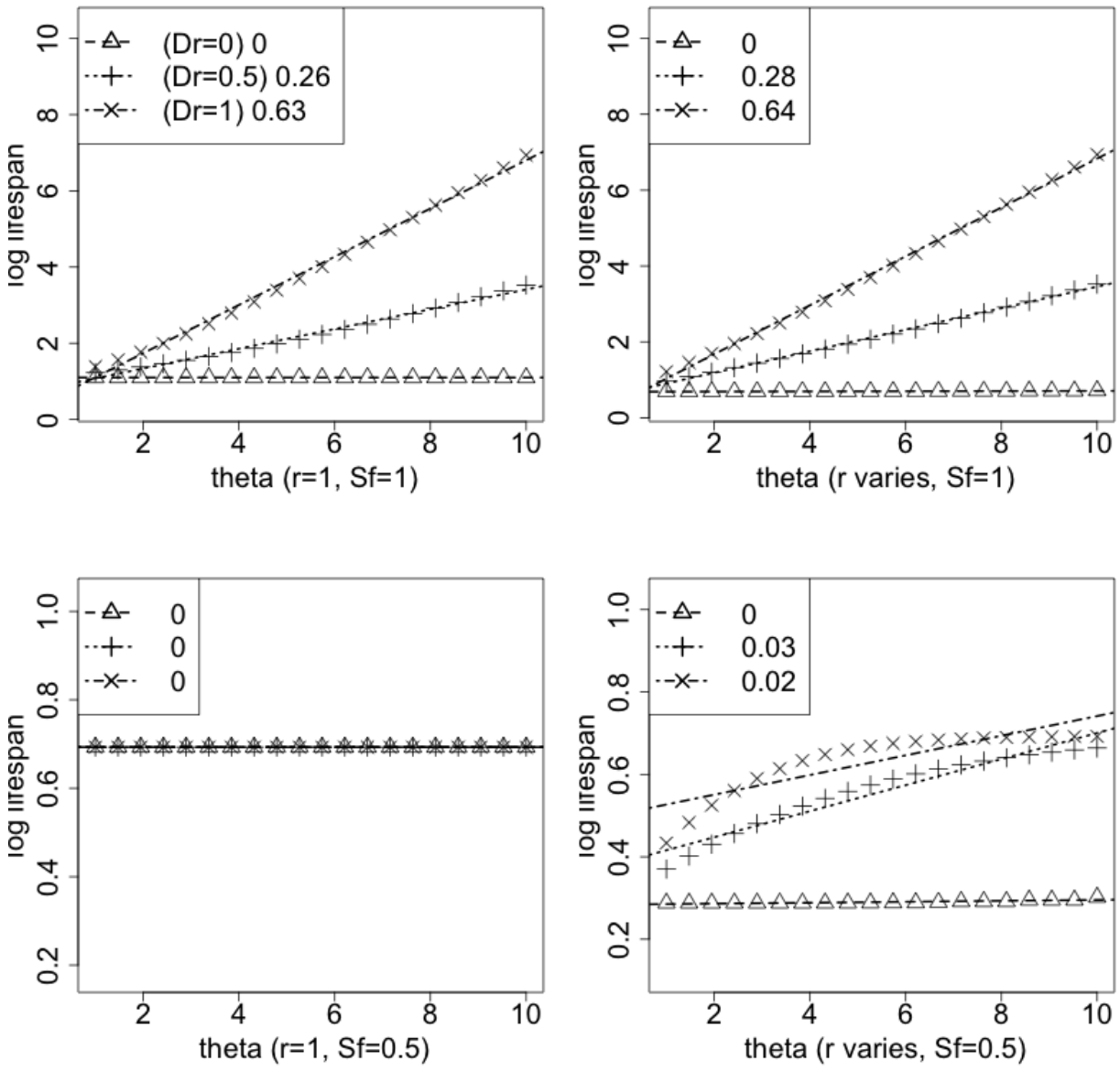

(a) X axis is θ, Y axis is log (lifespan).

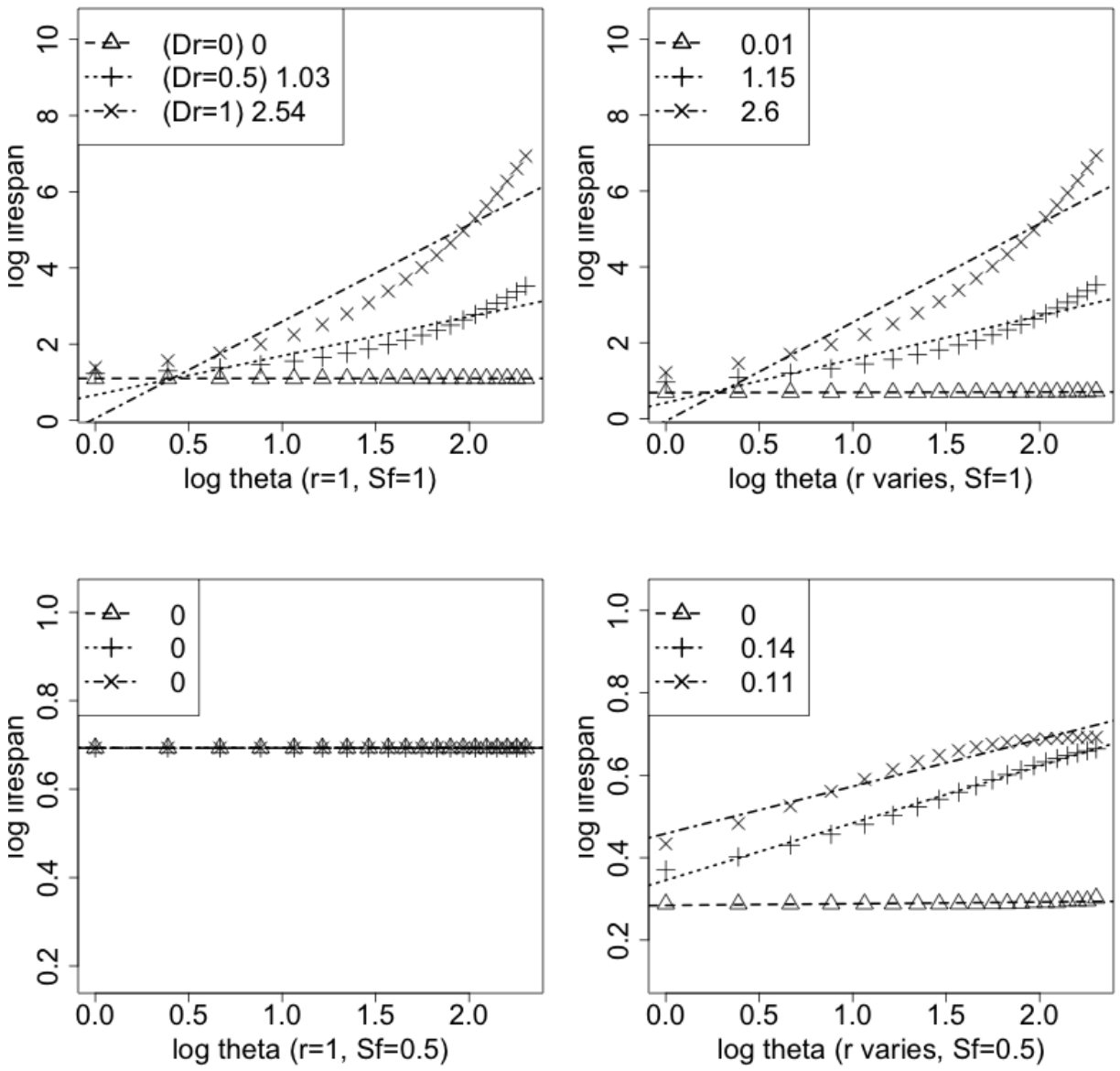

(b) X axis is log-transformed log(θ), Y axis is log (lifespan).

Figure 3.5: Relationship between θ and lifespan.

For graphs on the left, $r = 1$. For graphs on the right, r is proportional to $\frac{1}{\theta}$ and varies from 1 to 50. Different D_r values are represented by different point types as is illustrated in the legend of the first graph. The lines are each a linear fit between X and Y for a given D_r value with the slope specified in the legend of each graph.

Since the log of *per capita* birth (or death) rate is just the inverse of the logarithmic of lifespan, the pattern of it varying with θ should be perfectly symmetrical to the pattern in Fig. 3.5a against the X axis.

The first row of Fig. 3.5a shows that when individuals are selfish ($S_f = 1$) and $D_r > 0$, the predicted lifespan increases with θ (which is positively related to body size), suggesting that under these conditions, our prediction is consistent with the empirical observation that lifespan increases with body size. When $D_r = 0$, however, predicted lifespan does not change with θ.

On the left graph we have used a constant r (=1). A more realistic scenario is to set r to be related to θ: bigger species are observed to have lower intrinsic growth rates (Fenchel 1974). Therefore in the graph on the right we have assumed that r is proportional to $\frac{1}{\theta}$. The pattern is not much affected.

Next we look at the case where individuals are indifferent ($S_f = 0.5$). Results are shown in the second row of Fig. 3.5a. We can see that $r = 1$ leads to a flat line, i.e. no correlation, between lifespan and θ for all D_r values. When r is set to decrease with θ, although lifespan does increase with θ when $D_r > 0$, the slopes are very small compared to when $S_f = 1$.

In Fig. 3.5a we have log-transformed the lifespan but not θ because this gives the best linear relationship between X and Y (as is predicted by our model). On the other hand, empirical data on lifespan and body size have been mostly plotted on a log-log scale. To compare with those results, in Fig. 3.5b we re-plot predictions against θ on a log-log scale.

The empirical slope for a log-log plot between lifespan and body mass is around 0.2 (between 0.15 and 0.3) for both birds and mammals (Speakman 2005). Assuming θ is proportional to body mass, the result here indicates that 1) most species must have $D_r > 0$; 2) given the selfishness of individuals, the higher the D_r, the faster lifespan increases with body size; 3) an average individual is probably somewhere in between selfish and indifferent ($0.5 < S_f < 1$).

3.4 Discussion

In this chapter we have intensively explored a modified model for resource allocation which gives a number of predictions. Some of them are consistent with the first model (effect of θ and D_r on species coexistence at steady state), some are inconsistent (effect of θ and D_r on population resilience), but most are new predictions that are beyond the scope of the first model. Here we want to focus our discussion on the new predictions.

In both this model and the model developed in Chapter 2, D_r is a key factor determining the steady state coexistence pattern among species. If $D_r < 1$, all species have positive steady state abundances. However, the difference in abundance among species is larger with bigger D_r values. Considering stochasticity at the population level, i.e. environmental or demographic stochasticity (Morris *et al.* 2002), and that a species may have a non-zero minimum viable population size (Soulé 1987), it is less likely for species with smaller steady state abundances to survive in the long term. Therefore although in theory our model

predicts coexistence of all species as long as $D_r < 1$, in practice it predicts less stability for coexistence at steady state with bigger D_r. When $D_r = 1$ as is discussed in section 2.4, even without fluctuations or a non-zero minimum viable population size, species cannot coexist unless they all have the same θ: the species with the smallest θ are the only ones with non-zero abundances at steady state.

It is necessary to clarify that our model does not involve stochasticity at the population level. The community follows exactly the path that maximizes W_{total}, the number of microstates, and therefore the dynamics is deterministic. The coexistence and exclusion predicted here has nothing to do with demographic or environmental stochasticity. In future work population stochasticity can be introduced into the current framework for a more complete theory.

Although the interpretation of D_r is far from its final resolution (which will be further discussed in the next chapter), it has been generally accepted that it should be somehow related to within-species variation. In 3.3.1 we have proved that the higher the D_r, the more even reproductive success is distributed, which counteracts the effect of genetic drift (Lande 1976) and helps enhance the genetic diversity of the population. If D_r is positively related to functional variation (illustrated in Fig. 2.2 of Chapter 2), and assuming the functional traits have phylogenetic signal (Losos 2008), D_r should also be positively related to genetic variation. Then the result here suggests that there is a positive feedback for the population to become more and more genetically diverse: an increase in genetic variation will be reinforced in future generations by increasing the value of D_r. If this keeps happening, the eventual result will have to be diversification, when the population gets too genetically diverse to remain as one species. Then each new species with more homogenous genome will start with a small D_r and go through the process all over again. So far our theory has only been able to make predictions for communities where species identities are determined. This result could augment ability to predict speciation patterns from resource allocation statistics.

Either way, contingent on the relationship between D_r and genetic variation, many exciting predictions regarding the interaction of ecology and evolution can emerge from our theory. We will do a more thorough summary of analyses that can be done to achieve this goal in the next chapter. Here we will give an example: so far our theory consistently predicts that D_r determines how abundance correlates with body size. If D_r is positively related to genetic variation, we would expect to see better conformity with energy equivalence rule (EER, the prediction of our model when $D_r = 0$) for a community that is newly established or a rapidly evolving where each species is believed to have lower genetic variation. If the opposite is observed, then D_r should be negatively related to genetic variation.

Another interesting inference from the new predictions is the implication for body size evolution. Previously we only know that species with bigger θ end up with smaller abundance and therefore are more prone to extinction, which raises the question why all species do not become as small as possible. In this chapter we have shown that 1) bigger θ increases the evenness of reproductive success and therefore helps maintain genetic variation, and 2) bigger θ also increases the resilience of populations when D_r is small. Based on our interpretation that θ should be positively related to body size, these results suggest that there is a definite

benefit for species to grow bigger especially when their D_r is not big. Combined with our previous hypothesis on the relationship between D_r and genetic variation, a number of testable hypotheses can be made on the relationship between evolutionary trend for body size. For example, if D_r is positively related to genetic variation, we can infer that there is a tendency for new species to become bigger and for older species to become smaller.

Chapter 4

Maximizing resource allocation entropy on a functional space: implications for species coexistence, macroevolution and life history

Abstract

A new model is developed applying maximum entropy to resource allocation on a functional space. From this framework, a number of predictions for ecological and evolutionary processes for natural communities emerge. Steady state patterns (coexistence or exclusion) are affected by both body size and functional dispersion; their interaction generates possible evolutionary tradeoffs for species. Within this framework, the dichotomy of r-selected vs K-selected life history strategies can also be illuminated. This theory provides a way for different ecological theories, i.e. the niche theory and the neutral theory, to be combined in a unified framework. Concrete plans for empirical tests will be illustrated.

4.1 Introduction

In Chapters 2 and 3, I have explored the approach of maximizing Boltzmann entropy to predict population dynamics and community structure. This novel method yields a number of predictions including a steady state abundance-body size relationship, population dynamics (for one species and for multiple competitors), the within-species distribution of reproductive success and a lifespan-body size relationship.

To better understand this new model presented here, it is important to see how it differs from the approach in Chapter 3. In the introduction of Chapter 3, I listed the biological assumptions behind the resource allocation scenario. In addition to those, I also assumed that 1) species and individuals are the only relevant taxonomic units for resource allocation;

2) species identities and attributes are given as inputs and do not change through time; 3) the only attributes that differentiate one species from another are the species-specific resource requirement θ_i (number of resource units an individual of species i needs to survive one time interval) and the relative individual distinguishability $D_{r,i}$ (how distinguishable individuals of species i are compared to heterospecific individuals). If two species have the same θ and D_r, they will be equivalent in this model.

I started with these assumptions for simplicity. However, justifying them can be challenging. First, the definition for species is often ambiguous: it is not clear whether in this context we should use reproductive species, typological species, phylogenetic species or ecological species (Mallet 1995, Meier 2000, De Queiroz 2007). Nor is it clear why species rather than populations or genera or functional groups, for example, should be the relevant units for resource allocation. Secondly, one major difference among species in our model lies in the species-specific resource requirement θ_i, which is determined by the species average body size. Although body size is important, it is definitely not the only difference among species that matters. The relative individual distinguishability D_r is intended to capture additional differences among species, it does not yet clear what trait(s) it is based on, nor exactly how it can be calculated from data. Thus, if two traits are both relevant to resource allocation, and one species has higher variation in trait A while lower variation in trait B, and another species has lower variation in trait A while higher variation in trait B, it is not clear which species has higher D_r. Notice that the two traits can be incomparable (e.g. beak shape and foraging time). These problems are hard to solve in the current resource allocation scenario, where functional traits are not directly involved.

These problems suggest that, it is necessary to redefine the resource allocation process so that it is not taxonomy-based and more readily incorporates functional traits other than body size. One way to do this is to assume that resource is randomly allocated across a functional space, on which all individuals of the community can be mapped and microstates defined.

In the following I will first introduce the scenario of resource allocation to a functional space, and then explore a few specific cases where functional distribution patterns among species and individuals are given. In each of these cases, the same community- and population-level metrics can be predicted as in Chapter 3. The new formula for total number of microstates has the same parameters as in Chapter 3 (R_0, θ, D_r, r), only now the interpretation of D_r is more straightforward and measurable. Most importantly, the new model opens the possibility to explore the effect of functional distribution among species and individuals on all of our predictions, as well as to utilize information from other taxonomic levels in the model. Based on the results, plans for empirical tests will be demonstrated and future extensions summarized.

4.2 Method

Resource allocation to a functional space

Here I consider a scenario where a resource is randomly allocated across a functional space. The resource here can be thought of as a melded pool of all critical conditions for survival and reproduction, e.g. space, sunlight, water, nutrients, and each unit of it is of equal quality. The definition of functional space is similar to Hutchinson's definition of niche, an N-dimensional hypervolume with each axis being an environmental variable (Hutchinson 1965). Later in the discussion I will relate it directly to the niche space. The variables can also include geographic coordinates (x, y, z) and time.

Given this definition, I further assume that the functional space can be divided into discrete functional cells. Microstates for resource allocation are particular resource unit-functional cell matching patterns. To give an example, for Darwin's finches on the Galapagos islands (Grant & Grant 1989), taking food as the resource (including seeds, fruits, insects, etc.) and food hardness as the axis of the functional space, a microstate would be a particular food unit-hardness association among all food units across the hardness range. Using letters (A, B, ...) to represent resource units and numbers (1, 2, ...) to represent hardness levels, a microstate could be seed A - 10, seed B - 9, insect A - 2, fruit A - 1, ... Since maximizing the number of microstates as defined here will lead to a uniform distribution of resource across the functional space, the associated assumption for Galapagos islands is that the hardness distribution of food is uniform, i.e. randomly sampling a food unit, there is an equal chance for it to have any hardness value. If the variable is time or space, the associated assumption would be that resource is evenly distributed through time or across space. Which variable to choose depends on the system of interest and will be discussed later.

In this chapter I will focus on the simplest scenario assuming that the resource is uniformly distributed across the functional space. Uniform distribution is the MaxEnt solution when there are no other constraints than the boundaries of the random variable to be predicted. In the future scenarios with additional constraints (e.g. mean values of the functional variables) can be explored. Notice that this does not mean that the fitness landscape (Wright 1932) is flat for any species or individual; each species and individual can still have higher fitness at some functional locations than others. As will be illustrated later, where and how scattered a species is distributed on the functional space are considered as constraints given to this model. We are only assuming that species and individuals have equal optimized fitness, i.e. when they are at their optimal locations at the functional space, their fitness are equal. A similar argument has been used to justify the neutral theory (Clark 2009).

As in the previous chapters, the community here is defined as a group of species competing for the resource being allocated. To predict community patterns from the above resource allocation scenario, I need to map all species in the community onto the functional space. The mapping can be done by linking axis variables of the functional space to biological traits of the species. In other words, the axes of the functional space can also be considered as biological traits, as is often applied in niche-based studies (Violle & Jiang 2009). In the

example of Darwin's finches, the corresponding trait is beak shape (adapted to a certain hardness level). Applying this model to this case assumes that the chance of getting food is equal for birds with all beak shapes.

Once all individuals of the community are mapped onto the functional space, across- and within-species resource allocation patterns can be combined to represent microstates of resource allocation among functional cells. The simplest case would be that, if each species covers exactly one functional cell and does not overlap with any other species, each across-species resource allocation pattern corresponds to a distinct microstate on the functional space. In this case, since all individuals of the same species completely overlap, all within-species demographic grouping and resource allocation patterns correspond to the same microstate and therefore should not be counted in calculating the number of microstates. On the other hand, if each individual covers a different functional cell, each within-species demographic grouping and resource allocation combination corresponds to a different microstate on the functional space. Notice that for the former case, even if a species covers multiple functional cells, as long as it does not overlap with any other species, the number of across-species allocations is proportional to the number of microstates. The proportionality factor is the number of microstates each across-species allocation pattern corresponds to and is determined by the number of functional cells each species covers, the number of species, and the total resource available, and therefore is a constant. Since this factor does not influence the maximization, we will leave it out of the equations. The same applies at the individual level, i.e. the number of functional cells an individual covers is constant. The more important thing is how much different species and individuals overlap with each other functionally.

Here I define two parameters, O and O_i, to quantify respectively 1) how much different species overlap and 2) how much individuals of species i overlap on the functional space. For both O and O_i, the value is 0 when there is no overlapping, and 1 when there is complete overlapping. As is illustrated in the last paragraph, the extent to which species- and individual-level patterns should be counted as microstates is negatively related to O and O_i, respectively. In Chapter 2 I have defined D_{across} and D_{within} as distinguishability across- and within-species. Here I redefine them to be the complement of overlap:

$$D_{across} = 1 - O \tag{4.1}$$

$$D_{within,i} = 1 - O_i \tag{4.2}$$

Based on these definitions the total number of microstates W_{total} can be calculated from the number of across-species resource allocations W_{across}, the number of within-species demographic grouping $W_{grouping,i}$ and the number of within-species resource allocations $W_{within,i}$.

$$W_{total} = W_{across}^{D_{across}} \times \prod_{i}^{S_0} (W_{grouping,i} W_{within,i})^{D_{within,i}} \tag{4.3}$$

Eq. 4.3 is consistent with the rationale introduced earlier: when D_{across} and $D_{within,i}$ are both zero, species and individuals completely overlap with each other. This means that different species- and individual-level patterns all correspond to one microstate on the functional space so $W_{total} = 1$. When $D_{across} = 1$ and $D_{within,i} = 0$, species do not but conspecific individuals completely overlap. This means that across-species allocation patterns each corresponds to a distinct microstate on the functional space while within-species demographic grouping and resource allocation patterns do not affect the outcome, so $W_{total} = W_{across}$. When D_{across} and $D_{within,i}$ are both equal to 1, species and individuals are all completely separated from each other. This means that each across-species and within-species demographic grouping and resource allocation combination pattern corresponds to a distinct microstate, so $W_{total} = W_{across} \times \prod_i^{S_0}(W_{grouping,i}W_{within,i})$. The distribution patterns of species and individuals on the functional space for these cases are shown in graph 1-3 of Fig. 4.1.

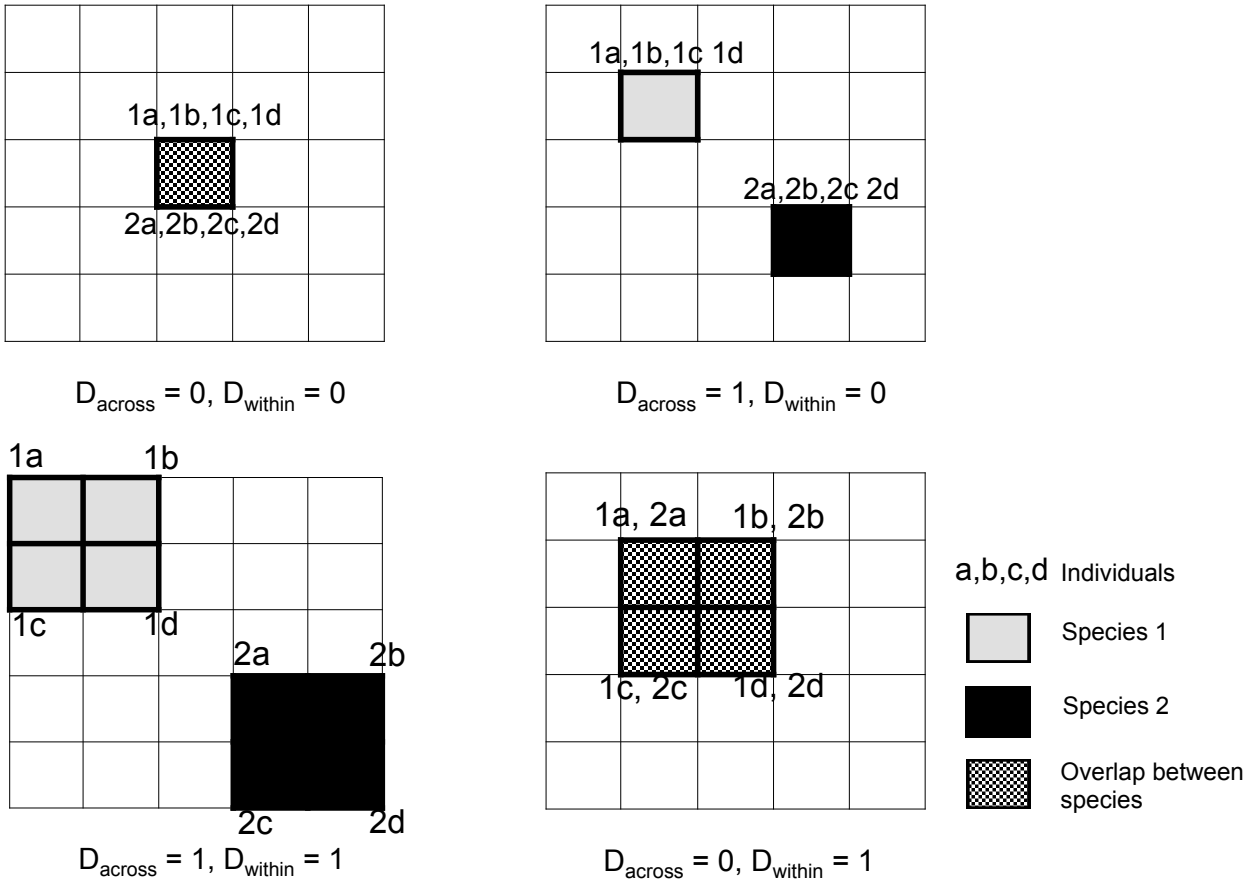

Figure 4.1: Species and individual distribution on the functional space

D_r is still defined as the ratio between D_{within} and D_{across}, so for species i:

$$D_{r,i} = \frac{D_{within,i}}{D_{across}} \tag{4.4}$$

Notice that this definition is not based on "distinguishability" as in the previous chapters, but the more biologically explicit idea of "functional overlapping": the bigger the $D_{r,i}$, the less functional overlapping there is within species i compared to across species. Substituting Eq. 4.4 into Eq. 4.3:

$$W_{total}^{\frac{1}{D_{across}}} = W_{across} \times \prod_{i}^{S_0} (W_{grouping,i} W_{within,i})^{D_{r,i}} \tag{4.5}$$

Notice that the exponent $\frac{1}{D_{across}}$ on the left has no influence on the maximization. Eq. 4.5 is very similar to the equation for W_{total} in Chapter 2 and 3 except that the exponent for $W_{grouping,i}$ and $W_{within,i}$ are now both $D_{r,i}$. Notice that the special case when $D_{r,i} = 1$ is the same as the previous model so the predictions for that case still holds: when all species have the same θ, the community has a neutral steady state; otherwise the species with the smallest θ deterministically excludes all other species. Given the new definition, $D_{r,i}$ can now be bigger than 1 when $D_{across} < D_{within,i}$ or $O > O_i$, in which case there is less functional overlap or more dispersion within species i than across species (graph 4 in Fig. 4.1).

The expressions for W_{across}, W_{within} and $W_{grouping}$ are the same as in Chapter 3:

$$W_{across} = \frac{R_0!}{\prod_i^{S_0} R_i! R_n!} \tag{4.6}$$

$$W_{within,i} = \frac{R_i!}{\prod_{k=1}^{r_i+1} (k\theta_i)!^{N_{i,k}}} \tag{4.7}$$

$$W_{grouping,i} = \frac{N_i!}{\prod_{k=0}^{r_i+1} N_{i,k}!} \tag{4.8}$$

In Eqs. 4.6-4.8, R_0 is the total resource available; r_i is the intrinsic growth rate, i.e. the maximum number of offspring an individual can have in one allocation period; N_i is the current abundance of species i; R_i is the amount of resource species i takes in the current allocation period; R_n is the amount of resource not allocated to any species ($R_n = R_0 - \sum_i^{S_0}$), and $N_{i,k}$ (k from 1 to r_i+1) is the macrostate variable which quantifies how many individuals from species i can get k resource units. $N_{i,0}$ is not an independent variable and can be calculated from $N_i - \sum_k^{r_i+1} N_{i,k}$. Substituting Eqs. 4.6-4.8 into Eq. 4.4 and log-transforming:

$$\begin{aligned}\log W_{total} = D_{across}(\log R_0! - \log R_n!) + \sum_i^{S_0}[(D_{within,i} - D_{across})\log R_i! \\ -D_{within,i}(\sum_{k=1}^{r_i+1} N_{i,k}\log (k\theta_i)! + \log N_i! - \sum_{k=1}^{r_i+1}\log N_{i,k}! - \log N_{i,0}!)]\end{aligned} \tag{4.9}$$

To maximize $\log W_{total}$, I take the partial derivative of $\log W_{total}$ over the macrostate variable $N_{i,k}$ (k from 1 to $r_i + 1$) and equate it to zero:

$$\begin{aligned}\frac{\partial \log W_{total}}{\partial N_{i,k}} = D_{across}k\theta_i\log R_n + k\theta_i(D_{within,i} - D_{across})\log R_i \\ -D_{within,i}k\theta_i(\log k\theta_i - 1) - D_{within,i}(\log N_{i,k} - \log N_{i,0}) = 0\end{aligned} \tag{4.10}$$

Eq. 4.10 gives the determining equation from which the macrostate variables $N_{i,k}$ can be solved. In the following, predictions from Eq. 4.10 on community structure and population dynamics will be examined and compared with those from the previous chapter. After that the connections between this framework and existing ecological theories will be clarified. Then I will introduce ways to empirically estimate functional overlapping and $D_{r,i}$. Based on this empirical methods to test the theory and directions it can be extended in future will be discussed.

4.3 Results

When $D_{across} = 0$ ($D_r = \infty$)

Substituting $D_{across} = 0$ into Eq. 10 we derive,

$$\frac{N_{i,k}}{N_i} = \frac{(\frac{eR_i}{k\theta_i})^{k\theta_i}}{\sum_{j=1}^{r_i+1}((\frac{eR_i}{j\theta_i})^{j\theta_i} + 1} \tag{4.11}$$

Notice that $D_{within,i}$ becomes the common multiplier for all terms and is dropped. From Eq. 4.11, the *per capita* net growth rate g_i can be calculated:

$$g_i = \sum_{k=0}^{r_i+1}(k-1)\frac{N_{i,k}}{N_i} = \frac{\sum_{k=1}^{r_i+1}(k-1)(\frac{eR_i}{k\theta_i})^{k\theta_i} - 1}{\sum_{j=1}^{r_i+1}((\frac{eR_i}{j\theta_i})^{j\theta_i} + 1} \tag{4.12}$$

At steady state, $\hat{g}_i = 0$ and therefore:

$$\sum_{k=1}^{r_i+1}(k-1)(\frac{e\hat{R}_i}{k\theta_i})^{k\theta_i} = \sum_{k=1}^{r_i+1}(k-1)(\frac{e\hat{N}_i}{k})^{k\theta_i} = 1 \tag{4.13}$$

In Eq. 4.13, the first non-zero term in the summation is $(\frac{e\hat{N}_i}{2})^{2\theta_i}$ for $k = 2$ and is bigger than 1 as long as the steady state abundance $\hat{N}_i \geq 1$ (since $e > 2$ and $2\theta_i > 0$). Therefore for Eq. 4.13 to hold, $\hat{N}_i$ has to be smaller than 1. Since actual abundance has to be at least 1, there is no meaningful steady state in this model when $D_{across} = 0$.

Meanwhile, Eq. 4.12 shows that g_i is only affected by the abundance and parameters (θ_i and r_i) of species i but not any other species. This means that the single species case gives the same prediction as the multiple competitor case, so the latter will not be explored separately.

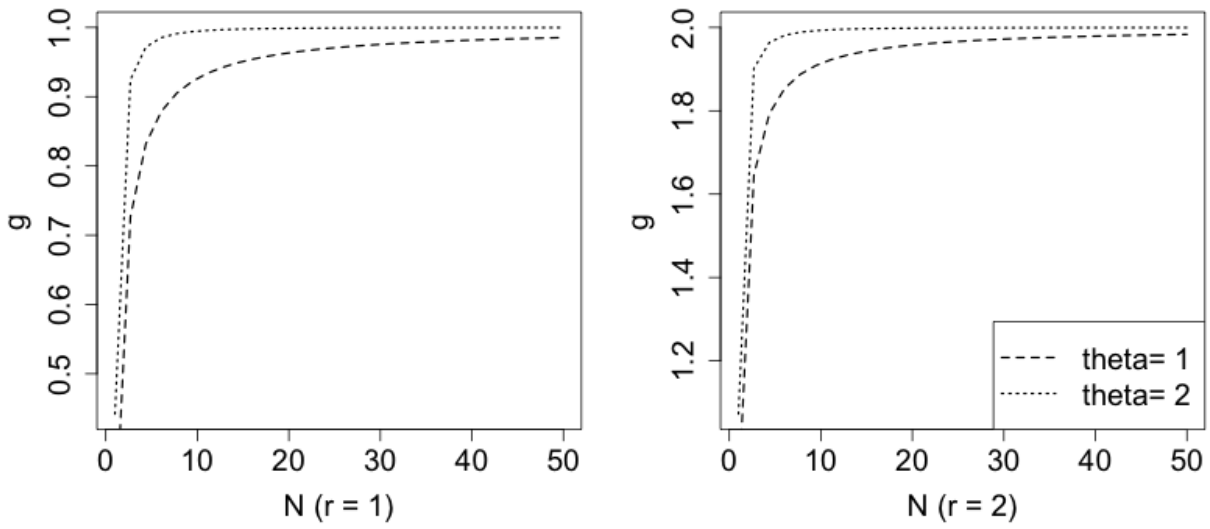

Figure 4.2: Dependence of *per capita* net growth rate g on abundance N when $D_{across} = 0$. R_0 does not affect this pattern. r is varied between the two graphs and specified in the label of the X axis. Different line types represent different θ values and are specified in the legend.

From Fig. 4.2 we can see that when $D_{across} = 0$, population growth has positive density dependence: the bigger the abundance N, the bigger the *per capita* net growth rate g and the faster the population grows. This effect is stronger with bigger θ.

In reality populations cannot grow forever; growth has to stop when the resource limit is reached. The result here tells us that when species have the same θ, the one with higher initial abundance is very likely to end up with much higher abundance due to the positive density dependence of growth; otherwise, the species with bigger θ is more likely to win over the other species.

When $D_{across} \neq 0$ but $D_{within} = 0$ $(D_r = 0)$

Substituting $D_{within,i} = 0$ into Eq. 4.10 we get:

$$R_i = R_n \tag{4.14}$$

Eq. 4.14 suggests that when $D_{within,i} = 0$, species i always gets the same amount of resource as R_n, the amount of resource not allocated to any species. This also means that when all species have $D_{within,i} = 0$, the resource distribution among species is perfectly even despite the initial state and potential differences in species attributes.

When $D_{across} > 0$ and $D_{within,i} > 0$ $(0 < D_{r,i} < \infty)$

When $D_{across} > 0$ and $D_{within,i} > 0$, $D_{r,i}$ can be used in place of $\frac{D_{within,i}}{D_{across}}$. Substituting it into Eqs. 4.10 & 4.12:

$$\frac{N_{i,k}}{N_i} = \frac{(\frac{R_n^{\frac{1}{D_{r,i}}} R_i^{\frac{D_{r,i}-1}{D_{r,i}}}}{\frac{k\theta_i}{e}})^{k\theta_i}}{\sum_{k=1}^{r_i+1}(\frac{R_n^{\frac{1}{D_{r,i}}} R_i^{\frac{D_{r,i}-1}{D_{r,i}}}}{\frac{k\theta_i}{e}})^{k\theta_i} + 1} \tag{4.15}$$

and

$$g_i = \sum_{k=0}^{r_i+1}(k-1)\frac{N_{i,k}}{N_i} = \frac{\sum_{k=1}^{r_i+1}(k-1)(\frac{R_n^{\frac{1}{D_{r,i}}} R_i^{\frac{D_{r,i}-1}{D_{r,i}}}}{\frac{k\theta_i}{e}})^{k\theta_i} - 1}{\sum_{k=1}^{r_i+1}(\frac{R_n^{\frac{1}{D_{r,i}}} R_i^{\frac{D_{r,i}-1}{D_{r,i}}}}{\frac{k\theta_i}{e}})^{k\theta_i} + 1} \tag{4.16}$$

In the following I will look at the predictions of Eqs. 4.15-4.16 for the same metrics explored in Chapter 3, i.e. steady state abundance, within-species resource allocation, single species population growth, multiple competitor dynamics and lifespan-body size relationship.

Steady state abundance

Substituting the steady state condition $g_i = 0$ into Eq. 4.16:

$$\sum_{k=1}^{r_i+1}(k-1)(\frac{eR_n^{\frac{1}{D_{r,i}}}\hat{N}_i^{\frac{D_{r,i}-1}{D_{r,i}}}\theta_i^{\frac{-1}{D_{r,i}}}}{k})^{k\theta_i} = 1 \tag{4.17}$$

First I will show how Eq. 4.17 can be analytically solved with approximations. The summation of Eq. 4.17 can be expanded as

$$(\frac{P_i}{2})^{2\theta_i} + 2(\frac{P_i}{3})^{3\theta_i} + 3(\frac{P_i}{4})^{4\theta_i} + ... = 1 \tag{4.18}$$

Where P_i is a positive value and is equal to $eR_n^{\frac{1}{D_{r,i}}}\hat{N}_i^{\frac{D_{r,i}-1}{D_{r,i}}}\theta_i^{\frac{-1}{D_{r,i}}}$. Since the first term on the left side of Eq. 4.18, $(\frac{P_i}{2})^{2\theta_i}$, is greater than 1 when $P_i \geq 2$, for Eq. 4.18 to hold, P_i has to be smaller than 2. Given $P_i < 2$ and that θ is positive, the magnitude of terms on the left should decrease with k faster than exponentially. Furthermore, when θ is much bigger than 1, all terms but the first (when $k = 2$) can be ignored and Eq. 4.18 can be approximated as:

$$(\frac{P_i}{2})^{2\theta_i} \approx 1 \tag{4.19}$$

Substituting $P_i = eR_n^{\frac{1}{D_{r,i}}}\hat{N}_i^{\frac{D_{r,i}-1}{D_{r,i}}}\theta_i^{\frac{-1}{D_{r,i}}}$ into Eq. 4.19 we get:

$$\hat{N}_i \approx \frac{2}{e}(\frac{2\theta_i}{e\hat{R}_n})^{\frac{1}{D_{r,i}-1}} \tag{4.20}$$

We can see that this approximated solution is very similar to the analytical solution for the first model in Chapter 2 where $\hat{N}_i = (C\theta_i)^{\frac{1}{D_{r,i}-1}}$ and C is a also constant determined by total resource available. Therefore the approximated analytical solution to steady state is the same as that in Chapter 2 and 3. This also turns out to be a good approximation especially when θ is big: in Fig. 4.3 the approximated solution is compared with the result of numerically solving Eq. 4.17 for the steady state.

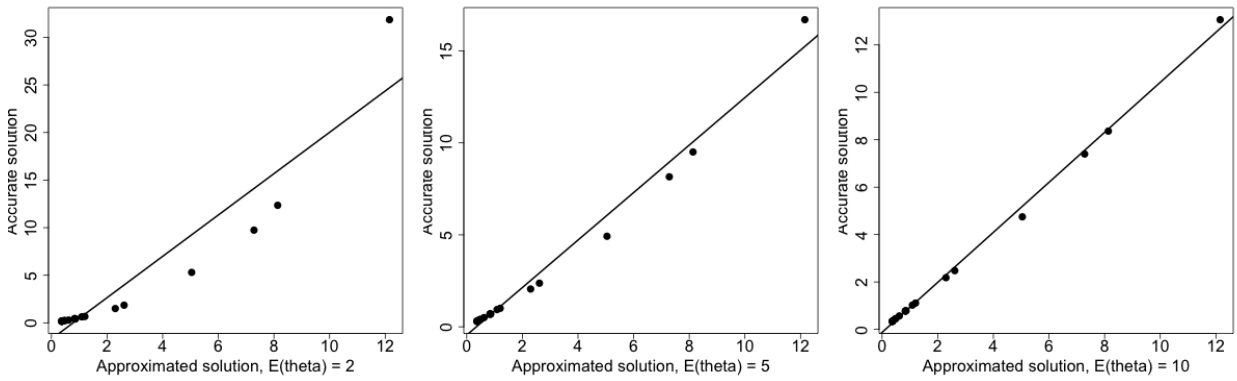

Figure 4.3: Comparing predictions for steady state abundances ($\hat{N}_i$) between the approximated solution (X axis; same with the model in Chapter 2) and the accurate numerical solution (Y axis).
$D_{r,i}$ is uniformly drawn from 0.1 to 0.9, r_i from 1 to 20. For the first graph, θ_i is uniformly drawn from 0 to 4, $R_0 = 20$. For the other graphs, R_0 and θ_i are both multiplied by a scale factor (2.5 or 5) so that their relative magnitudes are unchanged. The absolute value of the mean of θ is shown in the X label. The solid line is a linear fit between X and Y.

Fig. 4.3 shows that, as was inferred earlier, the steady state solution for the model in Chapter 2 is well correlated with the steady state solution in this new model especially when the absolute magnitude of θ is big.

Within-species resource distribution at steady state

Eq. 4.15 gives the relationship between $N_{i,k}$ and k which gives the within-species resource distribution. Substituting the approximated steady state solution (Eq. 4.19) into Eq. 4.15, I get the approximated steady state within-species resource distribution:

$$\frac{\hat{N_{i,k}}}{\hat{N_i}} \approx \frac{(\frac{2}{k})^{k\theta_i}}{\sum_{k=1}^{r_i+1}(\frac{2}{k})^{k\theta_i} + 1} \tag{4.21}$$

From Eq. 4.21 we can see that $D_{r,i}$ does not affect the within-species distribution at steady state; only θ_i does. The shape of this distribution is shown in Fig. 4.4.

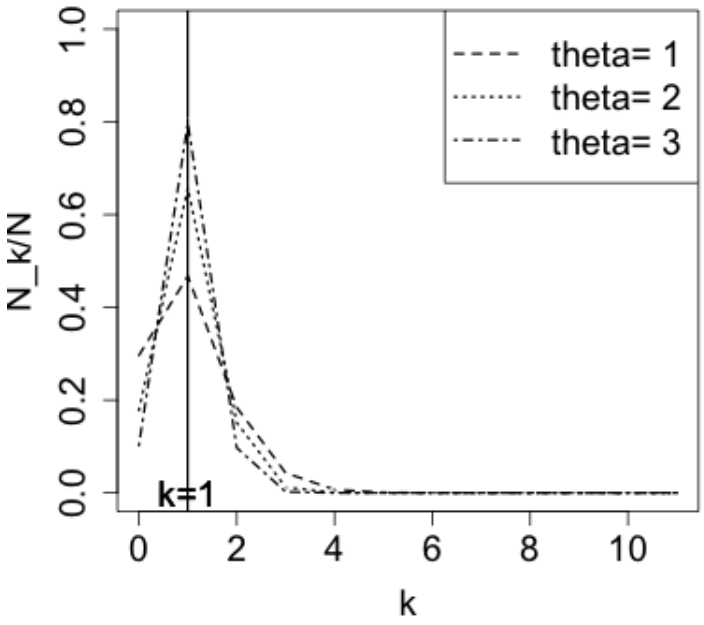

Figure 4.4: Within-species resource distribution at steady state ($\hat{N} = 100$, $r = 10$). The Y axis is $\frac{N_k}{\hat{N}}$. The X axis is k. Different line types represent different θ values (see the legend).

Notice that the shape of this distribution is independent of r once it passes a certain level. This is because N_k decreases very fast with k. For example, in Fig. 4.4 the value of $\frac{N_k}{N}$ is zero when $k > 5$, so $r = 10$ and $r = 20$ give the same shape of distribution.

Fig. 4.4 shows that the bigger the θ, the more peaked the distribution is at $k = 1$. Since net growth is zero at steady state, $k = 1$ or one resource unit per individual corresponds to a perfectly even resource distribution within the species. In this model, θ is positively related to body size; resource determines both survival and reproduction. Therefore the result here suggests that all else equal, reproduction opportunity is more evenly distributed among individuals when the species has bigger body size.

Single species population growth

Notice that when there is only one species in the community, there is no other species to overlap with so D_{across} is always equal to 1. This means that D_r is always equal to D_{within} and cannot be bigger than 1.

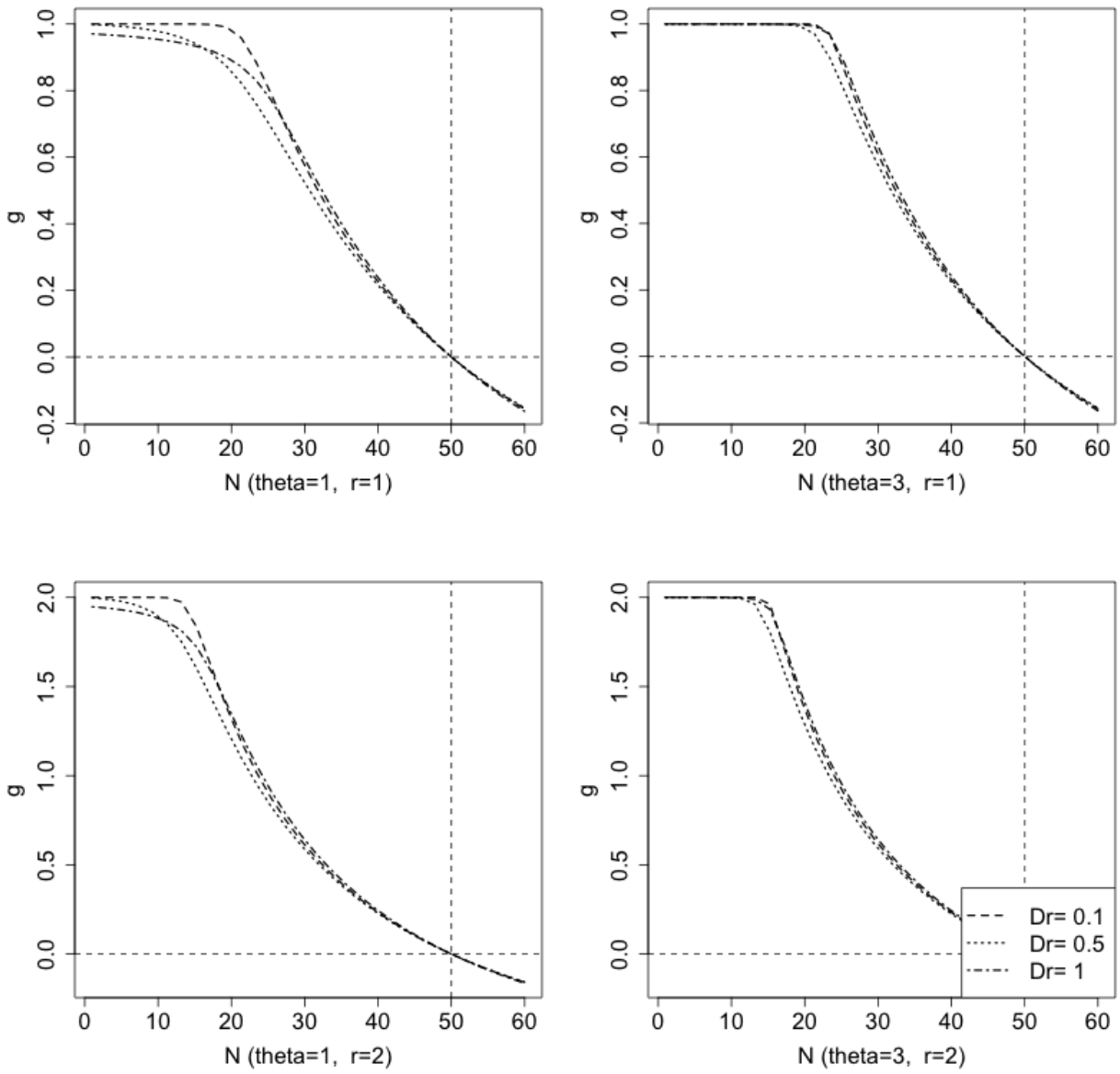

Figure 4.5: Density dependence of population growth for a one species community. For all graphs $\hat{N} = 50$. θ is varied between left and right while r is varied between upper and lower graphs; both are specified in the X label. Within each graph, different line types represent different D_r values (see the legend). The horizontal dotted line indicates $g = 0$ the vertical one $N = \hat{N}$.

Fig. 4.5 shows that similar to the result in Chapter 3, the slope of the $g-N$ curve changes with abundance in this model: when N is small, the slope gets more negative (steeper) as N increases; when N surpasses a certain level, the pattern is reversed and the slope gets slower as N increases. However, different from the result in Chapter 3, the effect of D_r is not very straightforward: the slope around steady state is the steepest when D_r takes an intermediate value ($= 0.5$). This suggests that the population has higher resilience around steady state when D_r is either smaller or higher than 0.5. The difference among different D_r is diminished as θ increases.

Two competitor dynamics

In this case the community has two species that exploitatively compete for the resource to be allocated. This scenario can be easily generalized to include more than two species without substantially changing the patterns predicted. Notice that when there are more than one species in the community, as discussed earlier, D_{across} can be smaller than $D_{within,i}$ in which case $D_{r,i} > 1$.

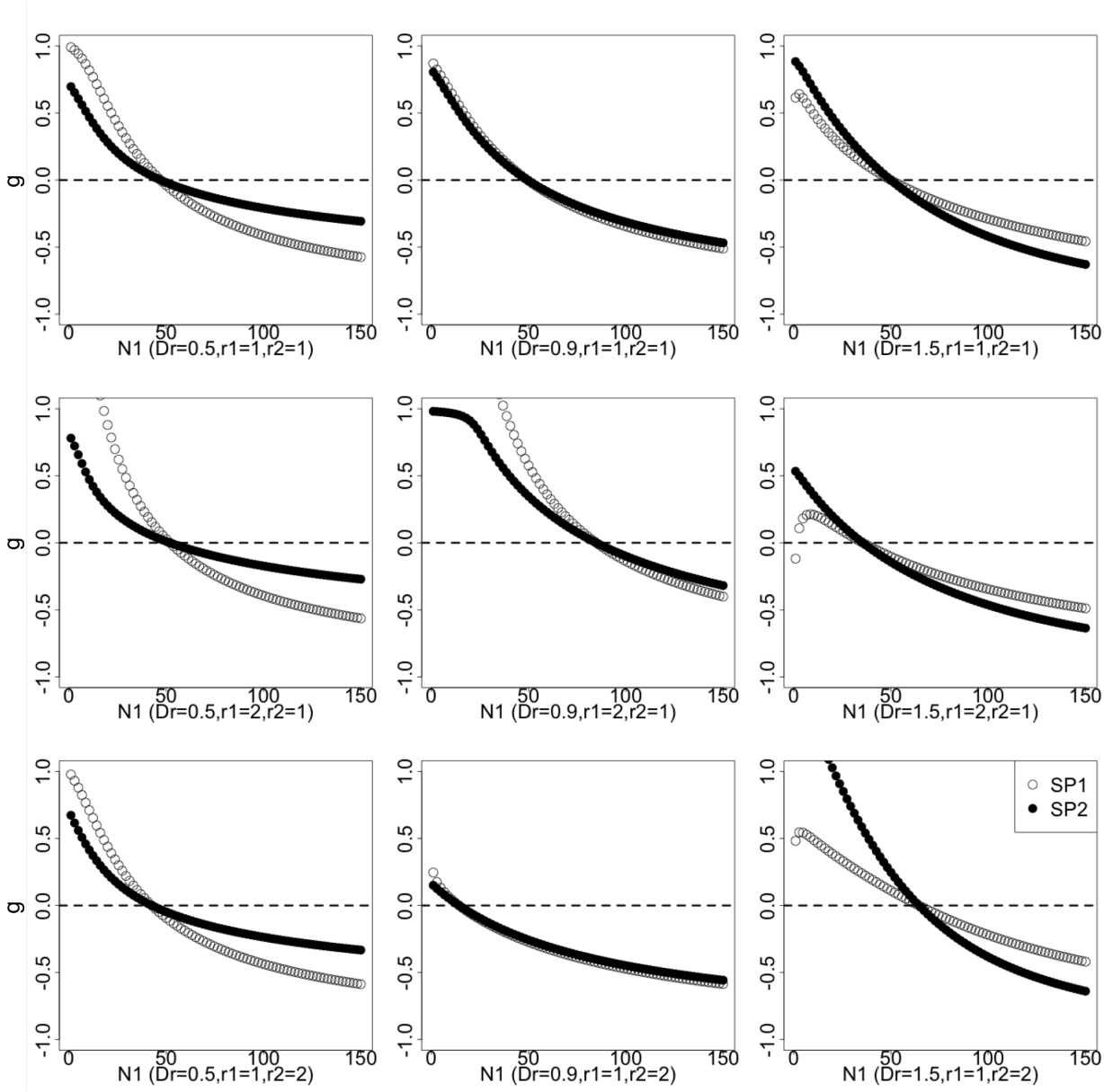

(a) $\theta_1 = \theta_2 = 1$.

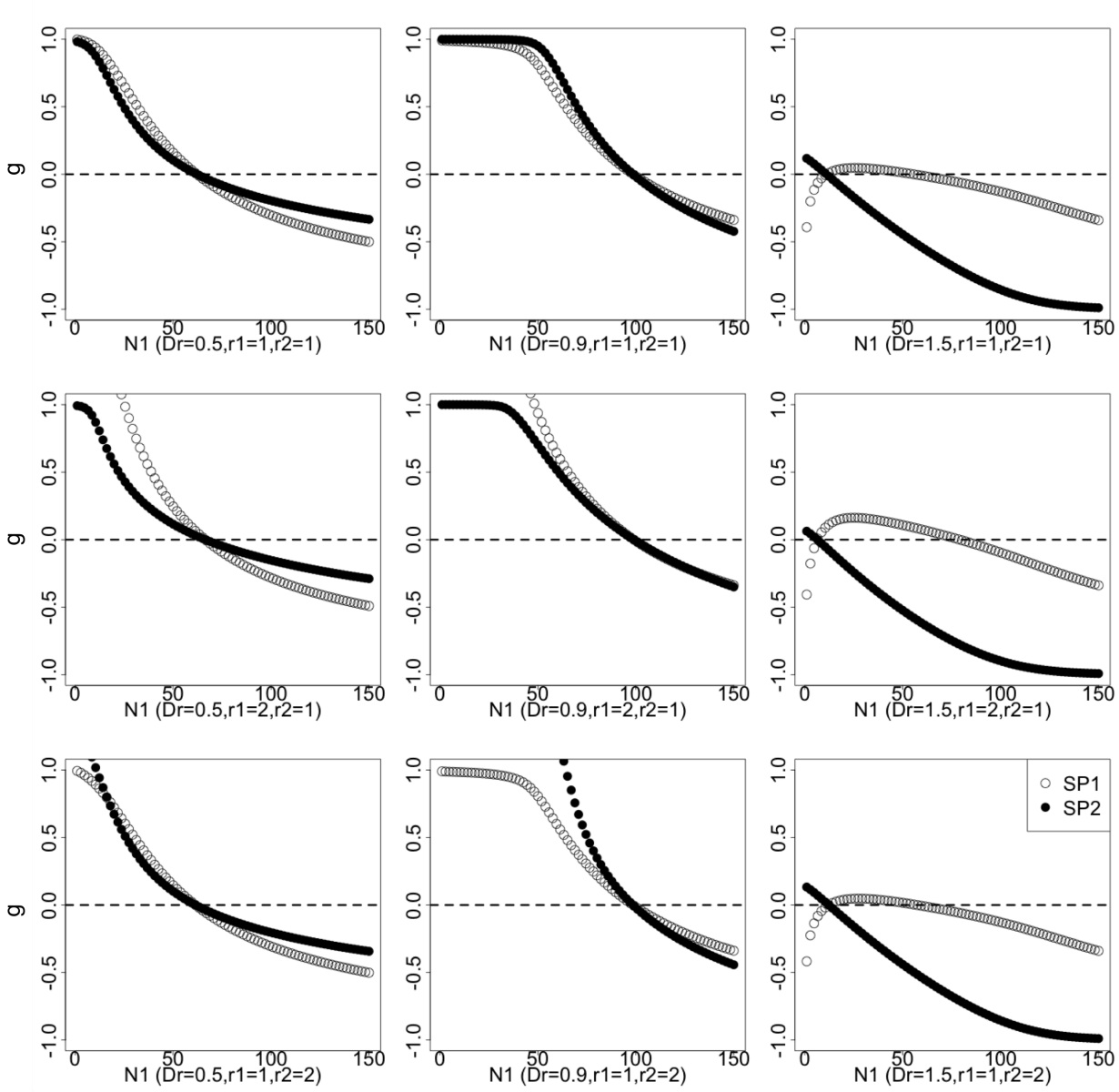

(b) $\theta_1 = 1, \theta_2 = 2$.

Figure 4.6: Dependence of *per capita* net growth rate on abundance in a two-species community.

Species 2 is controlled to be at its steady state level ($N_2 = \hat{N}_2$) while the abundance of species 1 is varied (X axis). *Per capita* net growth rate g (Y axis) is plotted for the two species, each with a different point type. D_r is varied among columns (left: 0.5, middle: 0.9 middle, right: 1.5), and r_1 and r_2 are varied among the rows (row 1: $r_1 = r_2 = 1$, row 2: $r_1 = 2, r_2 = 1$, row 3: $r_1 = 1, r_2 = 2$). D_r, r_1 and r_2 are specified in the X label. The horizontal dotted line is $g = 0$.

In Chapter 4.3 I defined conspecific density dependence as the dependence of the *per capita* net growth rate of a species (g_1) on the abundance of the same species (N_1), and heterospecific density dependence as the dependence of g_2 on N_1. Given this, if conspecific density dependence is more negative than heterospecific density dependence, a perturbation to the species abundances tends to be offset and species tend to coexist with each other. If, on the other hand, conspecific density dependence is less negative than heterospecific density dependence, a perturbation to the abundances tends to be reinforced, causing less chance for coexistence among the species.

From Fig. 4.6a and 4.6b we can see that the result here is very similar to that of Chapter 3: the bigger the D_r, the less negative conspecific density (g_1 on N_1) dependence is compared to heterospecific density (g_2 on N_1) dependence and therefore less chance for coexistence. Specifically when $D_r > 1$, conspecific density dependence is always less negative (or more positive) than heterospecific density dependence, which tends to enlarge the difference in abundance. This means that when $D_r > 1$, although there is a steady state where species coexist (where $g_1 = g_2 = 0$ in Fig. 4.6a and 4.6b), it is unstable and any perturbation can drive one species to exclusion. When θ is different among the species, all species except for the one with the smallest θ are excluded; when θ is the same for all species, the identity of the excluded species depends on the direction of the perturbation.

The effect of θ is similar to that in Chapter 3: all else equal, bigger difference in θ leads to less negative (or more positive) conspecific density dependence compared to heterospecific density dependence, which reinforces initial perturbations and leads to less chance for coexistence. Also similar to the conclusion in Chapter 3, here the values of r do not fundamentally change the result.

Lifespan-body size relationship

In Chapter 3 I defined a parameter S_f to quantify the selfishness of individuals of a given species. It is equal to the probability that an individual prioritizes itself over its offspring in resource allocation. Given this extra parameter, this model can predict the actual birth and death rate as well as the lifespan of a species at steady state. The calculation is the same as in Chapter 3. The relationship between predicted lifespan and θ is shown in Fig. 4.7.

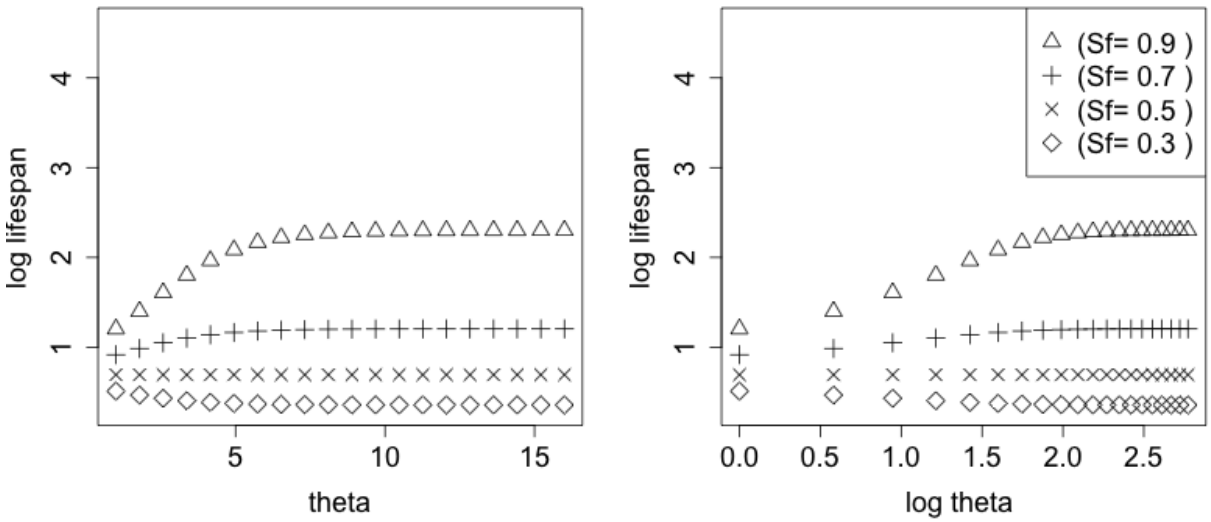

Figure 4.7: Relationship between θ and lifespan.
Y axis is log-transformed lifespan (number of reproductive intervals between birth and death). For the graph on the left, X axis is θ; in the graph on the right, X axis is log θ. Steady state abundance $\hat{N}$, D_r and r do not affect this pattern. Different selfishness values (S_f) are represented by different point types as is illustrated in the legend.

Notice that the pattern is not affected by D_r or r. This is because lifespan is completely determined by the k distribution at steady state ($\hat{N_{i,k}}$), which in this model is not affected by D_r or r (Fig. 4.4).

From Fig. 4.7 we can see that in this model, a positive lifespan-body size relationship is predicted when $S_f > 0.5$. Empirical studies have found that the slope of a log-log fit between lifespan and body size is around 0.2 (Speakman 2005). It is clear from Fig. 4.7 that lifespan is not in an exponential relationship (straight line on left graph) nor a power law relationship (straight line on the right graph) with θ: in both graphs, the slope decreases as θ increases.

Notice that the lifespan calculated here is actually the number of reproductive intervals between birth and death. For species with non-overlapping generations, this number is always one, i.e. each individual reproduces once before it dies. For species with overlapping generations, this number is bigger than one. Since bigger species usually have longer reproductive intervals, the patterns in Fig. 4.7 will be steeper if lifespan in absolute time is used.

In Section 4.4.3 Results I examined all the predictions of this new model that were explored in Chapter 3. Some of them are different: D_r does not affect the shape of within-species resource distribution or lifespan-body size relationship; the effects of θ and D_r on population resilience are not as significant. However, the majority of the predictions are consistent with those in Chapter 3. First steady state abundance approximately follows the same equation ($N_i = (C\theta_i)^{\frac{1}{1-D_{r,i}}}$); the higher the D_r or the bigger the difference in θ among the species, the less chance for species coexistence. Second, the within-species resource distribution is more even when θ is bigger, suggesting a more even distribution of reproductive success for species with bigger body size. Lastly, lifespan (measured as the number of reproductive intervals between birth and death) increases with body size when individual selfishness (S_f) is higher than 0.5.

In the next section I will first discuss how the new scenario of resource allocation explored here helps clarify the connections between this theory and existing ecological theories, then outline approaches to empirically test the predictions.

4.4 Discussion

D_r: connecting niche and species neutrality

In this new scenario of resource allocation, the definition of D_r is based on biologically specific metrics, i.e. across- and within-species functional overlapping. This helps clarify several points that were ambiguous in the previous framework. First, $D_{r,i}$ represents the level of trait dispersion of the species i: if species i is more dispersed in functional traits than species j, the functional overlapping within species i (O_i) is smaller than that within species j (O_j) and therefore $D_{r,i} = \frac{1-O_i}{O} > \frac{1-O_j}{O} = D_{r,j}$. Second, the theoretical upper limit

of D_r is not 1 but ∞. A species can have $D_{r,i} > 1$ when its individuals are functionally more dispersed than different species are.

Throughout this framework, D_r is a key factor determining the steady state coexistence pattern among species. Same as in Chapters 2 and 3, if $D_r < 1$, all species theoretically coexist; in practice where population stochasticity is present, there is a higher probability of exclusion with a bigger D_r. When $D_r = 1$, regardless of population stochasticity, all species except those with the smallest θ are excluded at steady state. In this chapter, the case when $D_r > 1$ (same for all species) is also explored. The result shows that although analytically there is a steady state where species coexist, it is not stable and the slightest perturbation can drive the species to exclusion (discussed in Section 4.3.3.4). In all, if all species have the same D_r but different θ, stable coexistence only happens when $D_r < 1$.

Based on the above it is easy to make connections between this theory and niche theory (Whittaker & Levin 1975, Pianka 1981); when the species each has a unique niche in the ecospace (the functional space in this theory), they have the maximal within-species functional overlapping ($O_i = 1$) but minimal across-species overlapping ($O = 0$). This means that $D_{r,i} = 0$ for all species (section 4.3.2), which leads to stable coexistence among all species just as the niche theory predicts.

Moreover, there are multiple connections with Hubbell's neutral theory (Hubbell 2001). Species neutrality can be interpreted in different ways in our theory. First of all, if we think of neutrality as equivalence in species attributes, it means that all species have the same θ, r and D_r. This leads to stable coexistence among species when $D_r \leq 1$. Secondly, if species neutrality means that all species completely overlap functionally, in this theory it corresponds to $D_{across} = 0$ and $D_{r,i} = \infty$ for all species. From section 4.3.1 we can see that this leads to exclusion of all species except for the one with the highest initial abundance. Thirdly, in a more relaxed sense, species neutrality could also mean that individuals are as functionally dispersed within-species as across-species, which corresponds to $D_{r,i} = 1$ in this theory. This leads to coexistence (neutral steady state) when all species have equal θ, and otherwise exclusion of all other species except the one with the smallest θ.

Recall that the neutral theory predicts that the steady state of any community (without speciation) to be exclusion of all species but one. This result is most similar to the second interpretation (i.e. species completely overlap functionally ($D_{across} = 0$)), which means that this can actually be the underlying assumption of the neutral theory. The fact that the other interpretations (equal attributes for all species, $D_{r,i} = 1$ for all species) have different predictions suggests that the framework presented here provides a means of clarifying the concept of species neutrality.

In summary, through the definition and incorporation of D_r in resource allocation, our theory bridges the niche- and neutrality-based view of community assembly under a unified framework: a small D_r represents functional clustering within species and predicts coexistence among species like the niche theory; a big D_r represents functional dispersion or no distinct niche for each species, which leads to predictions compatible with those of the neutral theory. Moreover, this theory highlights the middle ground where predictions can be made for communities where niche and neutrality apply to varying degrees.

Empirical measure of D_r

Here I summarize three different ways to calculate D_r from data. The first is the most data demanding, while the second and the third invoke additional assumptions.

Trait distribution-based

$D_{r,i}$ is the ratio between $D_{within,i}$ and D_{across}, which are the complement of functional overlapping within and across species (O_i and O, Eqs. 4.1-4.2). Therefore,

$$D_{r,i} = \frac{D_{within,i}}{D_{across}} = \frac{1 - O_i}{1 - O} \tag{4.22}$$

O_i and O can be measured from trait distributions. First suppose the functional space has only one dimension, i.e. one trait, Fig. 4.8 shows how across-species functional overlapping can be calculated from distributions of all species on this trait axis.

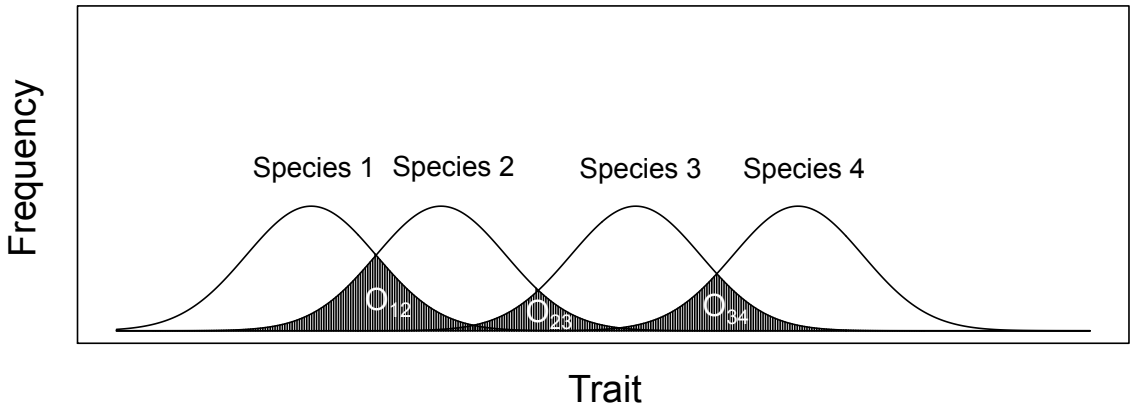

Figure 4.8: Calculate functional overlapping O among species from trait distributions. Each curve is the probability distribution of a trait (X axis) for a species (annotated at the peak of the curve). The shaded areas are overlaps between species (O_{12} between species 1 and 2, O_{34} between species 3 and 4, etc.). The overall functional overlapping across species is calculated by dividing total overlapping area (counted once for each species) by the maximum possible overlapping over all species, or $O = \frac{2O_{12}+2O_{23}+2O_{34}}{4(4-1)}$. See text for more explanation.

To calculate O, first plot trait distributions for all the species as in Fig. 4.8; then add up all the overlap among distributions (shaded area in Fig. 4.8). Notice that the overlap should be counted once for each species, i.e. the area where three species are overlapping should be counted three times. After the total overlap is calculated, divide it by the maximum possible overlapping over all species. The latter can be calculated by $S_0(S_0-1)$, where S_0 is the total number of species S_0. This is because when all species perfectly overlap, for each species, the area of overlapping with all the other species is $S_0 - 1$ (since the area under curve for one species is 1). This way $O = 1$ when all distributions completely overlap and $O = 0$ when they are completely separate. Notice that the trait can be either categorical (e.g. color, shape) or numerical (e.g. length, timing). This difference might affect how area-under-curve is calculated (summation for the former and integral for the latter), but not the fundamental idea behind the calculation.

When the functional space has multiple trait-axes, we can first do the calculation above, then take the product of the result for each trait. In other words, only when all the traits completely overlap can we get an $O = 1$. On the other hand, complete separation $O = 0$ happens as long as species are completely separated on at least one of the traits. The same method can be used to calculate within-species overlapping O_i by simply switching the distributions to be each for an individual instead of a species.

Trait difference-based

An alternative way to calculate functional overlapping is to use mean functional differences, assuming that the bigger the difference in mean trait values between two individuals or species, the less likely it is for them to overlap functionally:

$$\begin{aligned} 1 - O_i &\propto \mathrm{MPD}_{functional,i} \\ 1 - O &\propto \mathrm{MPD}_{functional} \end{aligned} \tag{4.23}$$

Where $\mathrm{MPD}_{functional,i}$ and $\mathrm{MPD}_{functional}$ are the mean pairwise distance between any two individuals of species i and between any two species in the functional space, respectively. D_r can then be calculated by

$$D_{r,i} = \frac{1 - O_i}{1 - O} = \frac{\mathrm{MPD}_{functional,i}}{\mathrm{MPD}_{functional}} \tag{4.24}$$

This method only applies to traits that can be ordered for mean pairwise distance to make sense. However, it provides a simple approximation when data on individual-level trait distribution is not available.

In the above two methods, expert knowledge is required to determine whether a trait (or more generally, any variable) is relevant to resource allocation and should be incorporated in the calculation for D_r. The fundamental standard is whether the resource tends to be evenly distributed along that trait. For example, in MacArthur's warbler study (MacArthur 1958), the resource (food) is believed to be evenly distributed through time so feeding time

is the trait that should be used to calculate D_r. If the resource is evenly distributed across space, then location should be used.

Phylogenetic distance-based

In some cases, functional data is not available or the resource allocation process is unclear so that it is hard to determine which trait(s) to use in the calculation of D_r. In those cases, it might be necessary to use genetic information as proxy for functional information. The underlying assumption for this would be that functional differences are correlated with genetic differences, or that the relevant functional traits have phylogenetic signal (Blomberg *et al.* 2003). Then we can simply substitute phylogenetic distance for functional difference in the calculation for $D_{r,i}$:

$$D_{r,i} = \frac{\text{MPD}_{phylo,i}}{\text{MPD}_{phylo}} \tag{4.25}$$

Here $\text{MPD}_{phylo,i}$ and MPD_{phylo} are the mean pairwise phylogenetic distance between any two individuals of species i and between any two species, respectively. Both functional and phylogenetic MPD are established metrics in bioinformatics (Webb *et al.* 2008) so I will not show the calculation details.

This method has two advantages over the functional difference-based method. First, we don't have to select traits or order them. Second, it makes use of the phylogenetic data and therefore expands the application of this model. However, it does assume that the relevant functional trait(s) have phylogenetic signal, which may not always be true (Ackerly 2009, Losos 2008).

Empirical tests

With a specific measure for D_r, the quantitative predictions of the model can be directly tested. The prediction for steady state abundance is:

$$N_i = (C\theta_i)^{\frac{1}{D_{r,i}-1}} \tag{4.26}$$

And therefore:

$$\log N_i(D_{r,i} - 1) = \log\theta_i + \log C \tag{4.27}$$

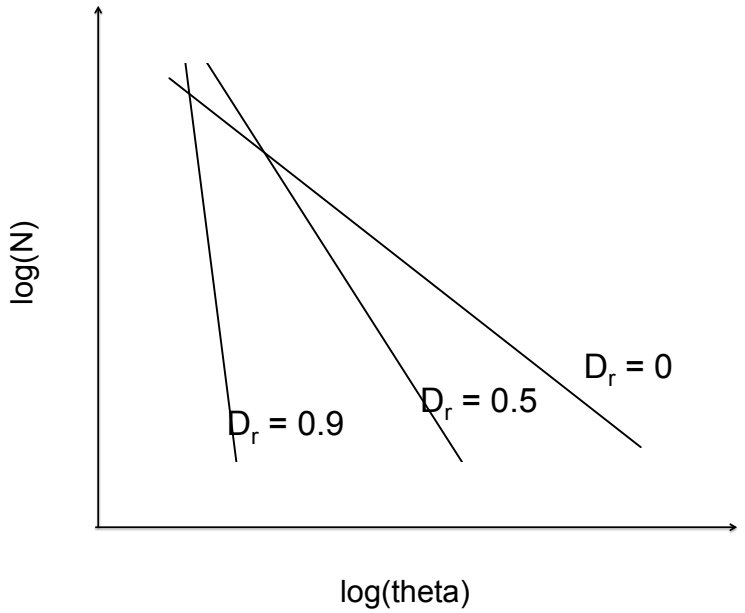

Figure 4.9: Steady state relationship between abundance N and resource requirement θ on a log-log scale when D_r is a constant for all species.
Three different cases for D_r are plotted for comparison and the values are specified next to the corresponding curves.

The steady state relationship between abundance and θ is also illustrated in Fig. 4.9. When available, data for abundance (N_i), body size (θ_i) and functional traits ($D_{r,i}$) can be fitted to a linear model in Eq. 4.27; the goodness of fit (R squared) shows how well this model describes the data.

Doing the above model fitting requires a lot of data and may not be pragmatic. When no such data are available, less data demanding tests can be done for the qualitative predictions of the model. In the following I group them into three broad categories: species coexistence, macroevolution and life history strategies. In the following I will use θ and body size interchangeably.

Species coexistence

Hypothesis I: Abundance decreases faster with body size when each species is functionally more dispersed.

From Fig. 4.9 we can see that, the bigger the D_r or trait dispersion, the faster the steady state abundance decreases with θ. To test this hypothesis, we can compare the abundance-body size relationships for communities among which functional dispersion potentially varies. For example, communities in tropical areas are believed to have less niche overlap across species (and therefore smaller D_r) than communities in temperate areas (Klopfer & MacArthur 1961). If that is the case, this model predicts that the correlation between abundance and body size is more negative for temperate communities. In general, the inference of whether a community has more functional dispersion than another requires expert knowledge on both communities and is context dependent. With no other information, a first guess can be made using the following standard:

Hypothesis II: Species in a community where body size distribution is highly skewed tend to be functionally clustered.

The model predicts that the bigger the difference in θ and the bigger the D_r, the less even the steady state abundances are. Therefore given the shape of the species abundance distribution, if the difference in body size is big, D_r has to be small which means species have to be functionally clustered.

Controlling not the abundance but the body size distribution, the steady state prediction also generates the following hypothesis:

Hypothesis III: Given the body sizes of all species, the abundance distribution is more even when species are functionally clustered.

Empirical studies have found that species abundance distribution can take the shape of a log-series distriution, a lognormal distribution and sometimes even a geometric distribution (Ulrich *et al.* 2010). This theory gives an explanation: communities with more even species abundance distributions are functionally more clustered.

Macroevolution

Hypothesis IV: Effective population size is bigger when body size is bigger.

As is illustrated in Results (section 4.3.3.2), this model predicts that a resource is more evenly distributed among individuals when the species has bigger θ (Fig. 4.4). In this model, more even resource distribution means more even reproductive opportunity among individuals. In population genetics, this corresponds to bigger effective population size, which is defined as the number of individuals that contribute offspring to the next generation or the efficiency of the population to pass genetic diversity on to future generations (Lande & Barrowclough 1987). The result here reveals that there is a tradeoff between body size and effective population size: according to Eq. 4.26, steady state abundance is higher when body size is smaller, but effective population size is comparatively smaller. Based on this, the polarization of r- and K-selected strategies can be interpreted as this: the former tries to maximize population size, while the latter tries to maximize effective population size relative to population size. More implications on life history strategies will be discussed later.

Further generalizing this result we have:

Hypothesis V: All else equal, a population is genetically more diverse when the body size is bigger.

Hypothesis VI: Diversification is faster for species with bigger body size.

This also provides an alternative explanation to Cope's rule (Brown & Maurer 1986, Hunt & Roy 2006): lineages tend to evolve to larger body size.

Since genetic diversity is usually correlated with phenotypic diversity (Reed & Frankham 2003), this result also suggests that there is possibly positive correlation between D_r and θ: the bigger the θ, the more genetically and functionally diverse the species is, the less functional overlapping within the species and therefore the higher the D_r. If this is the case,

Hypothesis VII: The slope of abundance varying with body size decreases with body size.

In other words, it should not be a straight line on the log-log plot between abundance and body size as is predicted when D_r is the same for all species. According to Eq. 4.26, the slope of this plot should be $\frac{1}{D_r-1}$, a negative function of D_r. If D_r is positively correlated with θ, then this slope should be in negative correlation with bigger θ.

Life history strategies

The selfishness parameter S_f quantifies how likely it is for the individual to give the resource to itself instead of an offspring. Therefore the bigger the S_f, the less investment the individual makes to reproduce. Based on this, the result for lifespan-body size relationship (section 4.3.3.5) can be interpreted as:

Hypothesis VIII: The more reproductive effort species make, the faster lifespan increases with body size.

Test for this hypothesis can also be based on the r- vs K-selected life history strategies. Species with r-selected strategy make more reproductive effort than species with K-selected strategy (Pianka 1970). According to the result here, only species with K-selected strategy have longer lifespan with bigger body size. The correlation between lifespan and body size for species with r-selected strategy should be much less positive or even negative (Fig. 4.7).

The application of the theory is not limited to what I have explored. In the following I will summarize prospective topics that can be further explored with this framework in the future.

Future extensions

Incorporate taxonomic levels other than species

Under the new resource allocation scenario, our model is now flexible to incorporate not just species and individuals but also higher taxonomic levels. For example, if functional overlapping among genera is known, we can generalize the equation for total number of microstates to be:

$$W_{total} = W_{genus}^{D_{genus}} \times \prod_{g}^{G_0} W_{across,g}^{D_{across,g}} \times \prod_{i}^{S_g} (W_{grouping,i} W_{within,i})^{D_{within,i}} \tag{4.28}$$

W_{genera} is the number of ways to allocate resource units among G_0 genera; $W_{across,g}$ is the corresponding number among the S_g species in genus g ($g = 1, 2, ..., G_0$). $D_{genera} = 1 - O_{genera}$ and O_{genera} is the level of functional overlapping among all genera; $D_{across,g}$ is the corresponding value for genus g. Other taxonomic levels can be added similarly.

In this theory the pattern at a given taxonomic level only matters if the functional overlapping at that level is small (so the exponent for the corresponding W is big). This can be used as a standard for whether to include information from a taxonomic level. For example, insects are functionally very different among orders (Zheng & Gui 1999). Therefore it makes much sense to include the order level in our model when predicting patterns for insects.

Incorporating ontogenetic growth

So far I have assumed that all species have equal reproductive interval, i.e. takes equal amount of time to grow into sexual maturity after born. In nature, species with bigger body size usually takes longer to mature than smaller ones. In the future this can be realized in our model by imposing longer waiting time for species with bigger θ to reproduce. This will enable our model to predict more realistic population dynamics and lifespan-body size relationship.

Predicting ecological network structure

In nature, species can interact with each other in many other ways than exploitative competition. Interspecific (trophic, mutualistic) relationships can also be taken as trait axes of the niche space. Based on the interpretation of D_r as trait dispersion, $D_{r,i}$ of a species should be bigger when it is a generalist and smaller when it is a specialist. In other words, the number of links between a certain species and other species should be positively related to its $D_{r,i}$. $D_{r,i}$ can be calculated from the steady state solution (Eq. 4.22) given the

total resource flow, the abundance and body size information of all species in the network. Then simulations can be done to find out the network structure that best satisfies a positive relationship between number of links and $D_{r,i}$ (and any other given constraints, e.g. total number of links in the network).

4.5 Conclusion

A model of population dynamics and species coexistence generated from a new perspective of the resource allocation process is explored. Many previous predictions on species coexistence, macroevolution and life history strategies have been proved to be robust. With a clearer interpretation of the D_r parameter as functional dispersion, empirical tests of the theory can readily be done. In this framework, several links can be established with the concepts of niche and species neutrality, suggesting new directions for existing ecological theories to be combined. This theory can be extended in many different directions to predict patterns at higher taxonomic level, ontogenetic growth, and ecological networks.

Bibliography

Abrams, P. & Ginzburg, L. (2000). The nature of predation: prey dependent, ratio dependent or neither? *Trends Ecol. Evo.*, 15, 337–341.

Ackerly, D. (2009). Conservatism and diversification of plant functional traits: evolutionary rates versus phylogenetic signal. *Proceedings of the National Academy of Sciences*, 106, 19699–19706.

Albert, C.H., Thuiller, W., Yoccoz, N.G., Douzet, R., Aubert, S. & Lavorel, S. (2010). A multi-trait approach reveals the structure and the relative importance of intra-vs. interspecific variability in plant traits. *Funct. Ecol.*, 24, 1192–1201.

Amarasekare, P. (2003). Competitive coexistence in spatially structured environments: a synthesis. *Ecol. Lett.*, 6, 1109–1122.

Anderson, R.P., Peterson, A.T. & Go, M. (2002). Using niche-based GIS modeling to test geographic predictions of competitive exclusion and competitive release in South American pocket mice. *Oikos*, 1, 3–16.

Armstrong, R.A. & McGehee, R. (1980). Competitive exclusion. *Am. Nat*, pp. 151–170.

Auger, S. & Shipley, B. (2013). Inter-specific and intra-specific trait variation along short environmental gradients in an old-growth temperate forest. *J. Veg. Sci*, 24, 419–428.

Baldwin, R.A. (2009). Use of maximum entropy modeling in wildlife research. *Entropy*, 11, 854–866.

Banavar, J.R., Maritan, A. & Volkov, I. (2010). Applications of the principle of maximum entropy: from physics to ecology. *Journal of Physics: Condensed Matter*, 22, 063101.

Barabás, G., Meszéna, G. & Ostling, A. (2012). Community robustness and limiting similarity in periodic environments. *Theor. Ecol.*, 5, 265–282.

Bellman, R. (1956). Dynamic programming and lagrange multipliers. *Proc. Natl. Acad. Sci. U.S.A.*, 42, 767.

Blackburn, T.M. & Gaston, K.J. (1994). Animal body size distributions: patterns, mechanisms and implications. *Trends Ecol. Evo.*, 9, 471–474.

Blomberg, S.P., Garland, T. & Ives, A.R. (2003). Testing for phylogenetic signal in comparative data: behavioral traits are more labile. *Evolution*, 57, 717–745.

Boltzmann, L. (1896). Entgegnung auf die wärmetheoretischen betrachtungen des hrn. e. zermelo. *Ann. Phys-Berlin*, 293, 773–784.

Boltzmann, L. & Gibbs, J.W. (1870). *Entropy in thermodynamics and information theory http://en. wikipedia. org/wiki*.

Brown, J.H. & Maurer, B.A. (1986). Body size, ecological dominance and cope's rule. *Nature*, 324, 248–250.

Calcagno, V., Mouquet, N., Jarne, P. & David, P. (2006). Coexistence in a metacommunity: the competition-colonization trade-off is not dead. *Ecol. Lett.*, 9, 897–907.

Chase, J.M., Abrams, P.a., Grover, J.P., Diehl, S., Chesson, P., Holt, R.D. et al. (2002). The interaction between predation and competition: a review and synthesis. *Ecol. Lett.*, 5, 302–315.

Chave, J. (2004). Neutral theory and community ecology. *Ecol. Lett.*, 7, 241–253.

Chesson, P. (1991). A need for niches? *Trends Ecol. Evo.*, 6, 26–28.

Chesson, P. (2000). General theory of competitive coexistence in spatially-varying environments. *Theor. Pop. Bio.*, 58, 211–237.

Clark, J.S. (2009). Beyond neutral science. *Trends Ecol. Evo.*, 24, 8–15.

Conlisk, E., Bloxham, M., Conlisk, J., Enquist, B. & Harte, J. (2007). A new class of models of spatial distribution. *Ecol. Monogr.*, 77, 269–284.

Damuth, J. (1981). Population density and body size in mammals. *Nature*, 290, 699–700.

De Queiroz, K. (2007). Species concepts and species delimitation. *Systematic biology*, 56, 879–886.

Dennis, B. & Desharnais, R. (1995). nonlinear demographic dynamics: mathematical models, statistical methods and biological experiments. *Ecol. Monogr.*, 3, 261–282.

Dewar, R.C. (2009). Maximum entropy production as an inference algorithm that translates physical assumptions into macroscopic predictions: Don?t shoot the messenger. *Entropy*, 11, 931–944.

Dewar, R.C. & Porté, A. (2008). Statistical mechanics unifies different ecological patterns. *J. Theor. Biol.*, 251, 389–403.

Dewdney, A. (1998). A general theory of the sampling process with applications to the ?veil line? *Theor. Pop. Bio.*, 54, 294–302.

Durrett, R. & Levin, S. (1998). Spatial aspects of interspecific competition. *Theoretical population biology*, 53, 30–43.

Fargione, J. & Tilman, D. (2005). Niche differences in phenology and rooting depth promote coexistence with a dominant C4 bunchgrass. *Oecologia*, 143, 598–606.

Fenchel, T. (1974). Intrinsic rate of natural increase: the relationship with body size. *Oecologia*, 14, 317–326.

Fisher, R.A., Corbet, A.S. & Williams, C.B. (1943). The relation between the number of species and the number of individuals in a random sample of an animal population. *J. Anim. Ecol.*, pp. 42–58.

George-Nascimento, M., Munoz, G., Marquet, P.A. & Poulin, R. (2004). Testing the energetic equivalence rule with helminth endoparasites of vertebrates. *Ecol. Lett.*, 7, 527–531.

Gilpin, M.E. & Ayala, F.J. (1973). Global models of growth and competition. *Proceedings of the National Academy of Sciences*, 70, 3590–3593.

Grant, B. & Grant, P. (1989). Natural selection in a population of darwin's finches. *Am. Nat*, pp. 377–393.

Green, J.L., Harte, J. & Ostling, A. (2003). Species richness, endemism, and abundance patterns: tests of two fractal models in a serpentine grassland. *Ecol. Lett.*, 6, 919–928.

Green, J.L. & Plotkin, J.B. (2007). A statistical theory for sampling species abundances. *Ecology letters*, 10, 1037–1045.

Haegeman, B. & Etienne, R.S. (2010). Entropy maximization and the spatial distribution of species. *Am. Nat.*, 175, E74–E90.

Haegeman, B. & Loreau, M. (2008). Limitations of entropy maximization in ecology. *Oikos*, 117, 1700–1710.

Haegeman, B. & Loreau, M. (2009). Trivial and non-trivial applications of entropy maximization in ecology: a reply to shipley. *Oikos*, 118, 1270–1278.

Harte, J. (2011a). *Maximum entropy and ecology: a theory of abundance, distribution, and energetics*. Oxford University Press.

Harte, J. (2011b). *Maximum entropy and ecology: a theory of abundance, distribution, and energetics*. Oxford University Press, Oxford, UK, pp. 141-175.

Harte, J., Conlisk, E., Ostling, A., Green, J.L. & Smith, A.B. (2005). A theory of spatial structure in ecological communities at multiple spatial scales. *Ecol. Monogr.*, 75, 179–197.

Harte, J. & Newman, E.A. (2014a). Maximum information entropy: a foundation for ecological theory. *Trends in ecology and evolution*, 29, 384–389.

Harte, J. & Newman, E.A. (2014b). Maximum information entropy: a foundation for ecological theory. *Trends Ecol. Evo.*, 29, 384–389.

Harte, J., Rominger, A. & Zhang, W. (2015). Integrating macroecological metrics and community taxonomic structure. *Ecology letters*, 18, 1068–1077.

Harte, J., Zillio, T., Conlisk, E. & Smith, A. (2008). Maximum entropy and the state-variable approach to macroecology. *Ecology*, 89, 2700–2711.

Hassell, M. (1975). density dependence in single-species populations. *J. Anim. Ecol.*, 44, 283–295.

He, F. (2010). Maximum entropy, logistic regression, and species abundance. *Oikos*, 119, 578–582.

Hernandez, P.A., Graham, C.H., Master, L.L. & Albert, D.L. (2006). The effect of sample size and species characteristics on performance of different species distribution modeling methods. *Ecography*, 29, 773–785.

Hubbell, S.P. (2001). *The unified neutral theory of biodiversity and biogeography (MPB-32)*. vol. 32. Princeton University Press.

Hunt, G. & Roy, K. (2006). Climate change, body size evolution, and cope's rule in deep-sea ostracodes. *Proceedings of the National Academy of Sciences*, 103, 1347–1352.

Hutchinson, G. (1961). The paradox of the plankton. *Am. Nat*, 95, 137–145.

Hutchinson, G.E. (1965). The niche: an abstractly inhabited hypervolume. *The ecological theatre and the evolutionary play*, pp. 26–78.

Jaynes, E.T. (1957). Information theory and statistical mechanics. *Physical review*, 106, 620.

Jaynes, E.T. (1982). On the rationale of maximum-entropy methods. *Proc. IEEE.*, 70, 939–952.

Kang, Y. & Chesson, P. (2010). Relative nonlinearity and permanence. *Theor. Pop. Bio.*, 78, 26–35.

Kelly, C.K., Blundell, S.J., Bowler, M.G., Fox, G.A., Harvey, P.H., Lomas, M.R. et al. (2011). The statistical mechanics of community assembly and species distribution. *New Phytologist*, 191, 819–827.

Kelly, C.K. & Bowler, M.G. (2002). Coexistence and relative abundance in forest trees. *Nature*, 417, 437–440.

Kendall, D.G. (1948). On the generalized" birth-and-death" process. *The annals of mathematical statistics*, pp. 1–15.

Khinchin, A.Y. (1957). *Mathematical foundations of information theory*. Courier Corporation.

Klopfer, P.H. & MacArthur, R.H. (1961). On the causes of tropical species diversity: niche overlap. *Am. Nat*, pp. 223–226.

Kramer-Schadt, S., Niedballa, J., Pilgrim, J.D., Schröder, B., Lindenborn, J., Reinfelder, V. et al. (2013). The importance of correcting for sampling bias in maxent species distribution models. *Diversity and Distributions*, 19, 1366–1379.

Kullback, S. (1959). Statistics and information theory. *J. Wiley and Sons, New York*.

Lande, R. (1976). Natural selection and random genetic drift in phenotypic evolution. *Evolution*, pp. 314–334.

Lande, R. & Barrowclough, G.F. (1987). Effective population size, genetic variation, and their use in population management. *Viable populations for conservation*, pp. 87–123.

Leirs, H., Stenseth, N.C., Nichols, J.D., Hines, J.E., Verhagen, R. & Verheyen, W. (1997). Stochastic seasonality and nonlinear density-dependent factors regulate population size in an African rodent. *Nature*, 389, 176–180.

Levin, S.A. (1970). Community equilibria and stability, and an extension of the competitive exclusion principle. *Am. Nat*, pp. 413–423.

Lewontin, R.C. (1974). *The genetic basis of evolutionary change*. Columbia University Press New York, pp. 95-159.

Lobry, C. & Harmand, J. (2006). A new hypothesis to explain the coexistence of n species in the presence of a single resource. *C. R. Biol.*, 329, 40–6.

Losos, J.B. (2008). Phylogenetic niche conservatism, phylogenetic signal and the relationship between phylogenetic relatedness and ecological similarity among species. *Ecology letters*, 11, 995–1003.

MacArthur, R.H. (1957). On the relative abundance of bird species. *Proceedings of the National Academy of Sciences*, 43, 293–295.

MacArthur, R.H. (1958). Population ecology of some warblers of northeastern coniferous forests. *Ecology*, 39, 599–619.

Mainali, K.P., Warren, D.L., Dhileepan, K., McConnachie, A., Strathie, L., Hassan, G. et al. (2015). Projecting future expansion of invasive species: comparing and improving methodologies for species distribution modeling. *Global change biology*, 21, 4464–4480.

Mallet, J. (1995). A species definition for the modern synthesis. *Trends Ecol. Evo.*, 10, 294–299.

Marks, C.O. & Muller-Landau, H.C. (2007). Comment on "from plant traits to plant communities: A statistical mechanistic approach to biodiversity". *Science*, 316, 1425c–1425c.

Marquet, P.A., Navarrete, S.A. & Castilla, J.C. (1995a). Body size, population density, and the energetic equivalence rule. *J. Anim. Ecol.*, pp. 325–332.

Marquet, P.A., Navarrete, S.A. & Castilla, J.C. (1995b). Body size, population density, and the energetic equivalence rule. *J. Anim. Ecol.*, 64, 325–332.

McGill, B.J. (2006). A renaissance in the study of abundance. *Science*, 314, 770–772.

McGill, B.J. (2010). Towards a unification of unified theories of biodiversity. *Ecol. Lett.*, 13, 627–642.

McGill, B.J. & Nekola, J.C. (2010). Mechanisms in macroecology: Awol or purloined letter? towards a pragmatic view of mechanism. *Oikos*, 119, 591–603.

McPeek, M.A. (2012). Intraspecific density dependence and a guild of consumers coexisting on one resource. *Ecology*, 93, 2728–2735.

Meier, R. (2000). *Species concepts and phylogenetic theory: a debate*. Columbia University Press.

Melbourne, B.a. & Chesson, P. (2005). Scaling up population dynamics: integrating theory and data. *Oecologia*, 145, 179–87.

Merow, C., Smith, M.J. & Silander, J.A. (2013). A practical guide to maxent for modeling species? distributions: what it does, and why inputs and settings matter. *Ecography*, 36, 1058–1069.

Morris, W.F., Doak, D.F. et al. (2002). Quantitative conservation biology. *Sinauer, Sunderland, Massachusetts, USA*.

Nathan, R. & Muller-Landau, H.C. (2000). Spatial patterns of seed dispersal, their determinants and consequences for recruitment. *Trends in ecology and evolution*, 15, 278–285.

Nee, S., Read, A.F., Greenwood, J.J. & Harvey, P.H. (1991). The relationship between abundance and body size in british birds. *Nature*, 351, 312–313.

Neill, C., Daufresne, T. & Jones, C.G. (2009a). A competitive coexistence principle? *Oikos*, 118, 1570–1578.

Neill, C., Daufresne, T. & Jones, C.G. (2009b). A competitive coexistence principle? *Oikos*, 118, 1570–1578.

Petchey, O.L. (2010). Maximum entropy in ecology. *Oikos*, 119, 577–577.

Phillips, R.a., Silk, J.R.D., Phalan, B., Catry, P. & Croxall, J.P. (2004). Seasonal sexual segregation in two Thalassarche albatross species: competitive exclusion, reproductive role specialization or foraging niche divergence? *Proc. R. Soc. B*, 271, 1283–91.

Phillips, S.J., Anderson, R.P. & Schapire, R.E. (2006a). Maximum entropy modeling of species geographic distributions. *Ecological modelling*, 190, 231–259.

Phillips, S.J., Anderson, R.P. & Schapire, R.E. (2006b). Maximum entropy modeling of species geographic distributions. *Ecol. Modell.*, 190, 231–259.

Phillips, S.J. & Dudík, M. (2008). Modeling of species distributions with maxent: new extensions and a comprehensive evaluation. *Ecography*, 31, 161–175.

Pianka, E.R. (1970). On r-and k-selection. *Am. Nat.*, 104, 592–597.

Pianka, E.R. (1981). Competition and niche theory. *Theoretical ecology principles and applications*, pp. 167–196.

Plotkin, J.B., Potts, M.D., Leslie, N., Manokaran, N., LaFrankie, J. & Ashton, P.S. (2000). Species-area curves, spatial aggregation, and habitat specialization in tropical forests. *Journal of theoretical biology*, 207, 81–99.

Pueyo, S. (2006). Diversity: between neutrality and structure. *Oikos*, 112, 392–405.

Pueyo, S., He, F. & Zillio, T. (2007). The maximum entropy formalism and the idiosyncratic theory of biodiversity. *Ecol. Lett.*, 10, 1017–1028.

Reed, D.H. & Frankham, R. (2003). Correlation between fitness and genetic diversity. *Conservation biology*, 17, 230–237.

Renner, I.W. & Warton, D.I. (2013). Equivalence of maxent and poisson point process models for species distribution modeling in ecology. *Biometrics*, 69, 274–281.

Renyi, A. (1961). On measures of entropy and information. In: *Fourth Berkeley symposium on mathematical statistics and probability*. vol. 1, pp. 547–561.

Roxburgh, S.H. & Mokany, K. (2007). Comment on ?from plant traits to plant communities: a statistical mechanistic approach to biodiversity? *science*, 316, 1425b–1425b.

Shannon, C.E. (1949). Communication in the presence of noise. *Proceedings of the IRE*, 37, 10–21.

Shannon, C.E. (1951). Prediction and entropy of printed english. *Bell system technical journal*, 30, 50–64.

Shipley, B. (2010a). Community assembly, natural selection and maximum entropy models. *Oikos*, 119, 604–609.

Shipley, B. (2010b). Community assembly, natural selection and maximum entropy models. *Oikos*, 119, 604–609.

Shipley, B. (2010c). *From plant traits to vegetation structure: chance and selection in the assembly of ecological communities*, Cambridge University Press, chap. 4, pp. 94–102.

Shipley, B., Vile, D. & Garnier, É. (2006a). From plant traits to plant communities: a statistical mechanistic approach to biodiversity. *science*, 314, 812–814.

Shipley, B., Vile, D. & Garnier, E. (2006b). From plant traits to plant communities: a statistical mechanistic approach to biodiversity. *Science*, 314, 812–4.

Siepielski, A. & McPeek, M. (2010). On the evidence for species coexistence: a critique of the coexistence program. *Ecology*, 91, 3153–3164.

Soulé, M.E. (1987). *Viable populations for conservation*. Cambridge university press.

Speakman, J.R. (2005). Body size, energy metabolism and lifespan. *Journal of Experimental Biology*, 208, 1717–1730.

Swenson, N.G. & Enquist, B.J. (2009). Opposing assembly mechanisms in a neotropical dry forest: implications for phylogenetic and functional community ecology. *Ecology*, 90, 2161–2170.

Tilman, D. (1981). Resource competition and community structure. *Mol. Ecol.*, 17, 1–296.

Tokeshi, M. (1993). Species abundance patterns and community structure. *Advances in ecological research*, 24, 111–186.

Tokeshi, M. (2009). *Species coexistence: ecological and evolutionary perspectives*. Wiley Blackwell, pp. 1- 464.

Toro, D.D., O'Connor, D. & Thomann, R. (1971). a dynamic model of the phytoplankton population in the sacramento-san joaquin delta. *Adv. Chem. Ser*, 106, 131–180.

Ulrich, W., Ollik, M. & Ugland, K.I. (2010). A meta-analysis of species–abundance distributions. *Oikos*, 119, 1149–1155.

Violle, C. & Jiang, L. (2009). Towards a trait-based quantification of species niche. *Journal of Plant Ecology*, p. rtp007.

Volterra, V. (1938). Population growth, equilibria, and extinction under specified breeding conditions: a development and extension of the theory of the logistic curve. *Hum. Biol.*, 10, 1–11.

Webb, C.O., Ackerly, D.D. & Kembel, S.W. (2008). Phylocom: software for the analysis of phylogenetic community structure and trait evolution. *Bioinformatics*, 24, 2098–2100.

White, E.P., Ernest, S.K., Kerkhoff, A.J. & Enquist, B.J. (2007a). Relationships between body size and abundance in ecology. *Trends Ecol. Evo.*, 22, 323–330.

White, E.P., Ernest, S.M., Kerkhoff, A.J. & Enquist, B.J. (2007b). Relationships between body size and abundance in ecology. *Trends in ecology and evolution*, 22, 323–330.

White, E.P., Thibault, K.M. & Xiao, X. (2012). Characterizing species abundance distributions across taxa and ecosystems using a simple maximum entropy model. *Ecology*, 93, 1772–1778.

Whittaker, R.H. & Levin, S.A. (1975). *Niche: theory and application.* vol. 3. Halsted Pr.

Wilson, M. & Lindow, S.E. (1994). Coexistence among Epiphytic Bacterial Populations Mediated through Nutritional Resource Partitioning Coexistence among Epiphytic Bacterial Populations Mediated through Nutritional Resource Partitioning. *Appl. Environ. Microb*, 60, 4468–4477.

Wilson, W.G. & Abrams, P.A. (2005). Coexistence of cycling and dispersing consumer species: Armstrong and McGehee in space. *Am. Nat.*, 165, 193–205.

Wright, J. (2002). Plant diversity in tropical forests: a review of mechanisms of species coexistence. *Oecologia*, 130, 1–14.

Wright, S. (1932). *The roles of mutation, inbreeding, crossbreeding, and selection in evolution.* vol. 1. na.

Young, J. & Willson, L.J. (1987a). Use of bose-einstein statistics in population dynamics models of arthropods. *Ecol. Modell.*, 36, 89–99.

Young, J. & Willson, L.J. (1987b). Use of Bose-Einstein statistics in population dynamics models of arthropods. *Ecol. Modell.*, 36, 89–99.

Zhang, Y.J. & Harte, J. (2015). Population dynamics and competitive outcome derive from resource allocation statistics: The governing influence of the distinguishability of individuals. *Theoretical population biology*, 105, 53–63.

Zheng, L. & Gui, H. (1999). Insect classification. *Nanjing: Nanjing Normal University Press (in Chinese)*.